On Sound and Silence

Amarins Nieske Heeringa

Publication of this dissertation was financially supported by
School of Behavioural and Cognitive Neuroscience (BCN)
University of Groningen
Nederlandse Vereniging voor Keel-Neus-Oorheelkunde en Heelkunde van het Hoofd-Halsgebied

Beter Horen BV
Daleco Pharma b.v.
EmiD BV
MED-EL
MediTop Medical Products B.V.
Olympus Nederland B.V.
Oticon Nederland B.V.

Cover design by Amarins Heeringa
Printed by & Lay Out by Proefschriftmaken.nl || Uitgeverij BOXpress
ISBN 978-94-6295-211-9

rijksuniversiteit
groningen

On Sound and Silence

Neurophysiological and behavioral consequences of acoustic trauma

Proefschrift

ter verkrijging van de graad van doctor aan de
Rijksuniversiteit Groningen
op gezag van de
rector magnificus prof. dr. E. Sterken
en volgens besluit van het College voor Promoties.

De openbare verdediging zal plaatsvinden op

maandag 22 juni 2015 om 16.15 uur

door

Amarins Nieske Heeringa

geboren op 24 februari 1986
te Menaldumadeel

Promotor
Prof. dr. P. van Dijk

Beoordelingscommissie
Prof. dr. R. Salvi
Prof. dr. ir. N. M. Maurits
Prof. dr. J. G. G. Borst

Index

Chapter 1

Introduction

A.N. Heeringa

Preface

Acoustic trauma has a major impact on several aspects of hearing. In the first place, it results in an elevation of the auditory thresholds, often accompanied by difficulties in understanding speech in noisy conditions. Additionally, people exposed to loud sounds might develop tinnitus, which is defined as the perception of a sound that cannot be attributed to an external sound source. Throughout this dissertation, the term tinnitus will refer to subjective tinnitus, which involves the cases where no physiological internal sound source, such as a sound produced by a pulsating blood vessel, is causing the tinnitus. The prevalence of people that perceive noise-induced tinnitus, but are not necessarily bothered by it, is quite large. Among young adults, 89.5% report experiencing transient tinnitus after loud music exposure (Gilles et al., 2012). Another consequence of exposure to loud sounds is hyperacusis. This is a condition in which the patient has a reduced tolerance and an increased sensitivity to sound. Hyperacusis can occur alone, but is often comorbid with tinnitus. The prevalence of hyperacusis in tinnitus patients varies between 55% and 79% (Dauman and Bouscau-Faure, 2005; Schecklmann et al., 2014). Both are potentially debilitating conditions for which there are no widely accepted treatments.

There is a general consensus that the pathology of both tinnitus and hyperacusis resides, at least partly, in the central auditory system (Eggermont and Roberts, 2004; Lanting et al., 2009; Knipper et al., 2013). However, despite numerous studies and hypotheses, the exact pathophysiological mechanism(s) behind tinnitus and hyperacusis remain(s) elusive. This will be the broad subject in this dissertation. I will try to answer a few specific research questions that are aimed to fill (or to contribute to filling) small parts of the gaps in the knowledge about the mechanisms behind noise-induced tinnitus and hyperacusis.

In the following part of this introduction, I will explain the methods that I used and the reasons why I used these specific methods to study the pathophysiological mechanism(s) behind noise-induced tinnitus and hyperacusis. This will be followed by an overview of the specific aims and research questions that are addressed in the subsequent chapters of this dissertation.

Why use the guinea pig to study the effects of acoustic trauma

There are a few important reasons to study pathophysiological mechanisms of tinnitus and hyperacusis in a living animal. First, as compared to *in vitro* techniques, the use of laboratory animals can provide crucial information, as the whole living body is far more complex than the sum of its parts. In other words, exposing a few auditory neurons in a petri dish to a traumatizing stimulus does not give the same results as exposing a living animal to loud sounds. Second, invasive techniques, such as *in vivo* electrophysiology, are inappropriate for use in humans, but can be applied on animals. Furthermore, animal studies allow for the careful control of a number of factors that might otherwise influence the outcomes when studied in human subjects, such as genetic background and degree of sound exposure. And last, the effectiveness and mode of action of specific treatments for tinnitus and hyperacusis

can be studied in detail in an animal model. In the last few decades, animal studies have proven to be useful in revealing physiological, molecular, and anatomical markers of noise exposure in the central auditory system (Knipper et al., 2010; Eggermont, 2013). In order to correlate these markers with a specific consequence of noise exposure, such as tinnitus or hyperacusis, behavioral models, which aim to show whether an animal has tinnitus or hyperacusis, have been designed (Hayes et al., 2014).

Even though the rat is also often used to study the pathophysiological mechanism(s) behind noise-induced tinnitus and hyperacusis, I chose for the guinea pig. In the guinea pig, the round window is easily accessible through the bulla behind the ear. This will be important for future studies, because it allows us to investigate the mode of action and effectiveness of drug treatments that need to be applied locally on the round window (Muehlmeier et al., 2011). Furthermore, the guinea pig has frequently been used in auditory neurophysiological studies (e.g. Rees and Palmer, 1989; Dunnebier et al., 1997; Shore, 2005; Mulders and Robertson, 2009). This allows for a direct comparison of my results to the literature. However, when I started this project in 2010, there was no behavioral model yet that could test for the presence of tinnitus or hyperacusis in the guinea pig. Therefore, one of the studies I conducted addressed possible measures to assess tinnitus in guinea pigs (Chapter 6).

How to study the effects of acoustic trauma on neurophysiological measures

"Neurophysiology" is derived from the Greek words "νευρο-" (neuro-) and "φυσιολογια" (physiology). It refers to the study of physiological mechanisms of the (central) nervous system. Several neurophysiological methods are available, which all have varying degrees of spatial and temporal resolution. In the current study, I used the auditory brainstem response (ABR) and *in vivo* electrophysiology, which are described in detail below.

The auditory brainstem response

I selected the ABR as an investigative technique because it is a rapid, commonly used, and reliable method to establish hearing thresholds and integrity of the auditory system (see below). Furthermore, the ABR can also be assessed in humans, which allowed me to compare my results to human studies.

The ABR is a recording of an evoked potential that derives from the cochlea and the auditory brainstem in response to an acoustic stimulus. In laboratory animals, the ABR is obtained by placing three electrodes subcutaneously, one at the vertex, one behind the ipsilateral pinna, and one behind the contralateral pinna, for reference, recording, and grounding, respectively. Clicks (0.1 ms) and short tone pips (3 ms) are commonly used as acoustic stimuli to evoke ABRs. By subtracting the signal recorded from the electrode behind the ipsilateral pinna from the signal recorded from the electrode at the vertex, a stimulus-related waveform can be measured (see Figure 1.1). This waveform is characterized by a number of peaks, which are referred to as the ABR waves and are labeled by the Roman

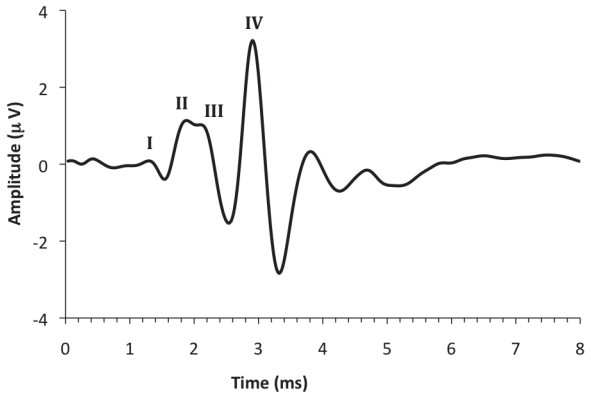

Figure 1.1 A representative example of an auditory brainstem response of a normal-hearing guinea pig evoked by a 0.1 ms click of 70 dB SPL. The positive peaks of the waveforms are labeled with the corresponding Roman numerals.

numerals I, II, III, and IV. ABRs can reveal several functional characteristics of the auditory system.

The most common application of the ABR is to determine auditory thresholds. Stimuli of decreasing sound levels are presented, which typically result in smaller amplitudes of the ABR waveforms. The lowest stimulus level at which prominent stimulus-related waveforms can still be observed is considered the auditory threshold for that particular stimulus. In the current dissertation, ABRs have been used to determine the auditory thresholds for the experiments described in Chapter 2, Chapter 5, and Chapter 6.

Furthermore, the waves of the ABR can be regarded as derived from different locations of the auditory pathway, although it is not entirely clear whether there are single sites in the brain responsible for the generation of the individual waves (Wada and Starr, 1983a, 1983b). Nevertheless, it is commonly accepted that wave I represents the summated activity of the auditory nerve and wave IV derives from a more central location, i.e. the auditory midbrain (see Figure 1.1 and Figure 1.3). When the auditory nerve integrity is compromised by moderate noise trauma, then the amplitude of wave I is reduced (Kujawa and Liberman, 2009; Lin et al., 2011). Furthermore, in tinnitus patients with normal auditory thresholds, the amplitude of wave I is also reduced but the wave IV amplitude is intact (Kehrle et al., 2008; Schaette and McAlpine, 2011; Gu et al., 2012). These findings show that studying the amplitudes of the ABR waves can be used as a tool to determine the integrity of the central auditory system. This approach has been applied in Chapter 2.

In vivo electrophysiology

The other method that I used extensively in the experiments conducted for this dissertation was *in vivo* electrophysiology. This method allows us to directly record neural activity from auditory neurons in the anesthetized animal. The activity of neurons consists of brief electrical

discharges, which appear as spikes in a neural signal recorded by the electrode. Recordings of these spikes in the presence and absence of external acoustic stimuli provides a powerful tool to study the integrity and functionality of the central auditory system after acoustic trauma.

Briefly, a linear 16-channel electrode is inserted in the brain of the anesthetized animal and extracellular currents are recorded. Subsequently, the signals are filtered and algorithms are applied to remove artifacts. Spike trains can be extracted by determining the instants when the signal exceeds a predefined threshold (see Figure 1.2). On one channel, spiking activity of multiple neurons is typically recorded. Several attempts were made to sort the spikes into individual sources, however, no single units could be identified from the traces. Therefore, all the neurophysiological data reported in this dissertation is considered multi-unit activity.

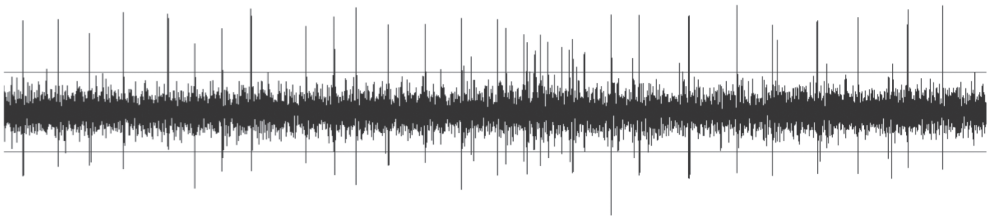

Figure 1.2 Example of a filtered neural signal and the corresponding spiking threshold.

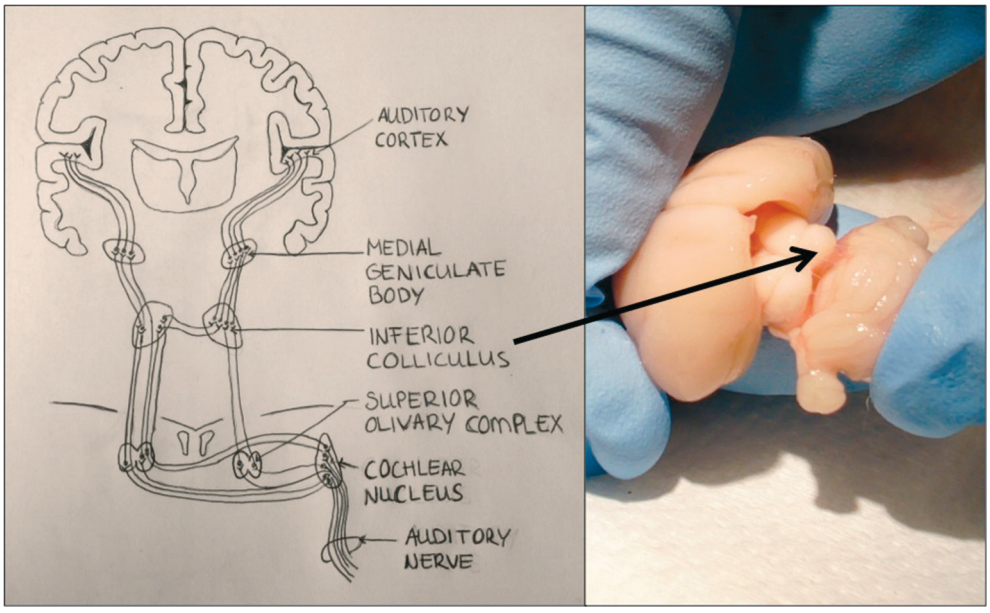

Figure 1.3 The central auditory system. On the left, a simplified, schematic illustration of the central auditory pathway is shown. The inferior colliculus is located at the level of the midbrain and connects the cochlear nucleus and superior-olivary complex to the auditory thalamus (medial geniculate body) and the auditory cortex. On the right, the inferior colliculi of the guinea pig are displayed.

All recordings reported in this dissertation derived from the auditory neurons in the inferior colliculus (IC), which is located in the midbrain and is connected to the cochlear nucleus, superior-olivary complex, and the thalamo-cortical system, among others (Figure 1.3).

I recorded both spontaneous (Chapter 2, Chapter 5) and acoustic stimulus-evoked activity (Chapter 2, Chapter 3, Chapter 4, Chapter 5). A number of analysis-techniques were used to analyze stimulus-evoked activity, which are described below.

Receptive fields

Receptive fields can be obtained by presenting pure tones that have a range of different frequencies and sound levels. Subsequently, the tone-evoked firing rates are inserted in a matrix that organizes frequency and sound level (Figure 1.4).

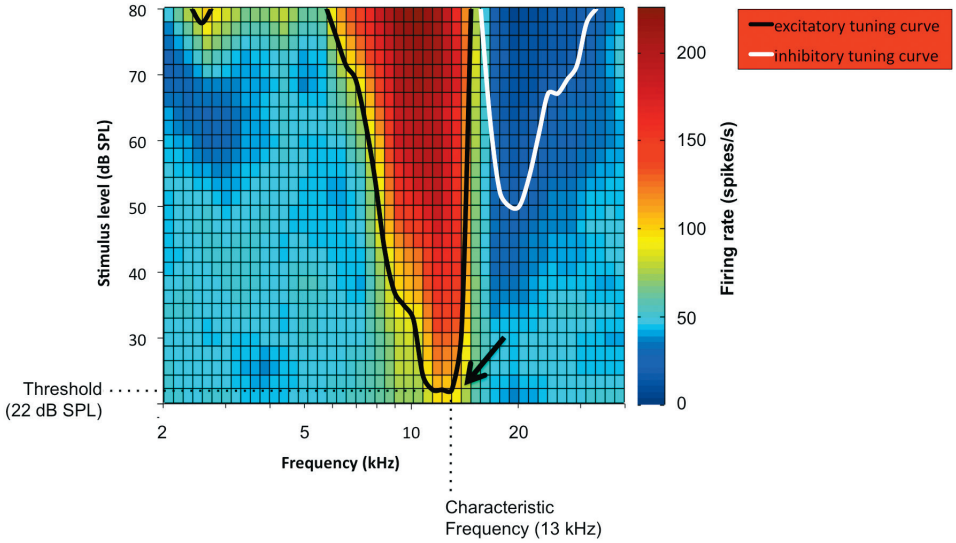

Figure 1.4 An example of a receptive field of an IC unit of the guinea pig. The color code indicates the firing rate in spikes/second. The excitatory receptive field is contoured by the excitatory tuning curve (black line). The characteristic frequency (CF) and threshold are defined by the lowest tip of the tuning curve (black arrow indicates the excitatory CF and threshold). The white line is the inhibitory tuning curve that contours the inhibitory receptive field, i.e. the range of tones that result in a reduction of the spontaneous firing rate.

The neurons in the inferior colliculus can have an excitatory and an inhibitory receptive field. The excitatory receptive field is defined by the range of frequencies and levels that elicit a significant increase in firing rate, whereas the inhibitory receptive field is considered to be the range of tones that elicit a significant decrease in firing rate as compared to the spontaneous

firing rate. The edge of the receptive fields are called the excitatory or inhibitory tuning curves (see Figure 1.4, black and white curves, respectively). The lowest tip of the tuning curve reveals the unit's characteristic frequency (CF) and its corresponding threshold (black arrow in Figure 1.4). In the IC of the guinea pig, the CFs of neurons along the dorso-lateral to medial-ventral axis are organized in an ascending manner. Such a systematic progression of CFs across a brain region is called a tonotopic organization. The CF and threshold, which characterize a multi-unit, were used in the experiments of the current dissertation to determine the location and degree of damage caused by acoustic trauma (Chapter 2, Chapter 3, Chapter 5).

Post-stimulus time histograms

Stimulus-evoked activity can also be organized in a post-stimulus time histogram (PSTH). A PSTH is obtained by presenting a short-duration stimulus (e.g. 100 ms) for a large number of times (e.g. 300 repetitions). Subsequently, spikes are accumulated in time-interval bins relative to the timing of the stimulus. Typically, these histograms are converted to show the average firing rate before, during, and after the presentation of the repeated stimulus (Figure 1.5).

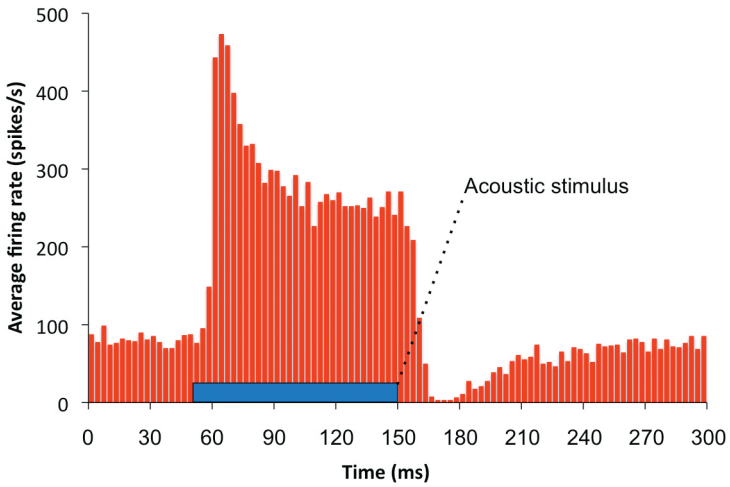

Figure 1.5 An example of a post-stimulus time histogram of an IC unit of the guinea pig. The average firing rate in spikes/sec relative to the timing of the stimulus is plotted as a histogram (bin size 3 ms). The stimulus (blue bar) was a 22-kHz pure tone of 70 dB SPL, with a delay of 50 ms and a duration of 100 ms. This neuron shows an excitatory response to this particular stimulus.

A PSTH provides information about response characteristics, such as the magnitude, the sign (enhancement or inhibition), and the latency of the response. Previous studies showed that PSTH response characteristics are affected by acoustic overstimulation (Willott and Lu,

1982; Wang et al., 1996). Furthermore, a PSTH of a neural response to amplitude-modulated sounds can reveal whether the spiking activity phase locks to the period of the modulation frequency (Rees and Palmer, 1989). This indicates how well the envelope of a stimulus is coded by the recorded multi-unit. In the experiments of the current dissertation, I used PSTHs to study the effects of acoustic trauma on excitatory and inhibitory responses to pure tones (Chapter 2) and on responses to amplitude-modulated noise (Chapter 3).

Wiener-kernel analysis

Another technique that I used in the current dissertation to analyze stimulus-evoked activity of the auditory system is called the Wiener-kernel analysis (Chapter 4, Chapter 5). For this analysis, spiking activity of the IC in response to a continuous Gaussian noise is recorded. Subsequently, the spike trains are cross-correlated with the broadband noise to obtain a set of Wiener kernels (Eggermont, 1993). These kernels provide information about the stimulus characteristics that evoke spikes. In other words, the technique allows us to look back at the acoustic signal preceding the spikes to investigate the stimulus characteristics that elicited the spikes. The Wiener-kernel analysis technique has also been referred to as a subject-centered approach and allows us to investigate the non-linear properties of the auditory system. Typically, the kernels up to the second-order are calculated. The first-order kernel is equal to the linear correlation between the spike train and the noise stimulus, and reflects the ability of a neuron to phase lock to the fine structure of the noise stimulus. The second-order kernel describes nonlinear characteristics of the system and can be further analyzed with singular-value decomposition (SVD). SVD decomposes the kernel into a number of parallel subsystems, each with a filter function (an eigenvector) and a gain function (the corresponding eigenvalue). The filter functions with the highest gains reveal the best frequencies of the neurons. Furthermore, the gain functions can be positive or negative, corresponding to excitation or inhibition, respectively. Thus, Wiener-kernel analysis, complemented with SVD of the second-order kernel, can reveal excitatory and inhibitory response characteristics, and, therefore, can be used as tool to study processes that critically depend on a balance between excitation and inhibition, such as tinnitus and hyperacusis. A more detailed description of the Wiener-kernel analysis and the SVD is provided in Chapter 4.

How to ask a guinea pig if he has tinnitus

In humans, the diagnosis of tinnitus is based on a declaration of the patient, which states that he or she perceives a sound that cannot be attributed to an external acoustic source. Diagnosing hyperacusis is also dependent on a declaration of the patient, who rates the sound levels according to a loudness scale ranging from quiet to painfully loud. Obviously, these diagnostic methods are not appropriate for animals. Therefore, several behavioral animal models were developed to determine whether an animal experiences tinnitus and/or hyperacusis (Turner, 2007; Hayes et al., 2014). A reliable behavioral model will allow us to assign neurophysiological correlates to tinnitus and/or hyperacusis. Therefore, I believe

that it is important to consider behavioral models when studying the pathophysiological mechanism(s) of noise-induced tinnitus and hyperacusis. The current models can be roughly divided into two categories, which are described below.

Conditioning paradigms

In 1988, Pawel Jastreboff and colleagues were the first to publish results of a behavioral model to determine tinnitus in animals (Jastreboff et al., 1988a). In this paradigm, the researchers trained water-deprived rats to stop licking a water dispenser at the offset of a continuous background noise. It is assumed that, if the animal is well trained, the amount of licks during the silent interval corresponds to how well the animal perceives silence. After induction of tinnitus, animals continued to lick from the water dispenser during silence, suggesting that they did not perceive silence. A number of control experiments were conducted to exclude other explanations for the increased licking behavior during silence (Jastreboff et al., 1988b). Over the last decades, several groups provided improved paradigms of the initial idea to condition an animal to show a particular behavior during silent intervals (e.g. Bauer et al., 1999; Rüttiger et al., 2003; Stolzberg et al., 2013).

Startle-reflex paradigms

The other widely used paradigm is the startle-reflex paradigm, which was developed by Jeremy Turner and colleagues in 2006 (Turner et al., 2006). Similar to the conditioning models, the startle-reflex paradigm assumes that tinnitus impairs the animal's ability to perceive a silent interval. The paradigm makes use of the startle reflex, which involves a startle response to an abrupt loud sound. A small silent gap in continuous background noise prior to this loud sound acts as a cue that inhibits the startle reflex. This is called the gap pre-pulse inhibition reflex. It is assumed that animals with tinnitus have difficulties detecting the silent gap and, thus, have a smaller gap pre-pulse inhibition reflex.

Behavioral models to detect tinnitus in guinea pigs

More recently, it has been shown that tinnitus can be detected in guinea pigs using the startle-reflex paradigm (Dehmel et al., 2012; Berger et al., 2013). However, guinea pigs have not been subjected to the conditioning paradigms. In Chapter 6, an attempt to develop a conditioning paradigm for guinea pigs is described. The results of these experiments led to a new idea, which might be used as a potential new paradigm of detecting tinnitus in guinea pigs.

Aims and outline of the remaining chapters

The overarching aim of the current dissertation is to study neurophysiological and behavioral consequences of acoustic trauma in the guinea pig. The presented results may provide additional insight in the pathophysiological mechanism(s) of noise-induced tinnitus and

hyperacusis. Gaining knowledge about the pathophysiology of tinnitus and hyperacusis advances the search for a treatment. Future research in this direction might result in an animal model that allows us to test drug treatments that need to be applied on the round window of the cochlea.

In **Chapter 2**, the time course of neurophysiological consequences of acoustic trauma was determined. The applied acoustic trauma was associated with rapidly recovering hearing thresholds. Wave I and wave IV amplitudes of the ABR were assessed. In addition, *in vivo* neurophysiological recordings from the IC provided a more detailed insight into excitatory and inhibitory responses in the auditory midbrain.

In **Chapter 3**, the effects of immediate acoustic trauma on neural responses of the IC to amplitude-modulated noise were identified. This provided insight into the changes induced by acoustic trauma on envelope coding in the IC.

The aim of the study presented in **Chapter 4** was to determine the applicability of Wiener-kernel analysis to noise-evoked spike trains of the IC. First- and second-order Wiener kernels were identified and classified, and were compared to classic excitatory and inhibitory tuning curves, obtained from responses to pure tones.

Chapter 5 describes the effects of immediate acoustic trauma on response characteristics of the IC, as revealed with Wiener-kernel analysis. We investigated whether a trauma-induced disrupted balance between excitation and inhibition (as shown in Chapter 2) could be confirmed and further defined with Wiener-kernel analysis.

In **Chapter 6**, possible behavioral methods to determine tinnitus in guinea pigs were studied. The initial aim of the study was to develop a conditioning model to detect tinnitus in guinea pigs. However, the first experiment showed that guinea pigs could not be trained to a silent interval in background noise. Instead, it appeared that the behavioral activity of the animals was inhibited during the silent interval. Therefore, another experiment was designed to evaluate the mobility during silence and noise in animals with and without exposure to acoustic trauma.

Chapter 7 provides a discussion about how the experiments conducted for the current dissertation add value to the current literature of this research field. Furthermore, future directions that are necessary in order to develop an animal model to test treatments for tinnitus are also described.

Chapter 2

The dissimilar time course of temporary threshold shifts and reduction of inhibition in the inferior colliculus following intense sound exposure

A.N. Heeringa and P. van Dijk

Published in: Hearing Research (2014), 312: 38-47. doi: 10.1016/j.heares.2014.03.004.

Abstract

Excessive noise exposure is known to produce an auditory threshold shift, which can be permanent or transient in nature. Recent studies showed that noise-induced temporary threshold shifts are associated with loss of synaptic connections to the inner hair cells and with cochlear nerve degeneration, which is reflected in a decreased amplitude of wave I of the auditory brainstem response (ABR). This suggests that, despite normal auditory thresholds, central auditory processing may be abnormal.

We recorded changes in central auditory processing following a sound-induced temporary threshold shift. Anesthetized guinea pigs were exposed for one hour to a pure tone of 11 kHz (124 dB sound pressure level). Hearing thresholds, amplitudes of ABR waves I and IV, and spontaneous and tone-evoked firing rates in the inferior colliculus (IC) were assessed immediately, one week, two weeks, and four weeks post exposure.

Hearing thresholds were elevated immediately following overexposure, but recovered within one week. The amplitude of the ABR wave I was decreased in all sound-exposed animals for all test periods. In contrast, the ABR wave IV amplitude was only decreased immediately after overexposure and recovered within a week. The proportion of IC units that show inhibitory responses to pure tones decreased substantially up to two weeks after overexposure, especially when stimulated with high frequencies. The proportion of excitatory responses to low frequencies was increased. Spontaneous activity was unaffected by the overexposure.

Despite rapid normalization of auditory thresholds, our results suggest an increased central gain following sound exposure and an abnormal balance between excitatory and inhibitory responses in the midbrain up to two weeks after overexposure. These findings may be associated with hyperacusis after a sound-induced temporary threshold shift.

Keywords: sound exposure; inferior colliculus; guinea pig; stimulus-evoked activity; inhibition; auditory brainstem response

Abbreviations: ABR, auditory brainstem response; ANOVA, analysis of variance; CF, characteristic frequency; fMRI, functional magnetic resonance imaging; GABA, γ-aminobutyric acid; IC, inferior colliculus; PSTH, post-stimulus time histogram; RM-ANOVA, repeated measures analysis of variance; SEM, standard error of the mean; SPL, sound pressure level; SpO_2, blood oxygen saturation

1. Introduction

Exposure to loud noises may result in tinnitus, i.e. an acoustic perception in the absence of an external sound source, and/or in hyperacusis, a phenomenon defined as over-sensitivity to acoustic input. However, the most common consequence of excessive exposure to noise is an elevation of hearing thresholds. The elevation of thresholds may be permanent or temporary. Noise exposure associated with a permanent threshold shift results in a variety of pathologies in the peripheral and central auditory pathway.

Peripherally, both inner and outer hair cells may degenerate after noise exposure (Salvi et al., 2000). Furthermore, a number of structural changes have been observed. Synaptic ribbons in the surviving inner hair cells, which are important for spike reliability in the auditory nerve, are reduced in number (Zuccotti et al., 2012). Afferent dendrites that innervate the hair cells may swell, and spiral ganglion cells degenerate (Duan et al., 2000). These phenomena explain the permanently elevated hearing thresholds after noise exposure. Subsequently, along the central auditory pathway, γ-aminobutyric acid (GABA) inhibitory neurotransmission in the inferior colliculus (IC) is reduced (Milbrandt et al., 2000; Dong et al., 2010a), whereas the strength of excitatory responses in the IC is increased (Willott and Lu, 1982; Niu et al., 2013). In the auditory cortex, the balance between excitation and inhibition is likewise disrupted (Scholl and Wehr, 2008). Moreover, spontaneous firing rates of units in the IC are altered following sound-induced hearing loss (Mulders and Robertson, 2009; Niu et al., 2013). It is thought that these central pathologies, among others, are correlated with tinnitus and hyperacusis (Eggermont and Roberts, 2004; Knipper et al., 2013).

These changes occur after a noise-induced permanent elevation of the hearing threshold. However, tinnitus and hyperacusis can also occur in the absence of permanent elevated hearing thresholds, suggesting abnormalities in the central auditory system. Indeed, in tinnitus patients with normal hearing threshold, it has been shown that the amplitude of wave I of the auditory brainstem response (ABR) is reduced, whereas the amplitude of ABR wave V remains unchanged (Schaette and McAlpine, 2011). This indicates an increased neural gain, since a reduced auditory nerve response (wave I) is enhanced in the brainstem to produce a normal auditory midbrain response (wave V). Further evidence of increased central gain came from a functional magnetic resonance imaging (fMRI) study, that showed sound-evoked hyperactivity of the IC in hyperacusis patients with normal audiograms (Gu et al., 2010).

Recently, it has been shown that the peripheral auditory system may also be permanently damaged by a noise exposure that is only associated with a temporary threshold shift. Following recovery of hearing thresholds, the amplitude of ABR wave I is chronically reduced, despite apparently unaffected hair cell integrity. This reduction of wave I is associated with a 50% loss of afferent nerve terminals on inner hair cells, and with disorganization and a reduced number of synaptic ribbons. Furthermore, within months, the auditory nerve slowly degenerates. Specifically, auditory nerve fibers that have high thresholds and low spontaneous

firing rates are affected more than those with low thresholds and high spontaneous rates (Kujawa and Liberman, 2009; Lin et al., 2011; Furman et al., 2013).

At present it is not known to what extent conditions that may affect the peripheral hair cell synapse influence response properties in the central auditory system. It is conceivable that damage to the peripheral synapse, such as a loss of synaptic ribbons, results in changes in central auditory processing, despite the presence of normal hearing thresholds. The current study aims at determining possible abnormalities in central auditory processing caused by sound exposures that are associated with rapidly recovering hearing thresholds. We assessed ABR waveforms after acoustic trauma that induced temporary threshold elevations in guinea pigs. These results are readily comparable to those in human subjects (Schaette and McAlpine, 2011). In addition, multi-unit recordings were made in the IC and provide a more detailed insight into excitatory and inhibitory responses in the auditory midbrain. Finally, the recordings of spontaneous neural activity provide a possible correlate of tinnitus.

2. Methods

2.1 Experimental groups

Fifteen male albino guinea pigs (Dunkin Hartley; Harlan Laboratories, Horst, the Netherlands) were used in this study. Guinea pigs weighed between 250 and 300 g upon arrival in the Central Animal Facility of the University Medical Center Groningen, where they were socially housed. Sound pressure levels (SPLs) in the housing room did not exceed 65 dB SPL (36 dB A). All neurophysiology was carried out six weeks after arrival, to ensure that all guinea pigs had approximately the same age and weight during recording of IC activity. Guinea pigs were exposed to a loud tone at either four weeks (n=3), two weeks (n=3), one week (n=3), or immediately (n=3) before neurophysiology. In addition, a control/sham group (n=3) was treated similarly, except for the sound exposure, two weeks before the neurophysiology. Thus all guinea pigs were allowed to acclimatize to laboratory conditions for at least two weeks before experimental procedures started (Figure 2.1A). All experiments were approved by the Animal Experiment Committee of the University of Groningen (DEC # 6068B) and were in compliance with Dutch and European law and regulations.

2.2 Sound exposure

Guinea pigs that were tone- or sham-exposed four weeks, two weeks, or one week before neurophysiology were anesthetized with isoflurane (5% for initiating and 2.5% for maintenance of anesthesia) in a mixture of medical air and oxygen. Animals that were exposed to the tone immediately before neurophysiology were anesthetized with ketamine/xylazine (70 mg/kg Ketamine, Alfasan, Woerden-Holland; 6 mg/kg Rompun (xylazine), Bayer-Healthcare, respectively). Heart rate and blood oxygen saturation (SpO_2) were monitored using a pulsoximeter. Body temperature was held constant at 38 °C by a heating pad. Two Piezo tweeters (PH8; Velleman) were positioned at approximately 5 cm from each ear, resulting in

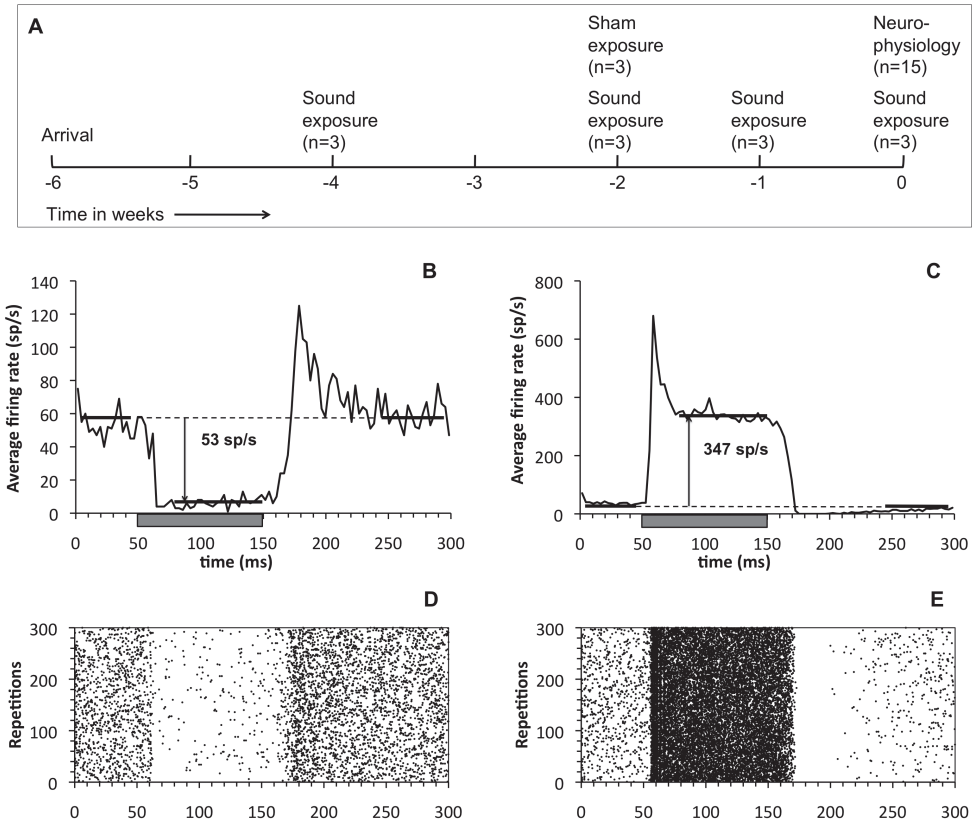

Figure 2.1 **A)** Experimental design. Neurophysiology was always performed six weeks after arrival in the central animal facility. Time of sound exposure differed between the groups: either four weeks, two weeks, one week, or immediately before neurophysiology. Sham exposure of the control group took place two weeks before neurophysiology. ABRs were recorded directly before and after sound exposure, and on the day of neurophysiology. **B) - E)** Examples of sound-evoked activity. Averaged stimulus-driven firing rate in sp/s (spikes/sec) over 300 presentations of a 22-kHz pure tone (gray bar) in a sham-exposed animal. PSTH **(B)** and its raw data traces **(D)** of a significant inhibitory response of an IC multi-unit (CF 8.9 kHz; threshold 37 dB SPL) with a response strength of 53 sp/s. PSTH **(C)** and its raw data traces **(E)** of a significant excitatory response of an IC multi-unit (CF 21.5 kHz; threshold 39 dB SPL) with a response strength of 347 sp/s. Horizontal black bars in panel B and C show how the response strength is calculated.

free field overexposure. Both pinnae were folded over the head, to create an unobstructed path from the speakers to the tympanic membrane. Animals were bilaterally exposed to a continuous tone of 11 kHz (124 dB SPL) for 1 hour. The trauma stimulus was designed in RPvdsEx (Tucker-Davis Technologies; TDT Inc.), generated by a Real-Time Processor (RP2.1, TDT Inc.) and amplified (Philips PM 5170 amplifier). A measuring microphone (Bruël & Kjær; type 2670) and amplifier (Bruël & Kjær; type 2610) were used to calibrate the stimulus level at the entrance of the ear canal. The sham-exposure group was treated as

the other groups, without the amplifier being connected. All subsequent stimulus levels will be expressed as dB SPL.

2.3 Neurophysiology

2.3.1 Auditory brainstem responses (ABRs)

ABRs were collected before and immediately after sound exposure, and on the day of the recordings from the IC. Anesthetics and monitoring of the animal were as described in section 2.2. The stimuli were 3 ms pure tones (3, 6, 11, and 22 kHz; 0.2 ms $\cos^2$ on and off ramps) and a 0.1 ms click that were designed in SigGenRP. Stimulus level started at 100 dB and decreased in steps of 10 dB. All stimuli were presented 1000 times at each level with a repetition rate of 33/sec. Presentation was controlled by BioSigRP software (TDT Inc.). Acoustic stimuli were generated by a Real-Time processor (RP2.1, TDT Inc.) and an attenuator (PA5, TDT Inc.), and presented via a free field electrostatic speaker driver and speaker (ED1 and ES1, TDT Inc.). The speaker was placed at approximately 2 cm in front of the nose of the animal. Stimuli were calibrated using a B&K microphone (type 2670) and amplifier (type 2610). Electrodes were placed subdermally at the vertex, behind the ipsilateral pinna, and behind the contralateral pinna, for reference, recording, and grounding, respectively. ABR signals were amplified (25K times) and filtered (0.3-3 kHz, -6 dB/octave slope) by a pre-amplifier (EG&G; model 5113), recorded by a second RP2.1, and saved on a PC using BioSigRP software.

2.3.2 Extracellular multi-unit recordings from the inferior colliculus

In vivo neurophysiological recordings from the IC were performed in a sound-attenuating booth at either four weeks, two weeks, one week, or immediately after sound exposure (Figure 2.1A). Neurophysiology of the control group was recorded two weeks after sham exposure. Animals were anesthetized with a mixture of ketamine and xylazine (70 mg/kg and 6 mg/kg, respectively; i.m.). To maintain a deep level of anesthesia, supplementary injections with half the original dose were administered every hour. A tracheotomy was performed for artificial respiration and a skull screw used for fixation of the head. Next, a craniotomy was made above the right IC. The head of the animal was slightly turned around the rostro-caudal axis, to position the craniotomy horizontally. The dura mater below the craniotomy was removed and cortical brain tissue aspirated, to allow visual placement of a single-shank 16-channel microelectrode array in the right IC. The electrodes in the array were arranged in a single column along the axis of penetration, were 100 μm apart, and had a contact surface equal to 413 μm2 (A1x16-10mm-100-413-A16; NeuroNexus). The microelectrode array was inserted into the IC in the lateral-dorsal to medial-ventral direction, in order to obtain recordings from a broad tonotopic gradient.

Acoustic stimuli were generated (RP2.1; TDT Inc.), attenuated (PA5; TDT Inc.), and presented (ED1, ES1; TDT Inc.) at ± 5 cm from the contralateral ear. Stimuli were calibrated using a B&K microphone (type 2670) and amplifier (type 2610) placed at the

entrance of the ear canal. Multi-unit neural activity was recorded using TDT hardware (preamplifier RA16PA and processor RX5) and software (RPvdsEx). MatLab programs (R2010b, MathWorks) were custom-made to store neural recordings and generate acoustic stimuli. Noise bursts (delay 50 ms, duration 100 ms, 10 ms $\cos^2$ gate) were presented while the microelectrode array was slowly inserted into the IC, using a micromanipulator (Kopf instruments). Real-time inspection of multi-unit activity before, during, and after the noise bursts revealed which channels on the microelectrode recorded from auditory neurons, and this was used for optimal placement in the IC.

Pure tones with a frequency of 3, 6, 11, and 22 kHz (delay 50 ms, 10 ms $\cos^2$ ramp, duration 100 ms, 300 ms recording time, 80 dB, 300 repetitions) were presented to elicit acoustically evoked activity, which was used to plot post-stimulus time histograms (PSTHs). In addition, receptive fields were obtained by recording neural activity resulting from stimulation with 300 ms pure tones of different frequencies (2-40 kHz, 25 steps, logarithmically spaced) and levels (0-80 dB, 15 steps, linearly spaced), presented randomly. Plotting the receptive field enabled us to determine the characteristic frequency (CF), i.e. the frequency at which the unit responds to the lowest sound level, and the corresponding threshold (Duque et al., 2012). And finally, two recordings without acoustical stimulation were acquired (180s duration), to assess spontaneous activity.

2.4 Data Analysis

ABR thresholds were determined by visual inspection and were considered the lowest stimulus level for which ABR wave IV, the most prominent and consistent waveform in our measurements, was clearly detectable. The tone-induced threshold shift was defined as the difference between the ABR threshold before and after the sound (or sham) exposure, and was calculated for every animal individually. Furthermore, the amplitudes of wave I and wave IV were determined by calculating the difference between P1 and N1, and between P4 and N4, respectively (Figure 2.2D shows an example of an ABR to 22 kHz, 70 dB tones in a sham-exposed guinea pig). The waveform amplitudes (in μV) were determined in the ABRs that were recorded on the day of neurophysiology. Only wave amplitudes in response to 22 kHz were taken into account, because waveform abnormalities are expected in ABRs in response to stimulation with tones one octave above the exposure frequency (Kujawa and Liberman, 2009).

Neural data were analyzed using custom-made MatLab programs (R2010b, MathWorks). To set a threshold for spike detection, the root-mean-square of filtered signals (300-3000 Hz, butterworth filter) was calculated and multiplied by three. Artifacts were removed using a custom-made algorithm. Units that had a clear response to white noise and a distinguishable receptive field were included in further analyses. Also, units without a clear receptive field, but that were recorded at an electrode located within 600 μm ventrally from a unit with a CF $<$ 8 kHz, were included. This last criterion included auditory IC neurons lacking a clear receptive field due to damage by sound exposure.

The proportion of units that suppressed or enhanced activity upon stimulation with pure tones and the respective mean change in spike rate were taken as a measure of inhibition and excitation, respectively. These measures were obtained from the PSTH, which was acquired between 0 and 300 ms, where the stimuli were presented between 50 and 150 ms. First, firing rates in the time windows 5-45 ms and 250-295 ms over all four recordings of that unit were averaged. Subsequently, the stimulus-evoked activity was calculated per stimulus by averaging activity over all 300 repetitions to that stimulus in the time window 80-150 ms and compared with the previously calculated firing rate before and after the stimulus. Thus, on-responses, i.e. the first response of a unit to an acoustic stimulus, were excluded in these analyses by starting the time window at 30 ms after onset of the stimulus. Significance of response strengths was determined by a Wilcoxon rank sum test and $p<0.001$ was considered significant. When the activity during stimulus presentation was not significantly different from firing rates before and after the stimulus, it was referred to as a 'no response'. Figure 2.1 shows an example of PSTHs of an inhibitory (panel B) and an excitatory (panel C) response to a pure tone of 22 kHz in a sham-exposed animal, and the corresponding time windows that were used to determine response strengths. Panel D and E of Figure 2.1 show the raw traces of the same data of the inhibitory and excitatory responses, respectively. The unit's CF and its corresponding threshold were determined by visual inspection of the receptive fields. Spontaneous firing rates were calculated by averaging firing rates of the two data files recorded in the absence of acoustic stimulation.

2.5 Statistics

Significance of ABR threshold shifts was calculated by a repeated-measures analysis of variance (RM-ANOVA; stimulus level as within-factor and group as between-factor), using a Bonferroni correction for multiple comparisons (IBM SPSS Statistics; Version 19). Differences in proportions of responses between the control group and the experimental groups were tested using a two-tailed bootstrapping test. This method made a probability distribution of the proportion of, for example, inhibitory responses under the assumption that the proportion of such a response is equal to that in the control animals (null hypothesis). Then, it calculated the chance that the experimental value was derived from that distribution ($p<0.05$ was considered significant after a Bonferroni correction). Differences between groups in firing rate changes and spontaneous activity were determined using a one-way analysis of variance (ANOVA), with a Bonferroni correction. Experimental groups were only compared to the control group, and not to each other, in all statistic tests.

3. Results

3.1 Hearing thresholds

Tonal exposure resulted in an immediate threshold shift of 30 dB at the exposure frequency (11 kHz) and of 60 dB one octave above the exposure frequency (Figure 2.2A; RM-ANOVA: immediately following exposure "Acute" vs. immediately following sham exposure "Control acute", $F=10.629$, $p<0.001$, one-sample t-test with Bonferroni correction for multiple testing). Thresholds recovered completely within one week following overexposure (RM-ANOVA, ns).

In addition to the ABR thresholds, we also studied the thresholds and the CFs of IC units. In sham-exposed animals, 52.5% of the recorded IC units had a CF above 11 kHz (Figure 2.3A) with thresholds ranging from 20 to 75 dB SPL. Immediately following overexposure, the percentage of recorded units with a CF above 11 kHz decreased to 6.0%, all with thresholds higher than 55 dB SPL. One week following overexposure, the proportion of units tuned to 11 kHz or higher had recovered to 43.2% (Figure 2.3C). Thresholds of units with CF ≥ 22 kHz were still elevated ±20 dB compared to control levels. From two weeks after overexposure, CFs and thresholds were similar to control levels (Figure 2.3D and 2.3E). Some IC units, however, did not show a distinguishable receptive field. The numbers of these units were 2, 87, 21, 25, and 8 for the control, acute, one-week, two-weeks, and four-weeks group, respectively.

3.2 ABR wave amplitudes

The amplitude of wave I of the ABR was decreased in every experimental group at stimulus levels ≤ 80 dB compared to the control group (Figure 2.2B; RM-ANOVA, $F=5.910$, $p<0.05$). However, for stimulus levels higher than 80 dB, the amplitude of wave I of control animals did not increase further, it rather stabilized at a lower amplitude. Contrarily, wave I amplitudes of the experimental groups monotonically increased with increasing stimulus level. There were no significant differences between the groups when only stimulus levels > 80 dB were taken into account (RM-ANOVA, ns).

Wave IV amplitudes were decreased for all stimulus levels when measured immediately after overexposure, but recovered within one week (Figure 2.2C; RM-ANOVA, $F=5.338$, $p<0.05$). See Figure 2.2D and 2.2E for representative examples of an ABR of the control group and of an ABR of the four-weeks post exposure group, respectively. Note the decreased wave I amplitude (P1 - N1) and recovered wave IV amplitude (P4 - N4) in the experimental group in panel E compared to panel D (sham-exposed animal).

3.3 Proportions of stimulus-evoked IC responses

Figure 2.4 displays how all recorded multi-unit responses in the IC were divided between no responses, inhibitory responses, and excitatory responses for stimulation with pure tones of

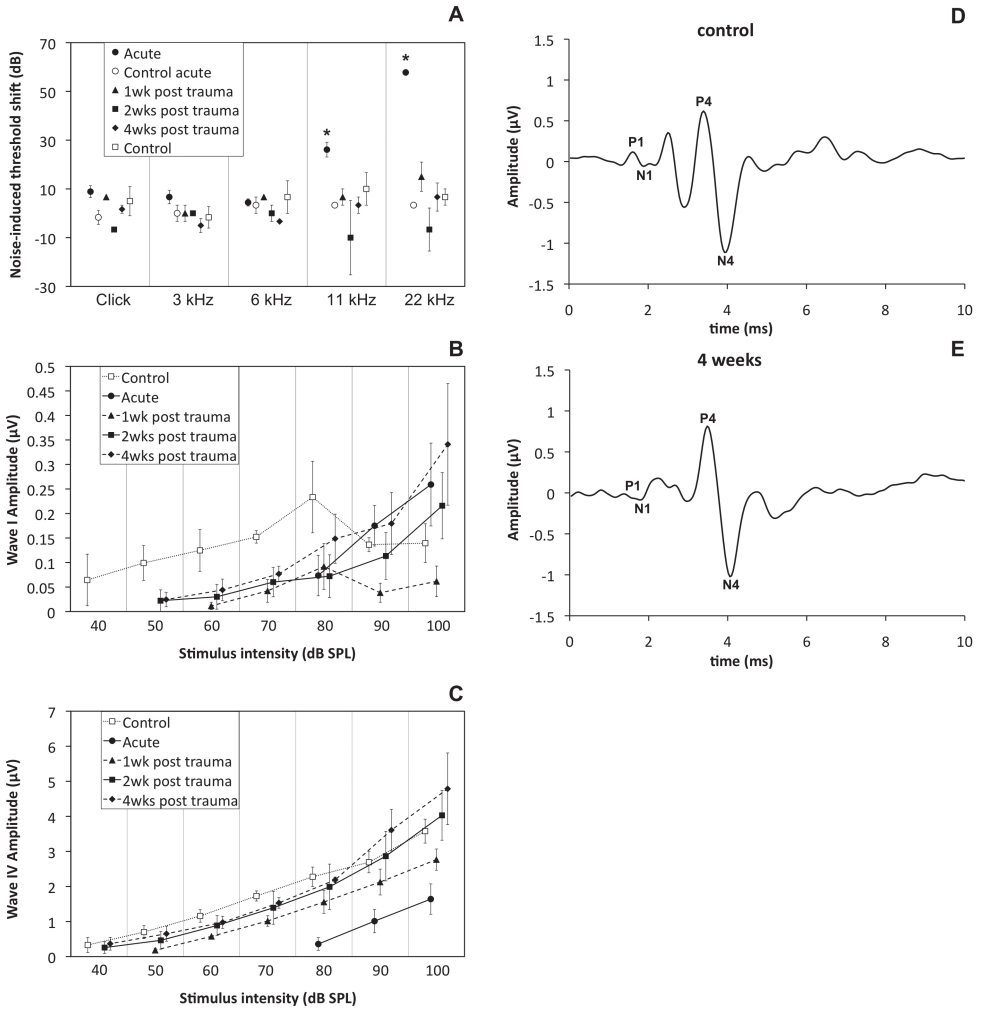

Figure 2.2 ABR recordings. **A)** ABR threshold shifts. Tone-induced ABR threshold shifts ± SEM measured immediately after sound exposure (closed circles) are significantly increased compared to ABR threshold shifts following sham exposure (open circles) at 11 kHz and at 22 kHz (see *; RM-ANOVA, $F=10.629$, $p<0.001$, one-sample t-test with Bonferroni correction for multiple testing). Sound-induced threshold shifts one week (closed triangles), two weeks (closed squares), and four weeks (closed diamonds) after exposure did not differ from two weeks after sham exposure (open squares). **B)** Wave I amplitudes. Average amplitudes ± SEM (in μV) of the ABR wave I of the tone-exposed groups (closed markers) up to 80 dB stimulus level are significantly different from the control group (open squares; RM-ANOVA, $F=5.910$, $p<0.01$). Groups did not differ at levels >80 dB (RM-ANOVA, ns). **C)** Wave IV amplitudes. The average amplitude ± SEM (in μV) of ABR wave IV of the group measured immediately following sound exposure (closed circles) is significantly different from the control group (open squares; RM-ANOVA, $F=5.338$, $p<0.05$). Examples of an ABR trace in response to a 22-kHz tone of 70 dB from a sham-exposed guinea pig **(D)** and a guinea pig measured four weeks post exposure **(E).** These examples demonstrate the permanently reduced wave I amplitude (P1-N1) and recovered wave IV amplitude (P4-N4) four weeks after sound exposure.

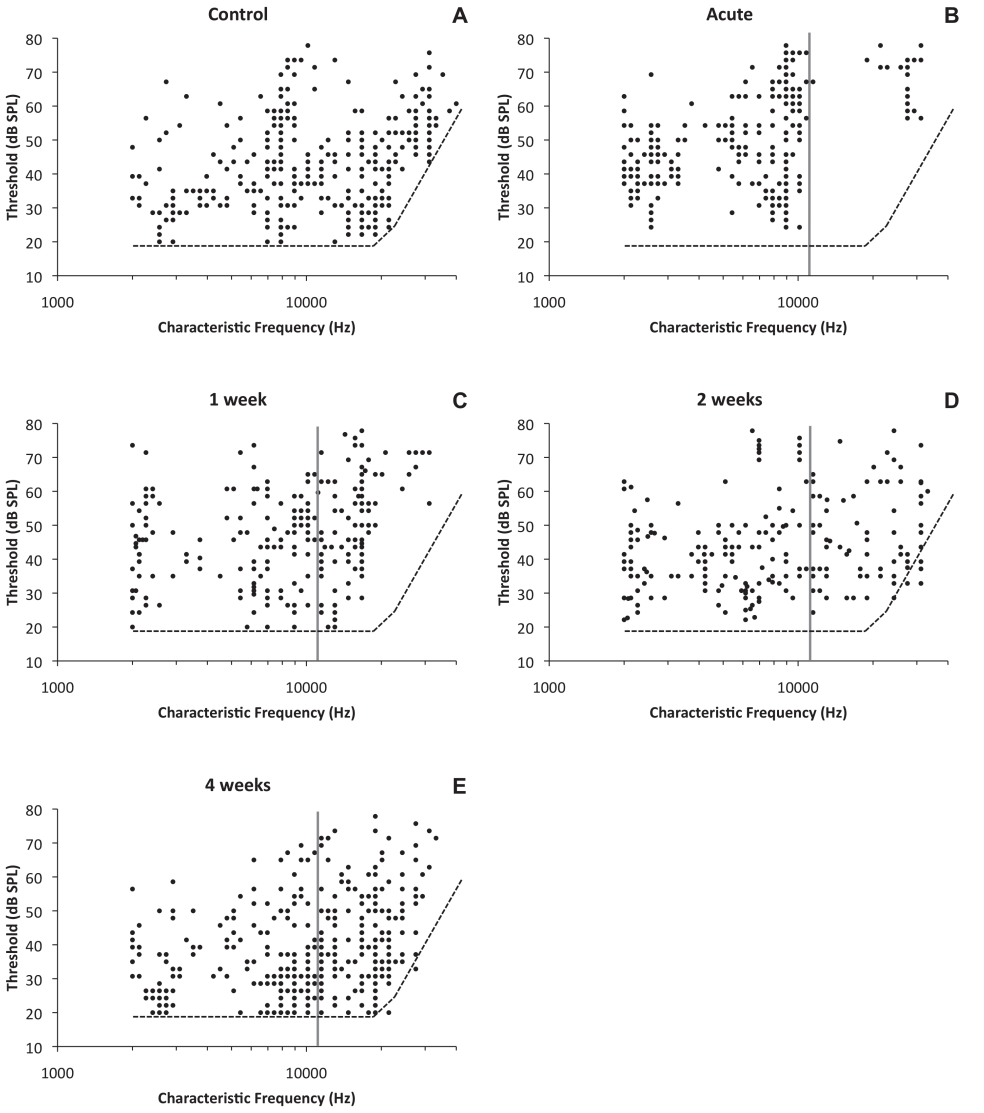

Figure 2.3 IC multi-units CFs and thresholds. The CF and threshold of all IC multi-units that were included in the study for the control group **(A)**, and the group measured immediately **(B)**, one week **(C)**, two weeks **(D)**, and four weeks **(E)** following sound exposure. The vertical gray line depicts the frequency of the exposure (11 kHz). The dashed line indicates the lowest thresholds measured in the sham-exposed group.

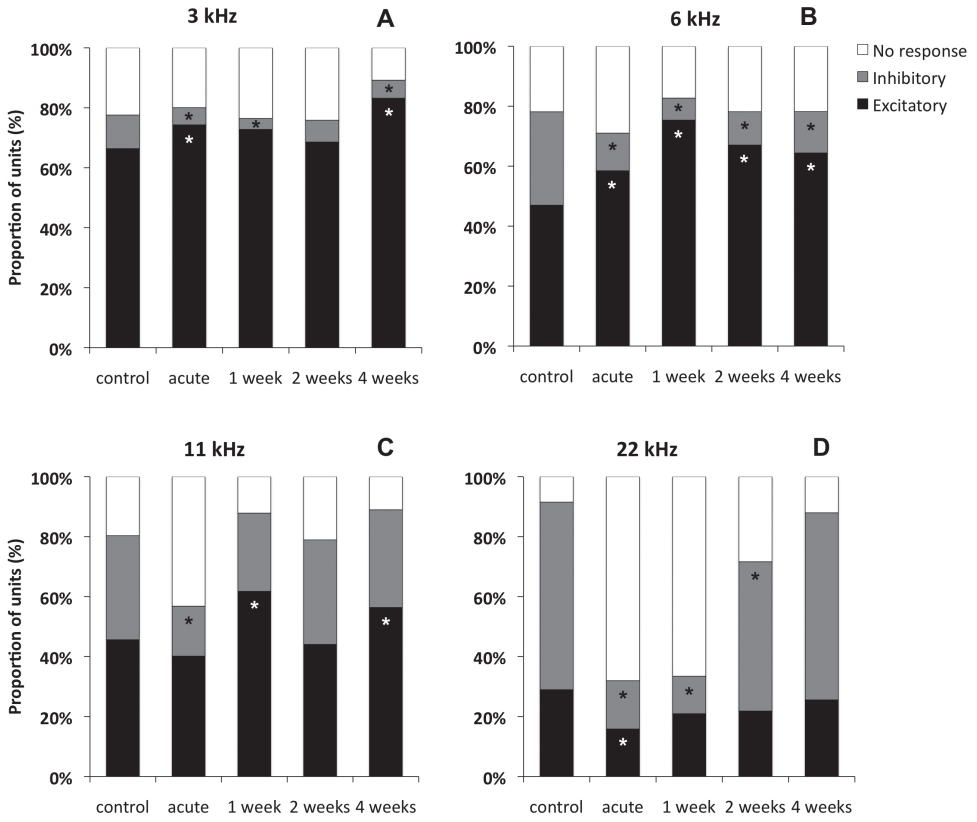

Figure 2.4 Proportions of stimulus-driven response types. The distribution of units between 'no responses' (white bars), 'inhibitory responses' (gray bars), and 'excitatory responses' (black bars) is shown for the five groups when stimulated with pure tones of 3 kHz **(A)**, 6 kHz **(B)**, 11 kHz **(C)**, and 22 kHz **(D)**. A '*' indicates a significant difference compared to the control condition, as determined by a two-tailed bootstrap method, corrected for multiple testing. See Figure 2.1 for examples of a PSTH and its raw data traces of an inhibitory response (Figure 2.1B and 2.1D, respectively) and of an excitatory response (Figure 2.1C and 2.1E, respectively).

3 kHz, 6 kHz, 11 kHz, and 22 kHz (panel A – D, respectively) for all experimental groups. The proportion of inhibitory responses to all frequencies decreased significantly immediately following overexposure (two-tailed bootstrap method; control vs. acute group for all tested frequencies, $p<0.05$). Furthermore, the proportion of excitatory responses significantly increased for stimulation with 3 kHz and 6 kHz, but decreased for 22 kHz. One week after overexposure, the proportion of inhibitory responses was still significantly reduced when stimulated with 3 kHz, 6 kHz, and 22 kHz. Also, the proportion of excitatory responses was increased when stimulated at the exposure frequency and one octave below the exposure frequency. Two weeks post trauma, the proportion of inhibitory responses to 6 kHz and 22 kHz was still slightly, but significantly, decreased, whereas the proportion of excitatory responses to 6 kHz was increased. Four weeks after overexposure, proportions of responses to 22 kHz were

recovered. In addition, when stimulated with 3-kHz and 6-kHz pure tones, the proportion of excitatory responses was increased and the proportion of inhibitory responses was decreased. Pure tones of 11 kHz elicited more excitatory responses compared to the control group.

3.4 Amplitude of stimulus-evoked IC responses

Immediately after overexposure, amplitudes of inhibitory responses to 11-kHz and 22-kHz tones, as measured by suppression of firing rate, were decreased as compared to the control group (Figure 2.5C and 2.5D, respectively; One-way ANOVA $F=18.752$, $p<0.001$; One-way ANOVA $F=30.860$, $p<0.001$, respectively). Similarly, the amplitudes of excitatory responses to 11 kHz and 22 kHz tones were also decreased immediately after overexposure (One-way ANOVA $F=14.818$, $p<0.001$; One-way ANOVA $F=23.717$, $p<0.001$, respectively). One week after overexposure, amplitudes of inhibitory responses to both 11 kHz and 22 kHz remained decreased. Moreover, amplitudes of excitatory responses to 22 kHz also remained decreased. Two weeks after overexposure, amplitudes of inhibitory responses to 22 kHz were still significantly decreased. Furthermore, amplitudes of excitatory responses to 3 kHz tones were significantly increased compared to the control group (Figure 2.5A; One-way ANOVA, $F=14.237$, $p<0.001$). Four weeks following overexposure, all responses were recovered, except that amplitudes of inhibitory responses to 3-kHz tones were significantly increased compared to the control group (One-way ANOVA, $F=4.976$, $p<0.001$). Throughout all time points measured, the amplitude of both inhibitory and excitatory responses to a 6-kHz tone did not significantly differ from the control group (Figure 2.5B; One-way ANOVA, ns).

3.5 Spontaneous activity

There were no effects of sound exposure on spontaneous firing rates of IC units at any time point (Figure 2.6A; One-way ANOVA, ns). Moreover, when only units with a CF above 11 kHz were taken into account, there were also no differences between any tone-exposed group and the control group (Figure 2.6B; One-way ANOVA, ns).

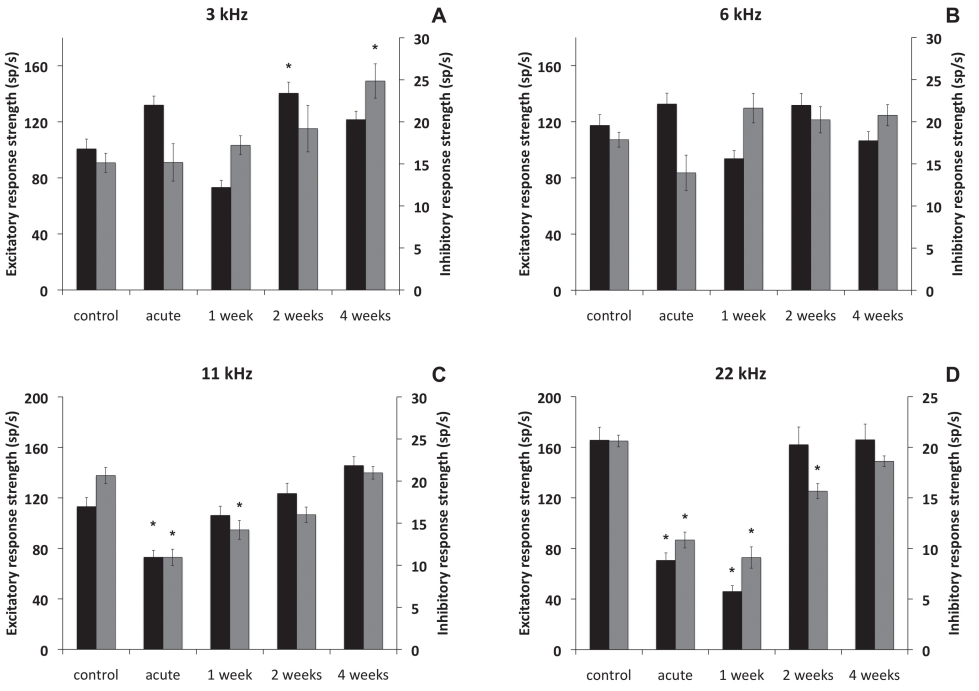

Figure 2.5 Amplitudes of stimulus-driven activity. Amplitudes (in sp/s ± SEM) of responses to pure tones of 3 kHz **(A)**, 6 kHz **(B)**, 11 kHz **(C)**, and 22 kHz **(D)**. The left vertical axis depicts mean amplitude of excitatory response in spikes/sec (black bars), the right vertical axis depicts mean amplitude of inhibitory response in spikes/sec (gray bars). Note that the amplitude of excitatory responses is an enhancement in firing rate, whereas the amplitude of inhibitory responses is a suppression of firing rate. A '*' indicates a significant difference between that experimental group and the control group, as determined by a One-way ANOVA ($p<0.001$).

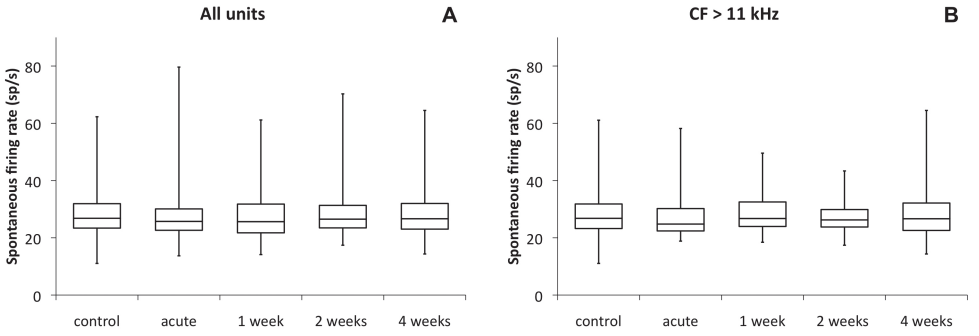

Figure 2.6 A box-plot of spontaneous multi-unit activity. The horizontal line in the box represents the median, the upper and lower borders of the box represent the 25%- and 75%-quartiles, and the error bars represent the maximum and minimum values of the data. **A)** Average spontaneous multi-unit activity (in sp/s) of all units per experimental group (One-way ANOVA; ns). **B)** Spontaneous multi-unit activity of units with a CF higher than 11 kHz (One-way ANOVA; ns).

4. Discussion

This study showed that a sound-induced temporary threshold shift was associated with a chronic reduction of ABR wave I amplitude, a temporary reduction of ABR wave IV amplitude, and a temporary reduction of tone-evoked inhibition in the IC. Although ABR thresholds recovered within one week, central auditory parameters required two to four weeks for full recovery or did not recover at all within four weeks.

Typically, the exposure used in this study has been described to cause a permanent elevation of hearing thresholds (e.g. Mulders and Robertson, 2009). Yet, in our study, thresholds were only briefly elevated. The rapid recovery of the thresholds, however, might be associated with the fact that the exposure was free field and bilateral. In contrast, the studies that report a permanent threshold shift up to twelve weeks after a similar exposure applied unilateral exposure, which resulted in a permanent threshold shift up to twelve weeks after exposure (Mulders and Robertson, 2011). Hypothetically, the free-field (bilateral) trauma stimulus activated the efferent auditory system (Buño, 1978; Liberman, 1989), which may protect against sound exposure (Zheng et al., 1997; Maison and Liberman, 2000).

Despite the rapidly recovered hearing thresholds, the central responses showed clear abnormalities, some of which were temporary and others permanent. The ABR responses suggest that different mechanisms were in place at high (> 80 dB) versus low to moderate (≤ 80 dB) stimuli. Remarkably, the control group showed a reduction in wave I amplitude to high levels (> 80 dB) when compared to levels ≤ 80 dB, which was not present in the traumatized animals. Purely speculatively, this could indicate a non-linear protective mechanism, possibly mediated by the efferent system (Zheng et al., 1997; Maison and Liberman, 2000). That mechanism could suppress the output of the cochlea to the auditory nerve, resulting in a reduced ABR wave I amplitude at high-level stimuli. The absence of this effect in traumatized guinea pigs suggests that the proposed protective mechanism may be damaged by sound exposure. Furthermore, an effect of time can be observed at high levels, in which the time after sound exposure is positively correlated with wave amplitude, suggesting damage that progresses in the weeks following the trauma (see Figure 2.2B).

For the lower levels (≤ 80 dB), the amplitude of wave I is reduced at all measured time points following sound exposure, in spite of recovered hearing thresholds. On the other hand, wave IV amplitude had recovered when the thresholds were recovered. This indicates that a central mechanism increased the neural gain between the cochlear nerve (wave I) and the auditory midbrain (wave IV), similar to what happens in tinnitus patients with normal thresholds (Schaette and McAlpine, 2011).

The multi-channel recordings in the IC showed a decrease in inhibition, both in strength and in proportion, immediately following overexposure. This was observed in response to all tested frequencies, even in response to tones outside the range of the temporary threshold shift. Inhibition gradually recovered over the four-week period following sound exposure. Our findings confirm studies that show disrupted inhibition in the IC at a molecular level following noise exposure (Szczepaniak and Møller, 1995; Dong et al., 2010a, 2010b).

As mentioned previously, the chronic reduction of wave I amplitude suggests degeneration of high-threshold cochlear-nerve fibers (Furman et al., 2013). ABR thresholds are obviously mediated by low-threshold fibers; hence the recovered thresholds suggest that any damage to the low-threshold fibers recovered after a week. Therefore, disrupted inhibition in the IC might have been a result of damage to high-threshold fibers. It can be speculated that high-threshold fibers (indirectly) innervate inhibitory projections in the IC, as these are triggered by high level stimuli (Ehret and Romand, 1997). This would explain why inhibition was abnormal when thresholds were already recovered, and demonstrates the presence of a 'hidden' hearing loss. This hearing loss is hidden in the sense that it is not revealed by a hearing threshold measure.

Conversely, tone-evoked excitatory responses increased in number and strength as a result of the sound exposure, especially in response to low-frequency tones. This finding is confirmed by other electrophysiological studies (Salvi et al., 1990; Sun et al., 2012) and in an fMRI study of tinnitus patients (Langers et al., 2012). Taken together, our results indicate an imbalance between inhibition and excitation in the IC, seen more prominently in the proportions than in response strengths.

We showed that free field exposure did not change spontaneous firing rates in the IC. Previous studies report mixed effects of noise trauma on spontaneous activity. It has been reported to decrease (Salvi et al., 1978; Niu et al., 2013), be unchanged (Wang et al., 1996), or to increase (Ma et al., 2006; Dong et al., 2010b) following sound exposure. It has been shown that, specifically, units tuned to frequencies at and above the trauma frequency can develop increased spontaneous firing rates (Mulders and Robertson, 2009). Selectively comparing high-frequency units of exposed animals with the control group, however, also did not reveal any significant differences. The absence of increased spontaneous firing rates, even though inhibition was reduced, is further supported by Dong and colleagues, who demonstrated a decreased expression of the α-subunit of GABA receptors two weeks after a temporary noise-induced threshold shift (Dong et al., 2010a). This subunit is specific for GABA-A receptors, which are ionotropic receptors mainly involved in stimulus-driven inhibition, but not in spontaneous activity.

In summary, our main findings point to an increased gain in the central auditory system, which followed a different time course compared to the tone-induced threshold shift. The increased central gain was reflected in recovered ABR wave IV amplitudes, while wave I amplitudes were chronically reduced. Furthermore, a substantial proportion of inhibition in the IC was temporary reduced, whereas excitation to low frequencies was slightly increased. Even though increased central gain was evident in stimulus-evoked activity, spontaneous activity was not affected.

We propose that temporary threshold shifts, induced by sound exposure, are associated with changes in the central auditory system that are involved in hyperacusis. A recent review by Knipper and colleagues (2013) hypothesizes that "an over-adaptive compensating central gain that spreads from the brainstem toward ascending pathways may

be associated with hyperacusis, but not with tinnitus" (Knipper et al., 2013). In addition, modeling of compensatory mechanisms of the central auditory system revealed that central gain corresponds to hyperacusis, whereas central noise, i.e. spontaneous activity, corresponds to tinnitus (Zeng, 2013). This model is supported by previous studies using animal models, which show that mechanisms of tinnitus are manifest in altered and/or elevated spontaneous activity (Eggermont and Roberts, 2004), whereas hyperacusis has been suggested to be correlated with a disruption of stimulus-driven activity (Eggermont, 2013). Furthermore, noise-induced synaptic ribbon loss in mice, in the absence of a permanent threshold shift, is associated with behavioral measures of hyperacusis, but not with behavioral measures of tinnitus (Hickox and Liberman, 2014). In humans, hyperactivity of the IC has also been linked to hyperacusis, in the absence of a threshold shift (Gu et al., 2010). The increased amplitudes of wave I and wave IV at high levels after sound exposure point to an increased stimulus-evoked activity in the brainstem, which is also indicative of hyperacusis.

This study reports on the consequences of acoustic overexposure on central auditory processing. We showed that a temporary threshold shift, due to free field overexposure, was associated with long-term central plasticity, expressed in disrupted stimulus-driven inhibition and enhanced excitation to low frequencies. We propose that these findings point to an underlying mechanism for hyperacusis.

Acknowledgements

The authors want to thank Hans Segenhout for technical support and Russ Snyder for showing us the surgical procedures involved in the IC recordings. We thank Geoffrey Manley for providing valuable suggestions for the English language in the manuscript.

This work was supported by the Heinsius Houbolt Foundation and the Stichting Gehoorgestoorde Kind. The study is part of the research program of our department: Healthy Aging and Communication.

Chapter 3

Effects of acoustic trauma on envelope coding in the inferior colliculus of the guinea pig

A.N. Heeringa and P. van Dijk

Submitted as an Express Letter to Journal of the Acoustical Society of America.

Abstract

The temporal fluctuations of a sound, as reflected by its envelope, are encoded in central auditory neurons to represent complex sounds, such as speech. Sensorineural hearing loss affects envelope coding at the level of the auditory nerve. The current study investigated the effects of acoustic trauma on envelope coding in the inferior colliculus. We found that envelope coding was enhanced immediately after acoustic trauma in neurons with a characteristic frequency below the trauma frequency, specifically in response to amplitude modulations ≤ 256 Hz. The observed changes in the auditory midbrain may relate to the problems that hearing-impaired people encounter while listening in noisy environments.

Keywords: envelope coding; inferior colliculus; acoustic trauma; guinea pig; amplitude modulation

Abbreviations: AM, amplitude modulated; AN, auditory nerve; CF, characteristic frequency; IC, inferior colliculus; MTF, modulation transfer function; PSTH, post-stimulus time histogram; SI, synchronization index; SPL, sound pressure level

1. Introduction

Natural sounds carry an important part of their information in the slow fluctuations of their amplitude. These envelope fluctuations support the perceptual separation of different sound sources (Grimault et al., 2002). Furthermore, a degraded speech signal, with only the envelope preserved, remains intelligible, demonstrating the importance of the envelope in speech understanding (Shannon et al., 1995). Thus, the envelope is involved in processing speech and separating it from other, less relevant, sound sources.

Hearing-impaired listeners often encounter problems with speech perception in noisy environments, in particular when one attempts to understand one target talker out of a number of competing talkers (Bronkhorst and Plomp, 1992). Remarkably, it has been shown that patients with sensorineural hearing loss have normal to better-than-normal envelope detection thresholds (Moore and Glasberg, 2001; Füllgrabe et al., 2003). Furthermore, in laboratory animals, noise-induced hearing loss results in enhanced envelope coding by the auditory nerve (AN). Especially AN fibers with high thresholds and steep rate-level functions have an enhanced response to amplitude-modulated (AM) sounds (Kale and Heinz, 2010). Coding of envelope information is also enhanced in the auditory-evoked potentials of chinchillas with noise-induced hearing loss (Zhong et al., 2014). These results suggest that hearing-impaired listeners might benefit from enhanced envelope coding, e.g. in understanding speech. However, the enhanced coding also applies to the background noise. Consequently, enhanced envelope coding may not help to improve the signal-to-noise ratio in a speech-in-noise communication (Kale and Heinz, 2010).

The current study aimed at identifying the effects of sound exposure on envelope coding at the level of the auditory midbrain. Spike trains of responses to AM noise were recorded in the inferior colliculus (IC) of the anesthetized guinea pig, before and immediately after bilateral exposure to a 124 dB SPL pure tone. Because the envelope coding is enhanced in the periphery, we hypothesized to see that reflected in the responses of more central neurons. This study provides results about the alterations in central processing caused by acoustic trauma and might give additional insight into the mechanisms involved in the problems encountered by hearing-impaired people during listening in a fluctuating background noise.

2. Methods

2.1 Animals

Six normal-hearing male albino guinea pigs (Dunkin Hartley; Harlan Laboratories, Horst, the Netherlands) were used for this study. Animals were anesthetized with a mixture of 70 mg/kg ketamine (10% Ketamine, Alfasan, Woerden-Holland) and 6 mg/kg xylazine (2% Rompun, Bayer-Healthcare; i.m.). Half the original dose was administered every hour to maintain a deep level of anesthesia. Body temperature was kept constant at 38 °C by a homeothermic heating pad (Harvard Apparatus), and heart rate and blood oxygen saturation were closely

monitored. A tracheotomy allowed for artificial respiration. The head of the animal was fixated by a skull screw. The right IC was surgically approached by a craniotomy and a subsequent careful ablation of the overlying cortical tissue. A linear 16-channel microelectrode array (A1x16-10mm-100-413-A16; NeuroNexus) was inserted in a dorsal-lateral to ventral-medial direction into the visualized IC. Online inspection of neural activity during the presentation of 100-ms noise bursts allowed for the optimal placement of the electrode in the IC. Neural spike trains were recorded before and immediately after a one-hour bilateral acoustic trauma. The acoustic trauma was an 11-kHz pure tone of 124 dB SPL, presented by two free-field Piezo tweeters (PH8; Velleman) that were positioned approximately 5 cm from each ear, respectively. The electrode remained inserted in the IC during exposure. The experiment was conducted in an anechoic sound-attenuating booth. The study was approved by the Animal Experiment Committee of the University of Groningen (DEC # 6068D) and was in compliance with Dutch and European law and regulations.

2.2 Acoustic stimuli

Acoustic stimuli were designed by custom-made MatLab programs (R2010b, Mathworks), generated using TDT hardware (RP2.1, PA5, and ED1), and presented by a free-field electrostatic speaker (ES1; TDT Inc.) positioned at ± 5 cm from the left ear, contralateral to the exposed IC. Pure tones (duration 300 ms, 10-ms cosine ramp) were presented to obtain receptive fields. The frequency of the pure tones ranged between 2 and 40 kHz (25 frequencies, logarithmically spaced steps) and the intensity ranged between 20 and 80 dB SPL (15 intensities, linearly spaced steps); each frequency-level combination was presented once. In order to study envelope coding, AM broadband noise was presented (duration 400 ms, 10-ms cosine gate, 300 repetitions, 70 dB SPL). The carrier noise had a spectrum that was flat within 1 dB between 2 and 40 kHz (butterworth filter) and was an unfrozen noise, i.e. for every repetition the carrier noise was newly regenerated. The amplitude of the carrier noise was modulated by multiplying the signal with

$$E(t) = 1 - \left(m\cos\left(2\pi f t\right)\right), \quad \{1\}$$

where m is the modulation depth, fixed at 50% ($m = 0.5$), and f is the modulation frequency, with a value between 8 and 1024 Hz in logarithmically spaced steps. All stimuli, including the trauma stimulus, were calibrated with a B&K microphone and amplifier (type 2670 and type 2610, respectively) positioned at the entrance of the ear canal.

2.3 Data analysis

The neural signal was amplified (RA16PA; Tucker Davis Technologies [TDT] Inc.), recorded (RX5; TDT Inc.), and stored on a PC using custom-made MatLab programs (digitized with

a sampling rate of 24,414 Hz). Next, signals were filtered (300-3000 Hz) and spikes were defined by the instants when the signal exceeded the threshold of 2.6 times the root-mean-square level of the signal. Responses to pure tones revealed the unit's receptive field, which was defined by the range of pure tones that elicited a significant increase in firing rate. The receptive field was contoured by the tuning curve; the lowest tip of the tuning curve defined a unit's characteristic frequency (CF) and corresponding threshold. Post-stimulus time histograms (PSTHs) were plotted from the neural responses to the AM stimuli. The tendency of a spike train to phase lock to the amplitude modulation of the stimulus was expressed by the synchronization index (SI), which was calculated by

$$SI = \frac{1}{N}\left|\sum_{j=1}^{N} e^{i\varphi(j)}\right|, \qquad \{2\}$$

where N is the number of spikes, i refers to $\sqrt{(-1)}$, and $\phi(j)$ is the phase of the j-th spike relative to the sinusoidal amplitude modulation ($E(t)$) of the acoustic stimulus (Eq. 1). Only the spikes that occurred during the presentation of the noise stimulus were taken into account. To eliminate the effect of response latency and the on-response, spikes occurring during an additional 25 ms relative to the start of the stimulus were not taken into account either. The modulation depth of the PSTH in percentage was calculated by multiplying the synchronization index with 200 (Rees and Palmer, 1989). The modulation response gain (G; in dB) was computed by

$$G = 20 \times \log_{10}\left(\frac{\%\ \text{modulation depth of PSTH}}{\%\ \text{modulation depth of stimulus}}\right), \qquad \{3\}$$

and represents the degree of neural synchrony relative to the modulation of the stimulus. A modulation response gain of 0 dB indicates that the neural modulation coding in the PSTH follows the modulation of the stimulus. If the response gain is higher than 0 dB, the auditory system has amplified the modulation. A modulation transfer function (MTF) is obtained by plotting the response gain (G in Eq. 3) against the modulation frequency of the stimulus (f in Eq. 1). The maximum response gain of the MTF was considered as a measure for envelope coding. All analyses were executed using custom-made MatLab software.

Paired-sample T-tests and Student's T-tests were used for statistical analyses, as appropriate (IBM SPSS Statistics; Version 22). P-values were Bonferroni corrected for multiple testing.

3. Results

Before acoustic trauma, IC multi units (n = 69) had a CF between 2.0 kHz and 35.3 kHz, with a corresponding threshold that ranged from 20 dB SPL to 74 dB SPL (Figure 3.1A). After a 1-h exposure to an 11-kHz pure tone of 124 dB SPL, CFs ranged from 2.0 kHz to 10.1 kHz (Figure 3.1B). The electrode remained in the IC during acoustic trauma, implying that the neural signal recorded from the units without a receptive field after exposure (n = 30, markers with arrows at the top of the panel in Figure 3.1B) derived from auditory units of the IC as well. Therefore, these units remained included in further AM analyses. Multi units that remained sensitive to pure tones after trauma (n = 39) had an average threshold shift of 14 dB (± 3.1 standard-error of the mean).

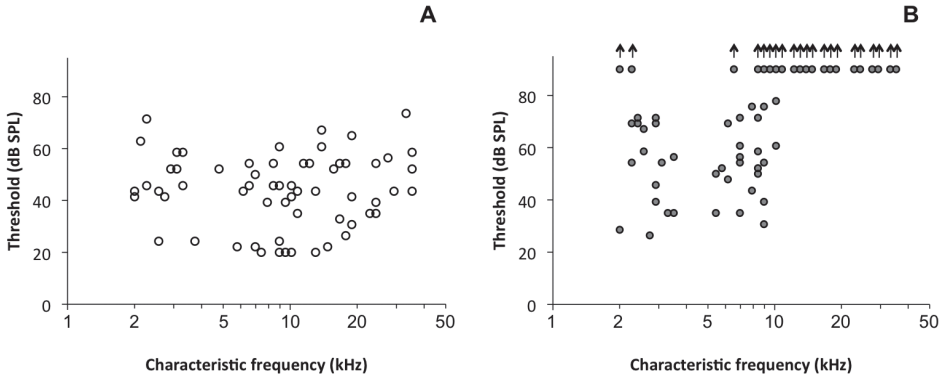

Figure 3.1 Characteristic frequency and thresholds of IC multi units. **A)** The CF and corresponding threshold of the IC units before acoustic trauma. **B)** The CF and corresponding threshold of the IC units immediately after acoustic trauma. Markers with upward arrows represent units that were included in the analyses, but did not have distinguishable receptive fields immediately after acoustic trauma. The location of these markers on the x-axis indicate the CF of these units before trauma.

Figure 3.2A shows a representative example of the MTF of an IC multi unit with a CF below the trauma frequency (CF = 4.8 kHz). Before exposure, this IC unit had a best modulation frequency of 256 Hz, at which the response gain was 1.68 dB (open markers). After exposure (filled markers), the highest response gain in the MTF increased to 6.36 dB in response to a 128 Hz amplitude modulation. In general, this unit showed an increased response gain for low modulation frequencies (f = 8 – 256 Hz) and a decreased response gain for high modulation frequencies (f = 512 – 1024 Hz). For a high-CF unit, that had a CF before acoustic trauma of 16.7 kHz, a similar clockwise 'tilting' of the shape occurred following acoustic trauma (Figure 3.2B). Response gain increased for the lower modulation frequencies (8 – 64 Hz, except for f = 32 Hz in which response gain was unchanged) and decreased for the higher modulation frequencies (f = 128 – 1024 Hz). Before acoustic trauma, the IC unit responded best to a

modulation frequency of 256 Hz with a response gain of 2.91 dB. After exposure, 256 Hz was still the best modulation frequency, but the unit coded less well for it, with a response gain of -2.41 dB.

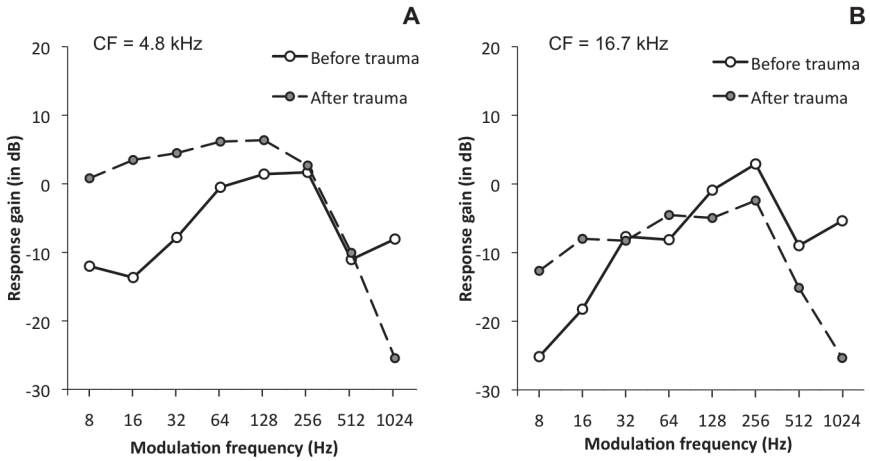

Figure 3.2 Modulation transfer functions. **A)** A representative example of the MTF of a low-CF unit (CF = 4.8 kHz). **B)** A representative example of the MTF of a high-CF unit (CF = 16.7 kHz). Open markers represent the MTF before exposure, filled markers represent the MTF immediately after exposure.

Figure 3.3A shows the average difference (± 95% confidence interval) between the response gain before and after acoustic trauma per modulation frequency. A positive difference indicates an increase in response gain following trauma. In low-CF units (CF < 11 kHz; closed markers), response gains to low modulation frequencies (f = 8 – 128 Hz) increased following exposure (difference > 0 dB), whereas response gains to modulation frequencies between 256 and 1024 Hz typically decreased (Figure 3.3A). High-CF units (CF > 11 kHz *before* exposure; open markers) showed a similar pattern, but with a general downward shift. For these units, the response gain remained unchanged (f = 16 Hz) or decreased (f = 8, 32 – 1024 Hz) following acoustic trauma. This decrease was larger for the high modulation frequencies.

The maximum response gain of the MTF was taken as a measure for envelope coding. For low-CF units (CF < 11 kHz), envelope coding was significantly increased following acoustic trauma (paired-sample T-test $T(43) = -9.300$, $p < 0.001$). For high-CF units (CF > 11 kHz), envelope coding was significantly decreased (Figure 3.3B; paired-sample T-test: $T(24) = 4.224$, $p < 0.001$). Envelope coding of units before exposure were more or less similar across the tonotopic map of the IC (Figure 3.3C) and did not significantly differ between low- and high-CF units (Figure 3.3B; Student's T-test: $T(67) = -2.000$, $p = 0.050$).

Acoustic trauma resulted in a significant difference in envelope coding between low- and high-CF units, in which low-CF units had higher maximum response gains (better envelope coding) than high-CF units (Figure 3.3D; Student's T-test: $T(29.710) = 7.976$, $p < 0.001$, degrees of freedom corrected for unequal variances).

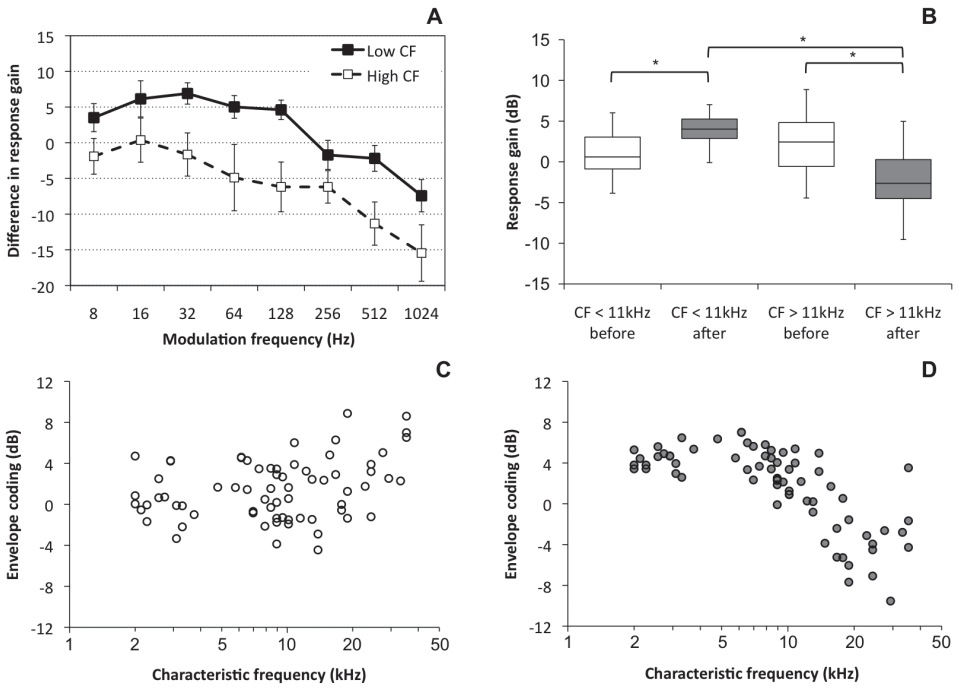

Figure 3.3 Envelope coding. **A)** The mean difference in response gain (± 95% confidence interval) induced by acoustic trauma. A positive difference in response gain (> 0 dB) indicates that the response gain increased as a result of acoustic trauma. Closed markers represent the IC units with a low CF (< 11 kHz), open markers represent IC units with a high CF (> 11 kHz). **B)** Box plots representing the minimum, 25% quartile, median, 75% quartile, and maximum of the response gains of IC units before (open boxplots) and after (filled boxplots) acoustic trauma. A distinction was made between units with a low CF (< 11 kHz) and units with a high CF (> 11 kHz). * represents a significant difference ($p < 0.05$ Bonferroni corrected). **C)** Envelope coding before acoustic trauma plotted as a function of the CF. **D)** Envelope coding measured immediately after acoustic trauma, plotted as a function of the CF that was determined before trauma.

4. Discussion

With the current study, we showed that immediate acoustic trauma resulted in enhanced envelope coding in multi units of the IC with a CF below the trauma frequency (< 11 kHz). In particular, response gains for the low modulation frequencies were enhanced.

Following acoustic trauma, there were no units with a CF of 11 kHz or higher, indicating that afferent input carrying high frequency information was impaired. Obviously, this input innervates mainly the high-CF units. Thus, the high-CF units were deprived from their main input, which presumably explains why these units showed reduced envelope coding after exposure (Figure 3.3B). At first sight, these findings appear inconsistent with the results of Kale and Heinz (2010), who showed in the AN that noise-induced threshold shifts are positively correlated with response gain. However, the authors corrected for threshold shifts by presenting the AM stimuli at the fiber's best-modulation level, which was approximately 20 dB louder for the AN fibers of hearing-impaired animals compared to control animals (Kale and Heinz, 2010; Fig. 7). In the current study, all AM stimuli were presented at the same level, both before and after sound exposure. Thus, our results demonstrated that enhanced envelope coding in the auditory midbrain was apparent even when threshold shifts were not corrected for.

To date, the neurophysiological mechanisms that are responsible for enhanced envelope coding observed after noise-induced hearing loss are not entirely known. Previous studies showed that enhanced envelope coding in chinchillas is present between 27 and 40 days after exposure (Kale and Heinz, 2010; Zhong et al., 2014). The current study showed that this effect was already apparent immediately following overexposure in the IC. This suggests that mechanisms involved in enhanced envelope coding were unmasked immediately after acoustic trauma and are likely to persist over time. In contrast to the results reported here, it has been shown that age-related hearing loss impairs auditory temporal-processing abilities in the IC (Walton et al., 1998). Thus, the effect of hearing loss on envelope coding differs between age-related and noise-induced hearing loss.

Enhanced envelope coding induced by acoustic trauma can be explained by a steepening of the rate-level function due to noise exposure (Kale and Heinz, 2010; Niu et al., 2013). In addition, there appears to be a second mechanism acting on the specific modulation frequencies after exposure. This mechanism seems to filter envelope coding at about -2 to -3 dB/oct and is effective for both low- and high-CF fibers (Figure 3.3A). This low-pass filter possibly suggests a reduced timing accuracy of auditory neurons, which would affect the response gain at high modulation frequencies more than at low modulation frequencies. Thus, the fact that modulation frequencies were not affected equally by the acoustic trauma resulted in an abnormal balance in the envelope information coded by the IC. Potentially, this mechanism may contribute to the difficulties hearing-impaired people encounter with auditory stream segregation.

In conclusion, the current study showed that envelope coding was enhanced in low-CF units of the IC immediately after acoustic trauma. Specifically, modulation gains in

response to low modulation frequencies ($f \leq 128$ Hz) were enhanced. Our results are consistent with responses in the auditory nerve and in auditory-evoked potentials after noise-induced hearing loss (Kale and Heinz, 2010; Zhong et al., 2014), but had not been shown before in the IC. The observed changes in envelope coding after acoustic trauma might be associated with the problems that hearing-impaired people encounter with listening to competing talkers (Bronkhorst and Plomp, 1992). An unnatural amplification of a specific range of modulation frequencies might affect the complex neural processes involved in auditory stream segregation (Grimault et al., 2002). Enhanced envelope coding after acoustic trauma may also be involved in the normal to better-than-normal envelope detection thresholds observed in patients with sensorineural hearing loss (Moore and Glasberg, 2001; Füllgrabe et al., 2003).

Acknowledgements

The authors want to thank Christian Lorenzi for his valuable discussions on the subject, Russ Snyder for showing us the surgical procedures involved in the IC recordings, and Annemieke Smit-van Oosten, Michel Weij, and Andre Zandvoort for technical support during the experiments.

This work was supported by the Heinsius Houbolt Foundation and the Stichting Gehoorgestoorde Kind. The study is part of the research program of our department: Healthy Aging and Communication.

Chapter 4

Wiener-kernel analysis of neural responses in the inferior colliculus of the guinea pig

A.N. Heeringa and P. van Dijk

Abstract

Wiener-kernel analysis is a technique to describe a nonlinear system in terms of a number of kernels. These kernels are obtained by cross-correlating the system's response to a broadband noise with that broadband noise. In the auditory system, Wiener-kernel analyses have been applied to the auditory nerve and the cochlear nucleus. The current study investigated the applicability of Wiener-kernel analysis to the inferior colliculus (IC).

First- and second-order kernels were determined for hundred multi units, recorded from the IC of nine guinea pigs. The second-order kernel was decomposed, using singular-value decomposition, into a number of parallel subsystems, each of which is characterized by a filter function (an eigenvector) and a gain factor (an eigenvalue). Positive and negative eigenvalues correspond to excitation and inhibition, respectively. The results of the Wiener-kernel analyses were compared with excitatory- and inhibitory-characteristic frequencies (CFs) obtained from pure-tone responses.

We detected significant stimulus-related oscillations in the first-order kernel of twelve IC units (2.1 – 3.3 kHz). A significant second-order kernel was found in all units, where the best frequency (BF) of the highest-ranking excitatory eigenvector corresponded well with the excitatory CF. The BF of the inhibitory eigenvector did not correspond to the inhibitory CF, but often corresponded to the BF of the excitatory eigenvectors.

We showed that Wiener-kernel analysis is a powerful tool to reveal excitatory- and inhibitory-response characteristics of the IC. This can be used to study neural processes that critically depend on a balance between excitation and inhibition, such as directional hearing, hyperacusis, and tinnitus.

Keywords: wiener kernel; inferior colliculus; guinea pig; white noise; singular-value decomposition

Abbreviations: AN, auditory nerve; BF, best frequency; CF, characteristic frequency; CN, cochlear nucleus; FFT, fast-Fourier transform; IC, inferior colliculus; REVCOR, reverse correlation; RMS, root-mean-square; SEM, standard-error of the mean; SVD, singular-value decomposition

1. Introduction

Neural spike trains evoked by external acoustic stimuli can be studied in many ways. In essence, there are two general approaches (Rieke et al., 1999). The first and most common approach is to present the system with a fixed stimulus and record the average firing rate. This approach, which is used to obtain, for example, tuning curves and post-stimulus time histograms, is called the experimenter-centered approach. The experimenter defines the stimuli, and observes the responses that follow in a neuron. The second approach often uses a Gaussian-noise stimulus and studies the events preceding a spike to gain knowledge about the characteristics in the stimulus that caused the occurrence of that spike. This approach is called the subject-centered approach (Eggermont et al., 1983).

Wiener-kernel analysis is a subject-centered technique and is often used to study functional properties of the auditory system (Korenberg and Hunter, 1990; Eggermont, 1993). The analysis typically provides the researcher with three kernels: the zeroth-, the first-, and the second-order Wiener kernel that together describe the characteristics of the system up to the second-order nonlinearities. The zeroth-order kernel is simply the average firing rate evoked by the Gaussian-noise stimulus. The first-order kernel represents the linear correlation between the input signal (the noise stimulus) and the output signal (the spike train), and is identical to the commonly-used reverse-correlation (REVCOR) function. A significant stimulus-related oscillation in the first-order kernel (or REVCOR function) reflects the neuron's ability to phase lock to the fine structure of an acoustic stimulus (de Boer and de Jongh, 1978). The second-order kernel could be referred to as a second-order REVCOR function that captures second-order nonlinearities of the neuron being studied. It is significant for phase locking and for non-phase locking fibers (Recio-Spinoso and van Dijk, 2006), and consequently allows for the application of a subject-centered approach across stimulus frequencies (van Dijk et al., 1994; Temchin et al., 2005).

When digitally sampled, the second-order Wiener kernel is a symmetric matrix. Although the computation of the kernel is relatively straightforward, it may be hard to obtain an intuitive interpretation of the functional properties of the system being studied. An exception to this statement are kernels obtained from the primary auditory nerve. These kernels are often well described by a so-called sandwich model, consisting of a band-pass filter, a nonlinear element, and a low-pass filter (van Dijk et al., 1994). The filters represent tuning in the inner ear and low-pass filtering in the hair cell and hair-cell synapse. The nonlinearity presumably corresponds to the transduction process in the hair cell stereocilia. As was shown by van Dijk et al. (1994), the impulse responses of the filters can be computed from the second-order kernel, thus providing a straightforward interpretation of the Wiener-kernel analysis.

However, for locations higher in the auditory system, such a simple model cannot be applied, because the signal has been further (nonlinearly) processed in a mostly unknown way. Then, to disentangle the functional meaning from the second-order kernel, its eigenvectors and eigenvalues can be computed by, i.e., singular-value decomposition (SVD; Lewis et al.,

2002a; Yamada and Lewis, 1999). SVD decomposes the kernel into parallel subsystems, each of which is characterized by a filter function (the eigenvector, u) and a gain function (the eigenvalue, w; Figure 4.1). Basically, all the subsystems together are a different representation of the same kernel. The eigenvector is the impulse response of the corresponding filter and the eigenvalue is a gain that represents the degree by which the subsystem contributes to the total second-order kernel. A subsystem contributes either positively (for positive gain/eigenvalues) or negatively (for negative gain/eigenvalues) to the neuron's response, and thus corresponds to either excitation or inhibition, respectively. Accordingly, SVD of second-order Wiener kernels provides a method to disentangle the inhibitory and excitatory neural responses of an auditory unit evoked by Gaussian noise.

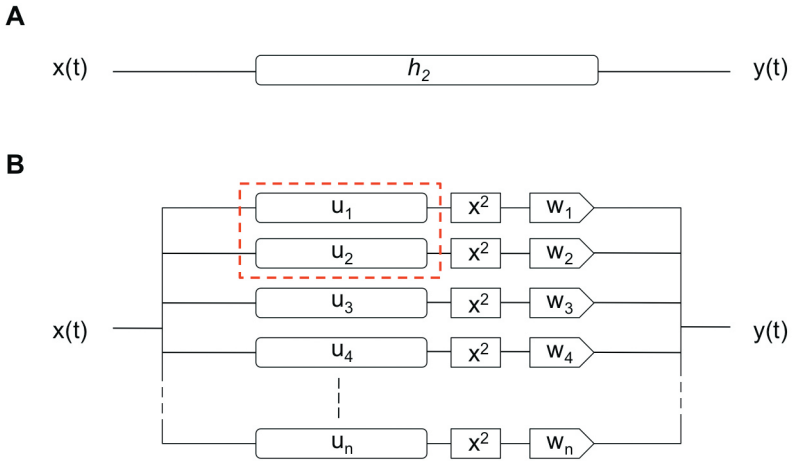

Figure 4.1 The second-order Wiener kernel. **A)** The second-order Wiener kernel (h_2) describes the second-order nonlinear response applied to the noise stimulus x(t) in order to obtain the spike signal from the IC y(t). **B)** The second-order kernel is a symmetrical square matrix, that can be decomposed into eigenvectors, each of which has an eigenvalue. Correspondingly, the kernel can be regarded as a number of parallel subsystems, which all consists of an impulse response (u; the eigenvector) and a weight factor (w; the eigenvalue). Each subsystem also squares the signal (x^2). The sign of the eigenvalues reflects excitation and inhibition for positive and negative values, respectively. Subsystems often occur in quadrature pairs, which are often ranked consecutively (dashed, red square). See also the study of Yamada and Lewis (1999).

Wiener-kernel analysis has been applied to study the response properties of the auditory nerve (AN) of a variety of species (e.g. van Dijk et al., 1994, 1997; Yamada and Lewis, 1999; Lewis et al., 2002a, 2002b; Recio-Spinoso et al., 2005; Temchin et al., 2005; Sneary and Lewis, 2007; Henry and Heinz, 2013) and to study responses of the ventral cochlear nucleus (CN) of the chinchilla and the cat (Wickesberg et al., 1984; Recio-Spinoso and van Dijk, 2006). Here, we applied Wiener-kernel analysis to study responses from the inferior colliculus (IC).

The IC receives and processes afferent input from the CN and the superior olivary complex, but also receives efferent auditory input and input from non-auditory centers (Ehret, 1997). This might be reflected in relative complex response properties of Wiener kernels of the IC, which might have been the reason why Wiener-kernel analysis has not yet been applied to recordings from the IC. The responses of the IC to external acoustic stimuli have been studied extensively with experimenter-centered and other subject-centered approaches. These studies revealed, amongst other things, that the IC has a distinct dorsal-to-ventral tonotopic organization and shows both excitatory and inhibitory responses to pure tones (Clopton and Winfield, 1973; Ehret, 1997; Heeringa and van Dijk, 2014). The Wiener kernels of the IC presumably reflect these diverse response patterns.

Our interest in applying Wiener-kernel analysis was coined by a more general interest in studying the physiological mechanisms involved in tinnitus and hyperacusis. Both these conditions are believed to be related to a disrupted balance of excitation and inhibition in the central auditory system (Eggermont and Roberts, 2014). With the possibility to decompose a kernel in excitatory and inhibitory subsystems (Yamada and Lewis, 1999; Figure 4.1), Wiener-kernel analysis potentially offers a useful tool to study disruptions of the balance between excitation and inhibition. The aim of the current study was to determine the applicability of Wiener-kernel analysis to IC multi units in the normal-hearing guinea pig. Zeroth-, first-, and second-order Wiener kernels were identified and classified, and the second-order kernel was decomposed with SVD in order to obtain an intuitive feeling for the contribution of the kernel to the response of neurons in the IC. Results were compared to an experimenter-centered approach, i.e. excitatory- and inhibitory-tuning curves from responses to pure tones.

2. Methods

2.1 Animal preparation

Nine normal-hearing adult albino guinea pigs (male; Dunkin Hartley; Harlan Laboratories, Horst, the Netherlands) were anesthetized with ketamine/xylazine (70 mg/kg 10% Ketamine, Alfasan, Woerden-Holland; 6 mg/kg 2% Rompun, Bayer-Healthcare, respectively; i.m.). Half the original dose was administered every hour to maintain a deep level of anesthesia throughout the experiment. Body temperature was kept constant at 38 °C using a heating pad, and heart rate and SpO_2 (blood oxygen saturation) were monitored with a pulsoximeter. A tracheotomy allowed for artificial respiration and a skull screw was placed to fixate the head of the animal. The right IC was approached by a craniotomy and partial aspiration of the overlying cortical tissue. A linear 16-channel microelectrode array (A1x16-10mm-100-413-A16; NeuroNexus) was inserted in the IC in the lateral-dorsal to medial-ventral direction. An uncoated silver wire, positioned through the craniotomy in rostral direction below the dura, served as ground. All experiments were approved by the Animal Experiment Committee of the University of Groningen (DEC # 6068B and 6068D) and were in compliance with Dutch and European law and regulations.

2.2 Stimulus presentation

All in vivo neurophysiological recordings were acquired in an anechoic sound-attenuating booth. The 16-channel neural signal was preamplified (RA16PA; Tucker Davis Technologies [TDT] Inc.) and recorded (RX5; TDT Inc.) in parallel at 16-bits AD resolution, with a 24,414 Hz sampling rate for each channel. Custom-made MatLab software (R2010b, Mathworks) was used to store the data on a PC. Acoustic stimuli were presented via a free-field electrostatic speaker (ES1; TDT) placed at ± 5 cm from the left ear (contralateral to the exposed IC), and were calibrated using a B&K microphone (type 2670) placed at the entrance of the ear canal and an amplifier (B&K; type 2610). The electrode was advanced into the IC, while successive noise bursts (duration 100 ms, 10 ms cosine ramp) were being presented via the speaker. Online inspection of the neural response signal during these presentations allowed for optimal placement of the electrode in the IC, in order to record from a maximum number of auditory units. Once sound-evoked responses were observed on at least six of the sixteen channels, the electrode position was fixed for the subsequent recordings.

For the acquisition of receptive fields, acoustic stimuli were generated using custom-made MatLab software and TDT hardware (RP2.1, PA5, and ED1). The sampling rate for stimulus generation was 97,656 Hz. Pure tones (10 ms cosine ramp, duration 300 ms) with a range of frequencies (2 – 40 kHz) and stimulus levels (0 – 80 dB SPL) were presented in random order.

To obtain recordings for Wiener-kernel analysis, Gaussian noise was digitally filtered to produce noise with a bandwidth from 2 to 40 kHz, and a flat spectrum at the entrance of the ear canal. The noise was recorded with a B&K microphone and varied within 1 dB over the 2-40 kHz bandwidth. Custom-made programs in C, Amadeus Lite (Version 2.0.7), an audio interface (Audiofire 4; Echo), and TDT hardware (PA5 and ED1) were used to design and present the noise. The stimulus was presented for 1 h with a constant stimulus level of 70 dB SPL, at 97,656 samples per second (*fs*). The stimulus, recorded by the B&K microphone, and the 16 neural channels, recorded by the TDT equipment, were stored on a PC hard disk for offline analysis.

2.3 Data analysis

2.3.1 Tuning curves

Neural signals were filtered (300-3000 Hz, butterworth filter) and their root-mean-square (RMS) was calculated. Spikes were defined by the instants when the signal exceeded the threshold of 3 x RMS. All recordings presented in this paper are multi-unit recordings, indicating that no spike sorting was executed and, therefore, it is not certain whether all spikes derived from the same neuron or from more than one neuron. MatLab programs were custom-made to calculate firing rates for every presented tone. This firing rate was inserted in a matrix that organized frequency versus stimulus level in an orderly manner. Units that had a distinguishable receptive field, as determined upon visual inspection of the matrix of

pure tone responses, were included in further tuning curve and Wiener-kernel analyses. To objectively determine the tuning curves, a baseline firing rate was considered, which was calculated by averaging the firing rates evoked by pure tones with the lowest stimulus level that visually did not seem to contribute to the receptive fields. An excitatory response was defined by a firing rate that was at least twice as high as the baseline firing rate. The excitatory-tuning curve was determined by connecting, per frequency, the lowest stimulus level that evoked an excitatory response. The excitatory characteristic frequency (CF) was considered the frequency at which the lowest stimulus level resulted in an excitatory response. Similarly, the inhibitory-tuning curve was constructed by determining per stimulus frequency the lowest level that elicited an inhibitory response, i.e. a firing rate that was at least twice as low as the baseline. The inhibitory CF was considered the stimulus frequency at which the lowest level resulted in an inhibitory response. See Figure 4.2A for an example of an excitatory- and an inhibitory-receptive field and tuning curve (black and white curve, respectively).

2.3.2 Wiener-kernel analysis

To calculate Wiener kernels, the spike-detection threshold was determined by visual inspection of the filtered (300-3000 Hz) neural signals. Custom-made programs in C were used to calculate the zeroth-, first-, and second-order kernels. For an extensive description of the calculation of Wiener Kernels from auditory responses to Gaussian noise, see Eggermont (1993). Briefly, the zeroth-order Wiener kernel (h_0) represents the average output of the system, i.e. the average firing rate during acoustic stimulation (N_0), and is calculated by

$$h_0 = \frac{N}{T} = N_0 \quad , \qquad \{1\}$$

in which N is the amount of spikes during the whole recording and T is the total duration of the recording in seconds. The first-order Wiener kernel (h_1) equals the cross-correlation between the input of the system, i.e. the acoustic signal, and the output of the system. For neural signals, this cross correlation is proportional to the average stimulus preceding the spikes. With the appropriate normalization constants, this average is given by (van Dijk et al., 1994):

$$h_1(\tau) = \frac{1}{AT}\sum_{i=1}^{N} x(t_i - \tau) \quad , \qquad \{2\}$$

where $x(t)$ is the acoustic stimulus signal, A is the power-spectral density of the acoustic stimulus, and t_i (with i=1,…,N) are the times at which a spike occurred. Each first-order kernel was visually inspected to check for significant stimulus-related oscillations. A fast-

Fourier transform (FFT) was performed, and the peak of this spectrum defined the best frequency (BF) of the first-order Wiener kernel. Furthermore, a group delay was determined by calculating the slope of the phase response at the BF.

To calculate the second-order Wiener kernel (h_2) the stimulus segments (length τ) preceding each spike were again taken into account. This kernel represents the second-order cross correlation, and is calculated by

$$h_2(\tau_1,\tau_2) = \frac{N_0}{2A^2}\left[R_2(\tau_1,\tau_2) - \Phi_{xx}(\tau_2 - \tau_1)\right], \quad \{3\}$$

in which Φ_{xx} is the autocorrelation function of the noise stimulus,

$$\Phi_{xx}(\tau) = \frac{1}{T}\int_0^T x(t)x(t-\tau)\,dt \quad \{4\}$$

and R_2 is the second-order cross correlation function, described by

$$R_2(\tau_1,\tau_2) = \frac{1}{N}\sum_{i=1}^{N} x(t_i - \tau_1)x(t_i - \tau_2) \ . \quad \{5\}$$

For digitally-sampled data, the first- and second-order Wiener kernel take the form of a vector and a symmetric square matrix, respectively. In this study, the analysis window was either τ = 10.5 or 21.0 ms. This corresponded to a vector size equal to $n = \tau \times fs$ = 1024 or 2048 samples for the first-order kernel. Correspondingly, the size of the matrix that contains the second-order kernel was 1024 x 1024 or 2048 x 2048.

2.3.3 Singular-value decomposition

SVD of the second-order kernel was performed using the built-in MatLab function s = svd(x) (R2010b, Mathworks). Second-order Wiener kernels with a size n x n were subjected to SVD, from which n subsystems, each with an eigenvector (u) of length n and a corresponding eigenvalue (w), were derived (Figure 4.1, see also Yamada and Lewis, 1999). The ranking of the eigenvectors was performed according to the absolute eigenvalues, where the first-ranked eigenvector had the highest absolute eigenvalue. Subsystems derived from decomposition of second-order kernels appear in quadrature pairs, which were often, but not always, two consecutively ranked vectors. Following Yamada and Lewis (1999), a dominance ratio was calculated by dividing the average eigenvalue of the highest-ranked quadrature pair with the average eigenvalue of the second highest-ranked quadrature pair. Note that a high dominance ratio reflects a relatively high contribution of the first two eigenvectors (or subsystems, Figure

4.1B) to the unit's response. An FFT of the eigenvectors revealed the frequency response and the phase response, from which a BF and a group delay could be determined, respectively.

To characterize the relative contribution of excitation and inhibition to the response of the IC, we focused on the subsystems with a rank 1-10, i.e. the first five quadrature pairs. We assessed the properties of the excitatory and inhibitory eigenvectors within the first five pairs. Furthermore, we reconstructed excitatory and inhibitory subkernels, by taking the outer product of each eigenvector with itself and then computing the eigenvalue-weighted sum of the resulted matrices (Yamada and Lewis, 1999). To reconstruct the excitatory kernel, only subsystems with a positive eigenvalue were considered; for the inhibitory kernel, only subsystems with a negative eigenvalue were considered.

3. Results

From nine normal-hearing guinea pigs, 100 recordings of IC multi units were included for further analyses. These units covered the tonotopic frequency range of the IC of the guinea pig, with excitatory CFs ranging from 2 to 35 kHz. Below, results from three multi units, that show representative features, will be described in detail. The population characteristics are presented subsequently.

3.1 Results for three exemplar multi units

Figure 4.2 displays results for an IC multi unit that responds to relatively low sound frequencies. The measurements with pure-tone stimuli revealed an excitatory CF at 2.5 kHz with a threshold at 24 dB SPL. In addition, there was an inhibitory receptive field, where the pure-tone stimuli elicited a firing rate significantly lower than the unit's baseline firing rate. The inhibitory-tuning curve had a CF at 11 kHz and a corresponding threshold at 69 dB SPL, which was well above the excitatory CF in frequency and threshold level.

The average noise-evoked firing rate, i.e. the zeroth-order Wiener kernel, was determined at 237 spikes/sec. The first-order Wiener kernel of this multi unit showed a stimulus-related oscillation with a BF at 2.1 kHz. This frequency corresponded with the excitatory CF. The first two quadrature pairs, derived from SVD of the second-order kernel, had BFs of 2.5 kHz and 2.2 kHz, respectively. These frequencies were consistent with the excitatory CF and with the BF of the first-order Wiener kernel. The fifth and sixth eigenvector, i.e. the third quadrature pair, had a negative eigenvalue and a BF at 2.6 kHz. This did not correspond to the inhibitory CF of 11 kHz, derived from responses to pure tones. However, this frequency did correspond to the excitatory CF and to the BF of the first excitatory quadrature pair. The inhibitory, third, quadrature pair had a longer response delay than the excitatory quadrature pairs: the unit's excitatory response to the presence of 2.5 kHz in the noise occurred after around 5.1 ms, whereas the inhibitory response occurred after 9.8 ms. In the reconstructed excitatory and inhibitory kernels, this difference in response delay is

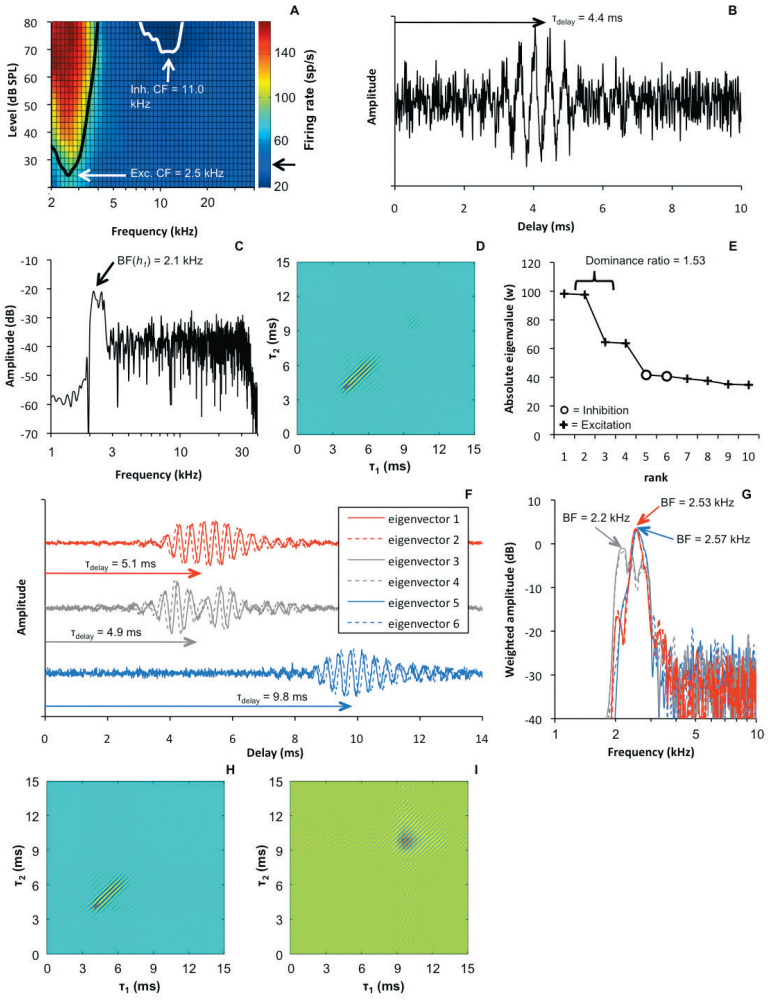

Figure 4.2 Representative example of a low-CF IC unit. **A)** The excitatory-tuning curve (black line) and the inhibitory-tuning curve (white line). The black arrow indicates the baseline firing rate (see Methods). **B)** The first-order Wiener kernel (h_1), which showed a stimulus-related oscillation. **C)** The amplitude spectrum of the first-order kernel. **D)** The second-order Wiener kernel (h_2), in which a matrix of τ_1, τ_2, and stimulus-related oscillations in color code is depicted. The original kernel of n = 2048 was zoomed in (0 – 15 ms); there were no stimulus-related oscillations outside this time window. To reduce noise, the kernel was reconstructed from the first 10 subsystems. **E)** The absolute eigenvalues of the ten highest-ranked subsystems. Crosses depict subsystems with a positive eigenvalue, open circles depict subsystems with a negative eigenvalue. **F)** Eigenvectors of the first-, second-, and third-ranked quadrature pairs, as derived from SVD analysis, depicted in the red, grey and blue lines, respectively. The first and second quadrature pair (red and grey lines) were excitatory subsystems (with positive eigenvalues), the third quadrature pair was an inhibitory subsystem (with a negative eigenvalue). The highest-ranked and second highest-ranked eigenvector of the quadrature pair is depicted with a solid and a dashed line, respectively. **G)** The amplitude spectrum of the eigenvectors plotted in panel **F**, the same legend applies. **H)** The excitatory second-order Wiener kernel, reconstructed from the subsystems with a positive eigenvalue (rank 1-4, 7-10). **I)** The inhibitory second-order kernel, reconstructed from the subsystems with a negative eigenvalue (rank 5 and 6).

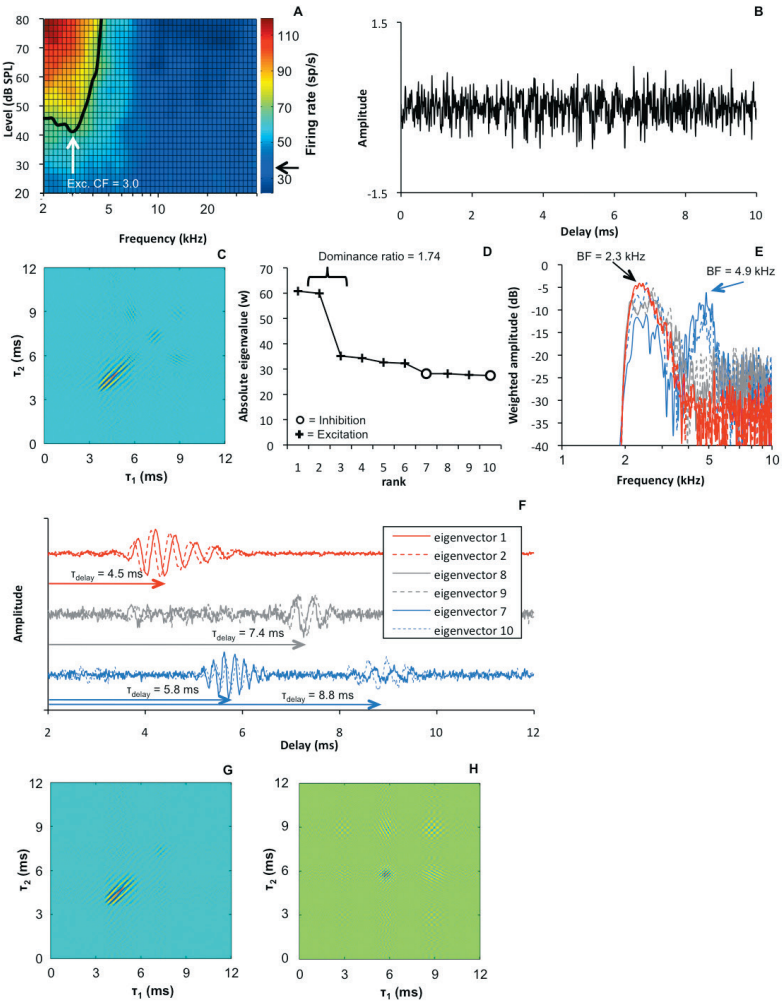

Figure 4.3 Representative example of a low-CF IC unit. **A)** The excitatory receptive field, contoured by the excitatory-tuning curve (black line). The black arrow indicates the baseline firing rate. **B)** The first-order Wiener kernel. **C)** The second-order Wiener kernel. The original kernel of $n = 2048$ was zoomed in (0 – 12 ms); there were no stimulus-related oscillations outside this time window. The kernel was reconstructed from the first 20 subsystems. **D)** The absolute eigenvalues of the ten highest-ranked subsystems. Crosses depict subsystems with a positive eigenvalue, open circles depict subsystems with a negative eigenvalue. **E)** The amplitude spectrum of the eigenvectors plotted in panel **F**, the same legend applies. **F)** Eigenvectors of the first-, fourth-, and fifth-ranked quadrature pairs, depicted in the red, blue and grey lines, respectively. The first and fifth quadrature pair (red and grey lines) were excitatory subsystems (with positive eigenvalues), the fourth quadrature pair (eigenvectors 7 and 10) was an inhibitory subsystem (with a negative eigenvalue; see panel d). The highest-ranked and second highest-ranked eigenvector of the quadrature pair is depicted with a solid and a dashed line, respectively. **G)** The excitatory second-order Wiener kernel, reconstructed from the excitatory subsystems (rank 1-6, 8 and 9). **H)** The inhibitory second-order Wiener kernel, reconstructed from the inhibitory quadrature pair (rank 7 and 10).

also visible (Figure 4.2H and Figure 4.2I, respectively). The remaining quadrature pairs that were not plotted had similar characteristics as the depicted excitatory quadrature pairs.

Results of another low-frequency unit are shown in Figure 4.3. Responses to pure tones revealed an excitatory CF at 3.0 kHz with a threshold of 41 dB SPL. This multi unit had no inhibitory receptive field, indicating that none of the presented pure tones resulted in a significant reduction of the firing rate.

The zeroth-order Wiener kernel had a value of 168 spikes/sec. Even though the multi unit responded to relatively low-frequency pure tones, it did not have a significant stimulus-related component in the first-order Wiener kernel (Figure 4.3B). Nevertheless, there was a clear response visible in the second-order Wiener kernel. Decomposing this kernel with SVD revealed both positive and negative eigenvalues in the first ten highest-ranked subsystems. The eigenvectors of the first quadrature pair (rank 1 and 2) had a BF of 2.3 kHz, corresponding with the excitatory CF. Eigenvectors rank 3, 4, 5, and 6 had a similar frequency response and group delay as the first quadrature pair, and were therefore not shown. Subsystems at rank 8 and 9, both with positive eigenvalues, formed a quadrature pair responding to the same BF as the first quadrature pair. The inhibitory quadrature pair, consisting of subsystems that were not ranked consecutively (rank 7 and 10), had two different frequency responses. One frequency response (BF = 2.3 kHz) was similar to the excitatory BF and one frequency response had a BF of 4.9 kHz.

The group delay of the first quadrature pair was 4.5 ms, whereas the group delay of the fifth quadrature pair, consisting of the excitatory subsystems at rank 8 and 9, was approximately 3 ms longer, at 7.4 ms. The inhibitory frequency response of the fourth quadrature pair (rank 7 and 10) that was similar to the excitatory BF occurred even later, at 8.8 ms. The other inhibitory frequency response (BF = 4.9 kHz) of the same quadrature pair had a group delay of 5.8 ms (Figure 4.3F).

Figure 4.4 shows the results of a high-CF unit. Pure tones evoked excitatory responses with a high CF at 10.1 kHz and a corresponding threshold at 10 dB SPL. This multi unit also had a large inhibitory-receptive field at the high-frequency boarder of the excitatory field. The inhibitory-tuning curve had a CF of 14.7 kHz, with a threshold at 50 dB SPL.

The zeroth-order Wiener kernel was determined at 607 spikes/sec. There was no stimulus-related response visible in the first-order Wiener kernel. The second-order Wiener kernel showed a clear response to the noise stimulus. The first quadrature pair, which contributed positively to the second-order kernel, had a BF response at 9.1 kHz, with a group delay of 3.3 ms. The second quadrature pair was also excitatory and had a BF response at 11.0 kHz with a group delay of 3.1 ms. This multi unit had an inhibitory quadrature pair that depicted two stimulus-related response bands, one with a BF of 6.6 kHz and on with a BF of 11.3 kHz. The response to 6.6 kHz had a group delay of 2.9 ms, indicating that this inhibitory response

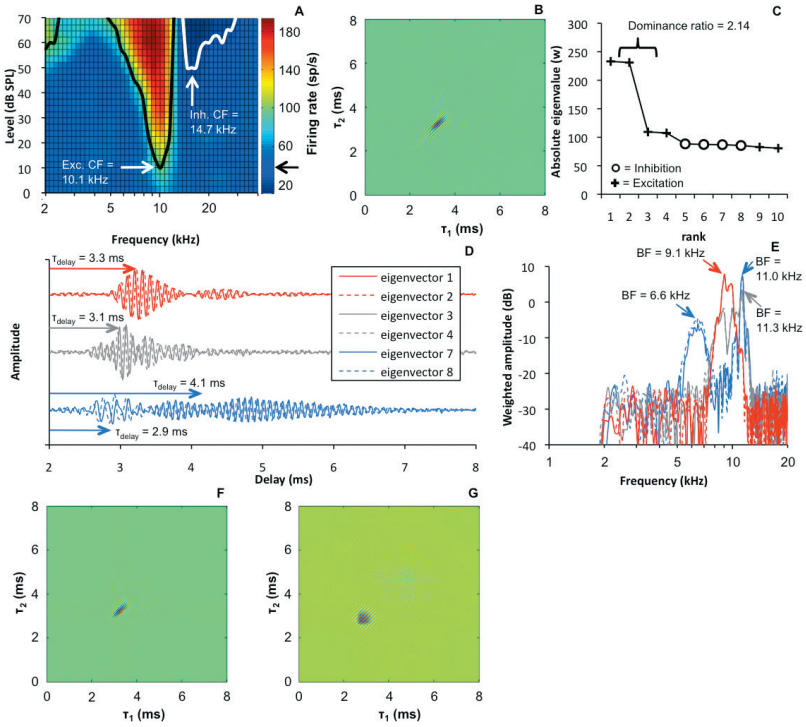

Figure 4.4 Representative example of a high-CF IC unit. **A)** The excitatory-tuning curve (black line) and the inhibitory-tuning curve (white line). The black arrow indicates the baseline firing rate. **B)** The second-order Wiener kernel (h_2). The original kernel (n = 1024) was zoomed in (0 – 8 ms); there were no stimulus-related components outside this time window. The kernel was reconstructed from the first 20 subsystems. **C)** The absolute eigenvalues of the ten highest-ranked subsystems. Crosses depict subsystems with a positive eigenvalue, open circles depict subsystems with a negative eigenvalue. **D)** Eigenvectors of the first-, second-, and fourth-ranked quadrature pairs, depicted in the red, grey and blue lines, respectively. The first and second quadrature pair (red and grey lines) were excitatory subsystems (with positive eigenvalues), the fourth quadrature pair (blue lines) was an inhibitory subsystem (with a negative eigenvalue). The highest-ranked and second highest-ranked eigenvector of the quadrature pair is depicted with a solid and a dashed line, respectively. Note that the x-axis is ranged from 2 to 8 ms. **E)** The amplitude spectrum of the eigenvectors plotted in panel **D**, the same legend applies. **F)** The excitatory second-order Wiener kernel, reconstructed from the excitatory subsystems (rank 1-4, 9 and 10). **G)** The inhibitory second-order Wiener kernel, reconstructed from the inhibitory subsystems (rank 5-8).

occurred slightly prior to the excitatory response and prior to the other inhibitory response of 11.3 kHz (delay 4.1 ms). This can be observed in the individual eigenvectors (Figure 4.4D) as well as in the reconstructed excitatory and inhibitory subkernels (Figure 4.4F and 4.4G, respectively).

Furthermore, the shape and width of the filter functions of the eigenvectors were not similar to the shape and width of the tuning curves. When the filter functions were inspected more closely, lobes around the peak could be observed (Figure 4.4E). For example,

the spectrum of the first quadrature pair had the highest peak at 9.1 kHz, but also smaller peaks at 8.0 kHz, 9.5 kHz, and 10.8 kHz, and the high-frequency peak of the inhibitory quadrature pair had two distinctive lobes at both sides of the peak, at 10.5 kHz and 11.6 kHz. A similar description accounts for the second excitatory quadrature pair. Those lobes could not be observed in the excitatory or inhibitory-tuning curves, representing responses to pure tones. The distance between the peaks of the lobes did not correspond to the best-modulation frequency (data not shown).

These three multi units represent the range of behaviors observed in the responses from the inferior colliculus. The first low-frequency unit (Figure 4.2) displayed a significant first-order kernel, reflecting the fact that phase information is coded by low-frequency neurons. The excitatory and inhibitory subsystems (eigenvectors of the second-order kernel) have overlapping pass bands (Figure 4.2G). The second unit (Figure 4.3) is also a low-frequency unit. Its receptive field did not show inhibition. Yet in the second-order kernel, inhibitory characteristics were clearly observed, with an inhibitory pass band well above the excitatory pass band (Figure 4.3E). The third and high-frequency unit (Figure 4.4) showed an elaborate pattern of excitation and inhibition. Inhibition was observed in the receptive field and in the second-order kernel, however, the inhibitory frequencies did not correspond. From the kernel it follows that inhibition had a shorter time delay than excitation in this unit. The subsystems obtained from the second-order kernel have partly non-overlapping frequency responses (Figure 4.4E).

3.2 Population characteristics

The mean firing rate evoked by the noise stimulus (the zeroth-order Wiener kernel) was 188 spikes/sec (± 16 spikes/sec standard error of the mean [SEM]). This was an average increase of 167 spikes/sec as compared to the mean spontaneous firing rate.

The best frequencies derived from the Wiener kernels were compared to the excitatory CF (Figure 4.5). A significant first-order Wiener kernel was observed in 12 of the 100 recorded multi units (see Figure 4.2B for an example). Eleven of these twelve multi units showed a good correspondence between the excitatory CF obtained from the receptive field, and the BF of the first-order kernel (Figure 4.5A). In one multi unit, the excitatory-tuning curve displayed a CF of 6.2 kHz, whereas the BF of the h_1 was 2.5 kHz. The BF of the significant first-order kernels ranged between 2.1 kHz and 3.3 kHz. Note that the presented noise had a low-cut off frequency at 2.0 kHz, which may have truncated low-frequency response components in these units. The best-frequency of the highest-ranked eigenvectors of the second-order Wiener kernel also showed a significant correspondence to the excitatory CF (Figure 4.5B).

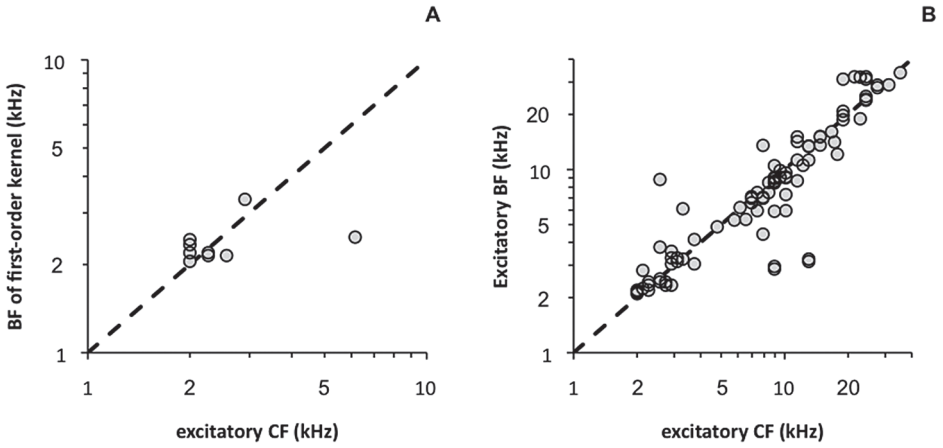

Figure 4.5 Correspondence between CFs obtained from tone responses and BFs obtained from Wiener-kernel analysis. **A)** The BF of the first-order Wiener kernel plotted against the excitatory CF. **B)** The BF of the excitatory first quadrature pair of the second-order kernel plotted against the excitatory CF.

Figure 4.6 depicts excitatory and inhibitory response characteristics revealed from the response to pure tones and the second-order kernels. Excitatory CFs were established in 98 of the 100 recorded multi units. The other two multi units did have a receptive field upon visual inspection, however, the criterion for an excitatory of inhibitory tone-evoked response was not met for any of the presented tones. Both multi units were recorded dorsal to the lowest excitatory CF measured, and, accordingly, these multi units were likely to have excitatory CFs < 2 kHz. Inhibitory receptive fields, and corresponding inhibitory CFs, were found in 36 of the 100 recorded multi units. In most of the multi units (33 of the 36), the inhibitory CF was higher than the excitatory CF (Figure 4.6A). Naturally, the excitatory CF never corresponded to the inhibitory CF, because one tone cannot both enhance and reduce the firing rate at the same time. The BFs of the inhibitory eigenvectors did not correspond to inhibitory CF, but often corresponded with the BFs of the excitatory eigenvectors (Figure 4.6B). The number of inhibitory subsystems within the ten highest-ranked subsystems was considered a measure for the amount of inhibition in the IC multi unit evoked by the noise stimulus. More than half of the multi units had no inhibitory subsystems (57%), however, there were also multi units with one inhibitory quadrature pair (i.e. two inhibitory subsystems; 26%), two inhibitory quadrature pairs (9%), or one or three inhibitory subsystems (both in 4% of the units, respectively; Figure 4.6C). Another measure for the amount of inhibition extracted from the decomposition of the second-order kernel was considered the ratio between the absolute sum of the negative eigenvalues and the sum of the positive eigenvalues. Note that the higher the absolute eigenvalue, the higher its contribution to the second-order kernel. The inhibition-to-excitation ratio ranged between 0.08 and 0.57, indicating that the contribution of excitation

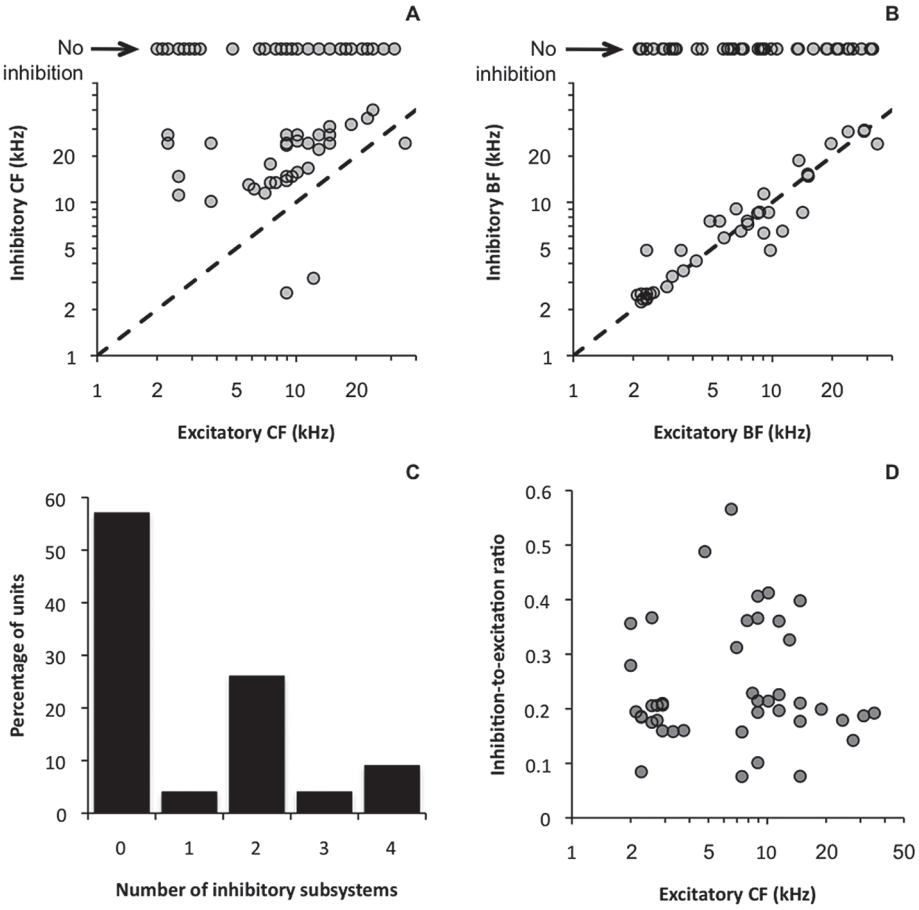

Figure 4.6 Excitatory and inhibitory tuning. **A)** The excitatory CF plotted against the inhibitory CF. Markers depicted at the top of the panel did not have an inhibitory receptive field (and CF). **B)** The BF of the highest-ranked excitatory eigenvector against the BF of the highest-ranked inhibitory eigenvector. Markers depicted at the top of the panel did not have inhibitory eigenvectors within the first ten subsystems. **C)** Distribution of the number of inhibitory subsystems within the ten highest-ranked subsystems. **D)** The absolute sum of the negative eigenvalues divided by the sum of positive eigenvalues (the inhibition-to-excitation ratio) is plotted against the excitatory CF.

to the second-order Wiener kernel was always higher than the contribution of inhibition. The height of the ratio was divided equally over the tonotopic axis of the IC (Figure 4.6D).

Group delays, as calculated from the slope of the phase response at the best frequency, are depicted in Figure 4.7. The highest-ranked eigenvectors had an average group delay of 4.74 ms (± 0.14 ms SEM). The shortest delays were found for subsystems with a high BF (Figure 4.7A). In most multi units that had both excitatory and inhibitory subsystems, the excitatory response occurred earlier, i.e. had a shorter group delay, than the inhibitory response (36 of

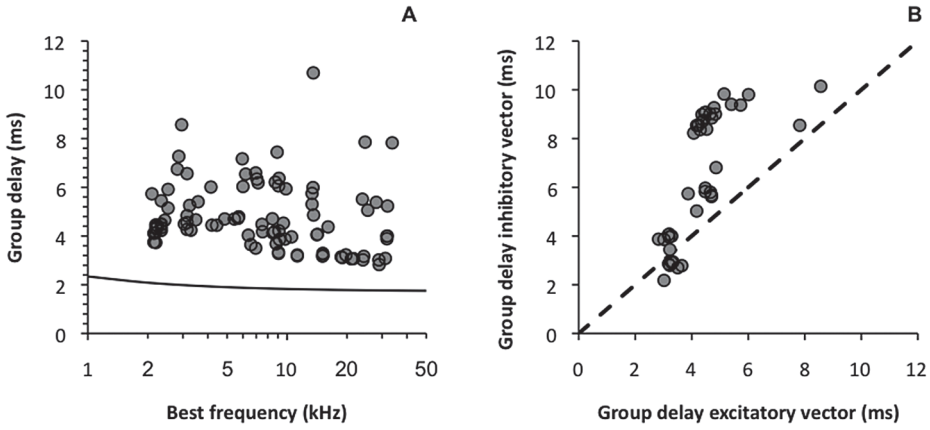

Figure 4.7 Group delays. **A)** The group delay of the highest-ranked eigenvector plotted against its best frequency. For comparison, the fit-function for group delays of AN fibers measured in the chinchilla, $\tau_{AN} = 1.721 + 1.863BF^{-0.771}$ is plotted (Recio-Spinoso et al., 2005; black solid line). **B)** The group delay of the highest-ranked excitatory eigenvector plotted against the group delay of the units highest-ranked inhibitory eigenvector. Markers depicted below the diagonal indicate multi units in which the highest-ranked inhibitory eigenvector has a shorter group delay than the highest-ranked excitatory eigenvector.

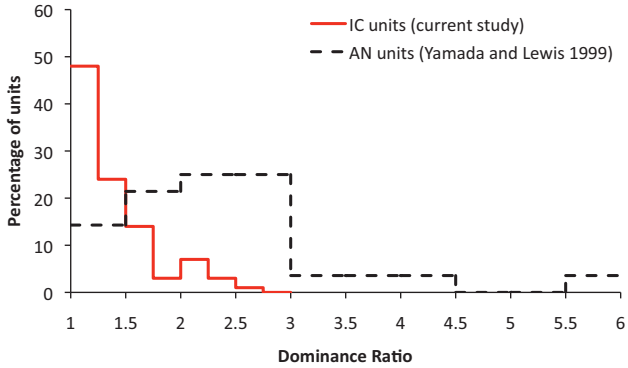

Figure 4.8 Dominance ratio. Distribution of dominance ratios for the 100 recorded IC multi units in this study (red solid line). For comparison, results for 28 units in the primary auditory nerve from the frog's basilar papilla are also shown (Yamada and Lewis, 1999; black dashed line). The numbers have been converted to show percentages of the total recorded units. A large dominance ratio indicates that the units response is dominated by the first quadrature pair of eigenvectors, as is typically observed in the primary units studies by Yamada and Lewis (1999).

the 43 units; Figure 4.7B). However, in seven multi units, the inhibitory eigenvector had a shorter group delay than the excitatory eigenvector.

Dominance ratios reflect the contribution of the first quadrature pair to the second-order Wiener kernel relative to the second quadrature pair (previously described by Yamada and

Lewis, 1999). Dominance ratios of IC multi units had an average value of 1.33 and a maximum of 2.72. The distribution of dominance ratios was skewed towards the lower values for IC units (Figure 4.8), indicating the relative important contribution of lower-ranked subsystems to the neuronal responses.

4. Discussion

The results of this study showed that Wiener-kernel analysis was applicable to characterize response patterns of multi units of the IC in normal-hearing guinea pigs. First-order Wiener kernels were found in 12% of the recorded multi units and had low-frequency oscillations between 2.1 kHz and 3.3 kHz. In all but one unit, these oscillations corresponded well with the excitatory CF, as determined from tone responses. A significant second-order kernel could be found in all neurons being studied. These kernels were decomposed in parallel subsystems, where the filter in each of the subsystems is given by an eigenvector of the kernel matrix. The best frequency of the first (highest-ranking) eigenvector corresponded well with the excitatory CF. The eigenvalue of the first eigenvector was always positive, indicating an excitatory contribution to the neuron's response. A portion of the eigenvalues was negative. The best frequencies of these inhibitory eigenvectors did not agree well with the inhibitory CF. Rather, the inhibitory BF was often similar to the excitatory BF. Additionally, we showed that group delays were often, but not always, shorter for the excitatory responses as compared to the inhibitory responses. Dominance ratios of IC multi units were several magnitudes smaller than those measured in the AN, reflecting the higher degree of complexity in the response properties of IC neurons.

The correspondence of the BF of the highest-ranked eigenvector and the tonal excitatory CF is consistent with earlier Wiener-kernel studies in the AN and the CN (Temchin et al., 2005; Recio-Spinoso and van Dijk., 2006). Furthermore, a significant stimulus-related oscillation was found in the first-order kernels of twelve low-frequency neurons. The BF of the first-order kernel also corresponded with the excitatory CF. Oscillations in the first-order Wiener kernel reflect the neuron's ability to phase lock to the fine structure in the acoustic stimulus (de Boer and de Jongh, 1978; Eggermont et al., 1983; Lewis et al., 2002b). Phase locking has been determined throughout the auditory system and only occurs in response to relatively low frequencies (Joris and Verschooten, 2013). In the current study, the highest first-order kernel oscillation was 3.3 kHz, which corresponds reasonably well with the upper limit of phase locking in the IC of the cat (Yin and Kuwada, 1983). Our findings indicate that the first-order Wiener kernel of an IC multi-unit reflects frequency selectivity.

Upon visual inspection, second-order Wiener kernels of the IC seemed similar to second-order kernels of the AN and the CN, with stimulus-related oscillations near the diagonal (Recio-Spinoso and van Dijk, 2006; Sneary and Lewis, 2007). SVD of the second-order kernels revealed a larger number of significant subsystems. This is also reflected by the low dominance ratios of IC units as compared to AN units (see Figure 4.8). The dominance ratio has been interpreted as a measure of the complexity of the response, in which low

dominance ratios correspond to high degrees of complexity (Yamada and Lewis, 1999). The complexity of the response in the IC probably reflects the fact that the IC is a 'higher-order' structure which integrates information from 'lower' nuclei.

Another measure that reflects this complexity is the fact that recordings of 60 minutes were required to obtain significant kernels from the IC. In the AN, recordings of a few minutes are sufficient (Recio-Spinoso et al., 2005; Temchin et al., 2005). This suggests that the spikes are not only conditioned by the stimulus, but might also be conditional to each other or be driven by other sources. At present we do not have a good explanation for the relative time-consuming nature of this analysis.

The advantage of the Wiener-kernel analysis over other methods that study stimulus-evoked spike trains, such as the spectrotemporal receptive field (STRF; Hermes et al., 1981) and the 'zwuis' stimulus (van der Heijden and Joris, 2003), is that Wiener-kernel analysis allows to separate excitatory and inhibitory responses of the inferior colliculus in a precise manner (Yamada and Lewis, 1999). By decomposing the second-order Wiener kernel with SVD, the excitatory and inhibitory frequencies, delays, relative weights, and pass bands can be determined. Since recent hypotheses suggest that acoustic trauma-induced pathologies, such as tinnitus and hyperacusis, are related to a disturbed balance between excitation and inhibition, gaining knowledge about the precise nature of this disturbed balance might provide additional insight in the noise-induced neurophysiological changes. Therefore, we selected the Wiener-kernel method to study properties of excitation and inhibition before and after acoustic trauma.

Separating excitatory and inhibitory responses by decomposition of the second-order Wiener kernel revealed a number of interesting findings. A large number of multi units (43%) had one or more inhibitory subsystem within the ten highest-ranked subsystems. Remarkably, the best frequency of the inhibitory eigenvectors did not correspond well with the inhibitory CF. This shows that information about reductions in the firing rate by pure tones is not readily available from Wiener-kernel analysis. However, the inhibitory BF did correspond to the excitatory BF (Figure 4.6B), suggesting that the inhibitory subsystems rather represent different processes that involve inhibition, such as adaptation or refractoriness (Sneary and Lewis, 2007). This shows that the classical methods and the Wiener kernels provide complementary information about inhibition in the IC. Group delays of the stimulus-related oscillations in the inhibitory eigenvectors were often longer than delays of the excitatory eigenvectors. However, in 7 of the 43 multi units with inhibition, the inhibitory response was faster than the excitatory response. In these multi units, adaptation or refractoriness could not have accounted for the presence of the inhibitory subsystem(s).

Another mechanism that might explain the presence of the inhibitory subsystems recorded from the IC is binaural hearing. Many neurons of the IC are sensitive to interaural time differences. Neural responses to interaural time differences consist of excitatory and inhibitory components. The inhibitory components can be both leading and lagging the excitatory components (Carney and Yin, 1989). In the current study, the stimulus was

presented by a free-field speaker, and therefore stimulated both the ipsi- and the contralateral ear. Accordingly, the spike trains recorded from the IC carried information about the interaural time difference. This might have been reflected in the response properties of the excitatory and inhibitory subsystems.

In the current study, we defined two measures for the amount of inhibition as revealed from the inhibitory subsystems of the second-order kernel: the number of inhibitory subsystems and the inhibition-to-excitation ratio. Inhibition plays a dominant role in the IC (Pollak et al., 2011) and it has previously been shown that inhibitory responses in particular are vulnerable to acoustic trauma (Heeringa and van Dijk, 2014). Both tinnitus and hyperacusis, two debilitating conditions that often result from exposure to loud sounds, are believed to be related to a disrupted balance between excitation and inhibition in the central auditory system (Eggermont and Roberts, 2014; Knipper et al., 2013). The measures of inhibition defined in the present work can be of additional use to further study the pathophysiological mechanism(s) of noise-induced tinnitus and hyperacusis.

Acknowledgements

We thank Hans Segenhout for technical support, Russ Snyder for showing us the surgical procedures involved in the IC recordings, and Fedde Tigchelaar for his assistance with the Wiener-kernel calculations.

This work was supported by the Heinsius Houbolt Foundation and the Stichting Gehoorgestoorde Kind. The study is part of the research program of our department: Healthy Aging and Communication.

Chapter 5

The immediate effects of acoustic trauma on the inferior colliculus: a Wiener-kernel analysis

A.N. Heeringa and P. van Dijk

A modified version of this chapter was submitted to Hearing Research

Abstract

Noise-induced tinnitus and hyperacusis are thought to correspond to a disrupted balance between excitation and inhibition in the central auditory system. We have previously shown that properties of excitation and inhibition of the inferior colliculus (IC) can be studied using Wiener-kernel analysis. The current study aimed at investigating the effects of immediate acoustic trauma on excitatory and inhibitory components of the IC, as revealed with Wiener-kernel analyses.

Neural responses were recorded from the IC of three anesthetized albino guinea pigs before and immediately after a one-hour bilateral exposure to an 11-kHz tone of 124 dB SPL. Before and after the traumatizing stimulus, neural activity was recorded during the presentation of a 1-h continuous Gaussian-noise stimulus of 70 dB SPL for Wiener-kernel analysis. Response characteristics obtained with Wiener-kernel analyses were complemented with excitatory and inhibitory responses to pure tones.

Both spontaneous and noise-evoked firing rates were significantly decreased immediately after acoustic trauma. Furthermore, multi units were tuned to lower frequencies as compared to before acoustic trauma. Wiener-kernel analysis showed that excitation and inhibition in low-CF multi units (CF < 3 kHz) was not affected, inhibition in mid-CF multi units (CF between 3 kHz and 11 kHz) disappeared whereas excitation was not affected, and both excitation and inhibition in high-CF multi units (CF > 11 kHz) disappeared after acoustic trauma. This specific differentiation could not be identified with the tone-evoked receptive-field analyses, in which inhibitory responses disappeared in all units and excitatory responses in only the high-CF units.

With this study, we showed that the effects of acoustic trauma can be identified with Wiener-kernel analysis. We confirmed an acoustic trauma-induced disrupted balance between excitation and inhibition, which was apparent in mid-CF units in particular. Our findings might give additional insight in the central pathophysiological mechanisms of noise-induced hyperacusis.

Keywords: Wiener kernels; inferior colliculus; acoustic trauma; singular-value decomposition; guinea pig

Abbreviations: ABR, auditory brainstem response; BF, best frequency; CF, characteristic frequency; IC, inferior colliculus; RMS, root-mean-square; SVD, singular-value decomposition

1. Introduction

Extensive acoustic overstimulation affects the balance between excitation and inhibition in the central auditory system (Scholl and Wehr, 2008; Dong et al., 2010a; Llano et al., 2012; Chapter 2). This disrupted balance between excitation and inhibition is thought to be an underlying mechanism of noise-induced tinnitus and hyperacusis (Noreña, 2011; Knipper et al., 2013). As there is currently no common treatment for patients with tinnitus and hyperacusis, gaining additional knowledge about this phenomenon can advance the search for such a treatment.

Recent research of our lab and others has shown that excitation and inhibition of the central auditory system can be well identified by applying Wiener-kernel analyses (Yamada and Lewis, 1999; Sneary and Lewis, 2007; Chapter 4). Wiener-kernel analysis is a technique that can be used to study functional properties of stimulus-evoked activity in the central auditory system (Korenberg and Hunter, 1990; Eggermont, 1993). To apply this analysis, neural responses from the auditory system to broadband Gaussian noise are measured. By correlating the broadband noise with the noise-evoked spike train, a set of Wiener kernels can be obtained. These kernels characterize the auditory system up to the level where the response was measured. In order to obtain functional properties of the second-order kernel, singular-value decomposition (SVD) can be applied to decompose the kernel into a number of parallel subsystems (Yamada and Lewis, 1999). Each subsystem is characterized by a filter function (an eigenvector of the kernel matrix) and a gain function (the corresponding eigenvalue; see Chapter 4, Figure 4.1). Eigenvalues can be positive or negative, reflecting excitatory and inhibitory subsystems, respectively. As such, the functional properties of excitation and inhibition in the IC can be obtained from the neural response to a single stimulus, the broadband Gaussian noise. For a more detailed description of the Wiener-kernel analysis technique and of decomposing the second-order kernel by SVD, see the Introduction of Chapter 4. Wiener-kernel analyses have previously been applied to responses of the auditory nerve and the cochlear nucleus (van Dijk et al., 1994; Yamada and Lewis, 1999; Lewis et al., 2002a, 2002b; Recio-Spinoso et al., 2005; Temchin et al., 2005; Recio-Spinoso and van Dijk, 2006; Sneary and Lewis, 2007). Recent results from our lab showed that Wiener-kernel analysis is also applicable to noise-evoked spike trains recorded from the inferior colliculus (IC; Chapter 4).

With the current study, we aimed at investigating the consequences of immediate acoustic trauma on excitation and inhibition in the IC, by studying the excitatory and inhibitory subsystems as derived from SVD of the second-order Wiener kernels. We hypothesized that inhibitory components in particular are affected by acoustic trauma. This study might further confirm earlier findings and extend our knowledge about the effects of acoustic trauma on excitation and inhibition in the central auditory system using the Wiener-kernel analysis technique. As such, this study might give additional insight in the central pathophysiological mechanisms of noise-induced tinnitus and hyperacusis.

2. Methods

Wiener-kernel analyses of noise-evoked neural responses of the IC of normal-hearing guinea pigs have previously been described in Chapter 4 of this dissertation. Details concerning the involved surgeries, stimulus presentation, neural recordings, and data analyses can be found in the Methods of Chapter 4. Here, we briefly summarize these procedures.

2.1 Animals

Three albino male guinea pigs (Dunkin Hartley; Harlan Laboratories, Horst, the Netherlands), weighing between 362 and 406 gram, were included in this study. These animals were a subgroup of the nine animals described in Chapter 4. Animals were anesthetized with intramuscular injections containing a mixture of 70 mg/kg ketamine and 6 mg/kg xylazine. Half the original dose was applied every hour to maintain a deep level of anesthesia. A tracheotomy was performed for artificial respiration during the experiment. A craniotomy, followed by partial aspiration of the overlying cortical tissue, allowed for visualization of the IC. A linear 16-channel microelectrode array (A1x16-10mm-100-413-A16; NeuroNexus) was placed in the IC in a dorsal-lateral to ventral-medial direction. Online inspection of the neural signal during presentation of successive noise bursts allowed for optimal placement of the electrode in the IC. During the entire experiment, the electrode remained at the same location in the IC. Thus, it can be assumed that neural activity was recorded from a fixed population of multi units throughout the entire experiment. The experiments were conducted in an anechoic sound-attenuating booth. The study was in agreement with Dutch and European regulations and was approved by the Animal Experiment Committee of the University of Groningen (DEC # 6068D).

2.2 Auditory brainstem response

Before and after acoustic trauma, hearing thresholds were determined by recordings of the auditory brainstem response (ABR). Thresholds for 3-ms tone pips of 3 kHz, 6 kHz, 11 kHz, and 22 kHz were determined. The threshold shifts (in dB) were calculated for every frequency to get an indication about the damage induced by the acoustic trauma. Methodological details about this procedure can be found in the Methods of Chapter 2.

2.3 Stimulus presentation

A free-field electrostatic speaker (ES1; Tucker Davis Technologies, Inc. [TDT]) was placed at approximately 5 cm from the left ear, contralateral to the exposed IC. Pure tones (duration 300 ms), with a frequency ranging from 2-40 kHz and an intensity ranging from 20-80 dB SPL, were presented to acquire receptive fields. Subsequently, a continuous Gaussian-white noise of 70 dB SPL was presented for 1 hour to acquire data for Wiener-kernel analysis. The noise had a spectrum that was flat within 1 dB between 2 kHz and 40 kHz.

For acoustic trauma, two free-field piezo tweeters (PH8; Velleman) were positioned at ± 5 cm from each ear. Animals were bilaterally exposed for 1 hour to a continuous 11-kHz tone of 124 dB SPL. To create an unobstructed path for the sounds to reach the tympanic membrane, both pinnae were folded over the head of the animal. All acoustic stimuli were presented with a sampling rate of 97,656 Hz and were calibrated using a Brüel & Kjær (B&K) microphone placed at the entrance of the ear canal and a B&K measuring amplifier (type 2670 and 2610, respectively).

2.4 Neural recordings

The 16-channel neural signal was preamplified (RA16PA; Tucker Davis Technologies [TDT] Inc.), recorded (RX5; TDT Inc.), and stored on a PC using custom-made MatLab software (R2010b, Mathworks). Neural signals were filtered (300-3000 Hz, butterworth filter) and the root-mean-square (RMS) was calculated. Spikes were defined by the instants when the signal exceeded a threshold. This threshold was determined by 3 times the RMS value for the responses to pure tones and the spontaneous-firing-rate recordings, and by visual inspection for the Wiener-kernel analyses. All recordings presented in this chapter are multi-unit recordings, indicating that no spike sorting was executed and, therefore, it is not certain whether all spikes derived from the same neuron or from more than one neuron.

2.5 Data analysis

MatLab programs were designed to analyze the firing rates evoked by pure tones and create matrices from which the excitatory and inhibitory receptive fields could be obtained. Units without a distinguishable receptive field before acoustic trauma were excluded from further analyses. The excitatory and inhibitory tuning curves contoured the excitatory and inhibitory receptive fields, respectively, and revealed a unit's excitatory characteristic frequency (CF), inhibitory CF, and the corresponding thresholds. Furthermore, neural activity was recorded for 180 s to obtain a unit's spontaneous firing rate. Wiener kernels and the subsequent SVD of the second-order kernels were calculated using custom-made programs in C and MatLab programs. SVD analysis of the second-order kernels revealed parallel subsystems, each consisting of a filter function (eigenvector) and a gain function (eigenvalue). The eigenvalue of a subsystem was either positive or negative, referring to an excitatory or an inhibitory subsystem. Subsystems derived from decomposition of second-order kernels appear in quadrature pairs, which are often, but not always, two consecutively ranked subsystems. From the frequency and phase response curves of the eigenvectors, the best frequency (BF) and the group delay was calculated, respectively. The results obtained with Wiener-kernel analysis were compared to and complemented with the excitatory and inhibitory CF. Detailed description of these analyses can be found in the Methods of Chapter 4.

2.6 Statistics

Statistical differences of spontaneous and noise-evoked firing rates, best frequencies, characteristic frequencies, and group delays between before and after acoustic trauma were determined with a Paired-sample T-test (IBM SPSS Statistics; Version 22). A p-value below 0.05 was considered significant and the outcomes were corrected for multiple comparisons.

3. Results

Data from 33 IC multi units were used to study the immediate effects of acoustic trauma on central excitation and inhibition, as determined by Wiener-kernel analysis. Exposure for 1h to an 11-kHz tone of 124 dB SPL resulted in elevated thresholds for all measured ABR frequencies. Auditory thresholds for 3 kHz and 6 kHz were both elevated with 13 dB on average. Thresholds for 11 kHz and 22 kHz (tones at and above the trauma frequency) were elevated with an average of 40 dB and 46 dB, respectively. A representative example of a low-, a mid-, and a high-CF multi unit are discussed below, followed by statistical analyses comparing response characteristics on the level of the population before and immediately after acoustic trauma.

3.1 Effects of acoustic trauma on a low-CF multi unit

Figure 5.1 shows results of a low-CF multi unit recorded before and immediately after acoustic trauma. Responses to pure tones revealed an excitatory receptive field with a CF of 2.0 kHz and a corresponding threshold of 35 dB SPL (Figure 5.1A). Acoustic trauma did not majorly change the excitatory receptive field (Figure 5.1B; CF = 2.1 kHz, threshold = 26 dB SPL). There was no inhibitory receptive field before and after acoustic trauma.

Both the spontaneous and the noise-evoked firing rate of this multi unit slightly decreased after acoustic trauma. The spontaneous firing rate decreased from 27 spikes/sec to 25 spikes/sec and the noise-evoked firing rate decreased from 232 spikes/sec before exposure to 205 spikes/sec after exposure. Significant stimulus-related oscillations were observed in the second-order Wiener kernel before and after acoustic trauma (Figure 5.1E and 5.1D). Excitatory and inhibitory subsystems, as obtained from decomposing the second-order kernel with SVD, were detected at both time points. The BF of the first (excitatory) quadrature pair (i.e. the first two subsystems) was not affected by acoustic trauma (BF before = 2.1 kHz; BF after = 2.1 kHz) and corresponded to the excitatory CF. The third quadrature pair (fifth and sixth subsystems) had a negative eigenvalue before as well as after acoustic trauma (Figure 5.1C). The inhibitory BF of this quadrature pair was also not majorly affected by acoustic trauma (BF before = 2.5 kHz; BF after = 2.2 kHz).

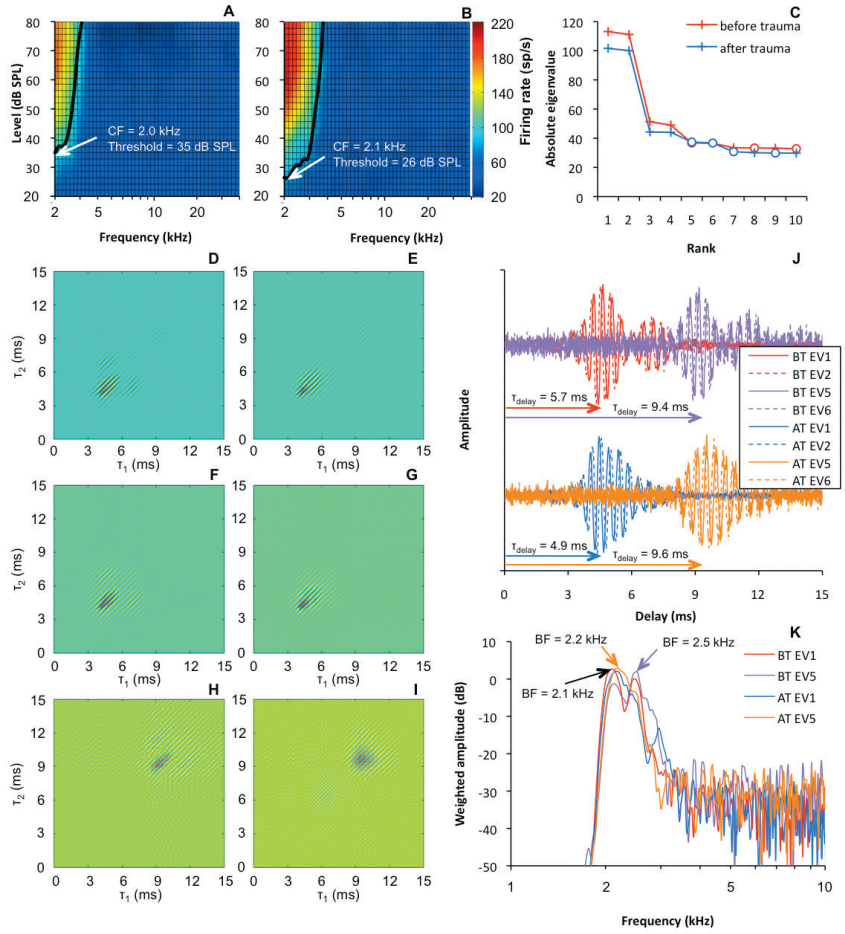

Figure 5.1 Representative example of a low-CF multi unit. The excitatory receptive field is contoured by the excitatory tuning curve (black line) before **(A)** and after **(B)** acoustic trauma. **C)** The absolute eigenvalues of the ten highest-ranked subsystems before (red curve) and after (blue curve) acoustic trauma. Crosses depict subsystems with a positive eigenvalue, open circles depict subsystems with a negative eigenvalue. The second-order Wiener kernel before **(D)** and after **(E)** acoustic trauma. The original kernel of n = 2048 was zoomed in (0 – 15 ms); there were no stimulus-related oscillations outside this time window. The excitatory kernel, reconstructed from the subsystems with a positive eigenvalue, before **(F)** and after **(G)** acoustic trauma. The inhibitory kernel, reconstructed from the subsystems with a negative eigenvalue, before **(H)** and after **(I)** acoustic trauma. **J)** Eigenvectors (EV) of the first- and third-ranked quadrature pairs, as derived from SVD analysis, depicted in the red and purple lines, respectively, before acoustic trauma (BT), and depicted in blue and orange lines, respectively, after acoustic trauma (AT). The first quadrature pair (red and blue lines) consisted of excitatory subsystems (with positive eigenvalues), the third quadrature pair (purple and orange lines) consisted of inhibitory subsystems (with negative eigenvalues). The highest-ranked and second highest-ranked eigenvector of the quadrature pair is depicted with a solid and a dashed line, respectively. **K)** The amplitude spectrum of the eigenvectors plotted in panel **J**, the same legend applies. As the frequency responses of the individual eigenvectors within a quadrature pair are assumed to be relatively similar (see also Chapter 4, Figure 4.2 – 4.4), only the frequency response of the highest-ranked EV of the quadrature pair is depicted here.

3.2 Effects of acoustic trauma on a mid-CF multi unit

Figure 5.2 shows the effects of acoustic trauma on the response characteristics of a mid-CF multi unit. Before exposure, the excitatory tuning curve had a CF of 6.2 kHz and a corresponding threshold of 50 dB SPL. After exposure, the receptive field shifted to lower frequencies and two excitatory CFs could be identified, at 2.4 kHz and at 3.7 kHz, both with a threshold of 59 dB SPL. This multi unit had no inhibitory responses to pure tones before and after acoustic trauma.

Firing rates measured in the absence and presence of the noise stimulus were both decreased after acoustic trauma. The spontaneous firing rate decreased from 24 spikes/sec to 14 spikes/sec and the noise-evoked firing rate decreased from 198 spikes/sec to 160 spikes/sec after acoustic trauma. Before acoustic trauma, this multi unit had distinct stimulus-related oscillations in the second-order kernel and showed both excitatory and inhibitory subsystems in the ten highest-ranked subsystems (Figure 5.2C). The first (excitatory) quadrature pair had a BF of 5.4 kHz. In addition, the third quadrature pair had negative eigenvalues, representing inhibition with a BF at 7.5 kHz. After exposure, the subsystems with a negative eigenvalue disappeared, i.e. acoustic trauma affected the presence of inhibition in this multi unit (see Figure 5.2, panel C and I). Furthermore, the BF of the first (excitatory) quadrature pair was lower as compared to before exposure. The excitatory BF after exposure was 2.8 kHz and corresponded to the lower excitatory CF, as revealed from the responses to pure tones (Figure 5.3, panel B and K).

3.3 Effects of acoustic trauma on a high-CF multi unit

Figure 5.3 shows the effects of acoustic trauma on a high-CF multi unit. Responses to pure tones revealed an excitatory-receptive field (CF = 16.7 kHz, threshold = 33 dB SPL) that disappeared completely after acoustic trauma. No inhibitory responses to pure tones were observed before or after acoustic trauma.

Spontaneous firing rates were decreased after acoustic trauma (from 21 spikes/sec to 14 spikes/sec), but noise-evoked firing rates of this multi unit were not affected (155 spikes/sec pre trauma, 158 spikes/sec post trauma). Before acoustic trauma, the frequency tuning to high-frequency pure tones (CF = 16.7 kHz) corresponded to the stimulus-related oscillations observed in the second-order kernel (BF = 16.1 kHz). After exposure, stimulus-related components were apparent, however, the frequency response was majorly affected (see Figure 5.3, panel E, K, and G). The first (excitatory) quadrature pair had a BF of 2.8 kHz. Both before and after exposure, no inhibitory subsystems were observed.

These three multi units exemplify that inhibition, as defined by the presence of subsystems with a negative eigenvalue, was preserved in a low-frequency multi unit, but not in a mid-frequency multi unit. Furthermore, the examples showed that frequency tuning of a low-CF multi unit was not affected by acoustic trauma, whereas in the mid-CF multi unit, a

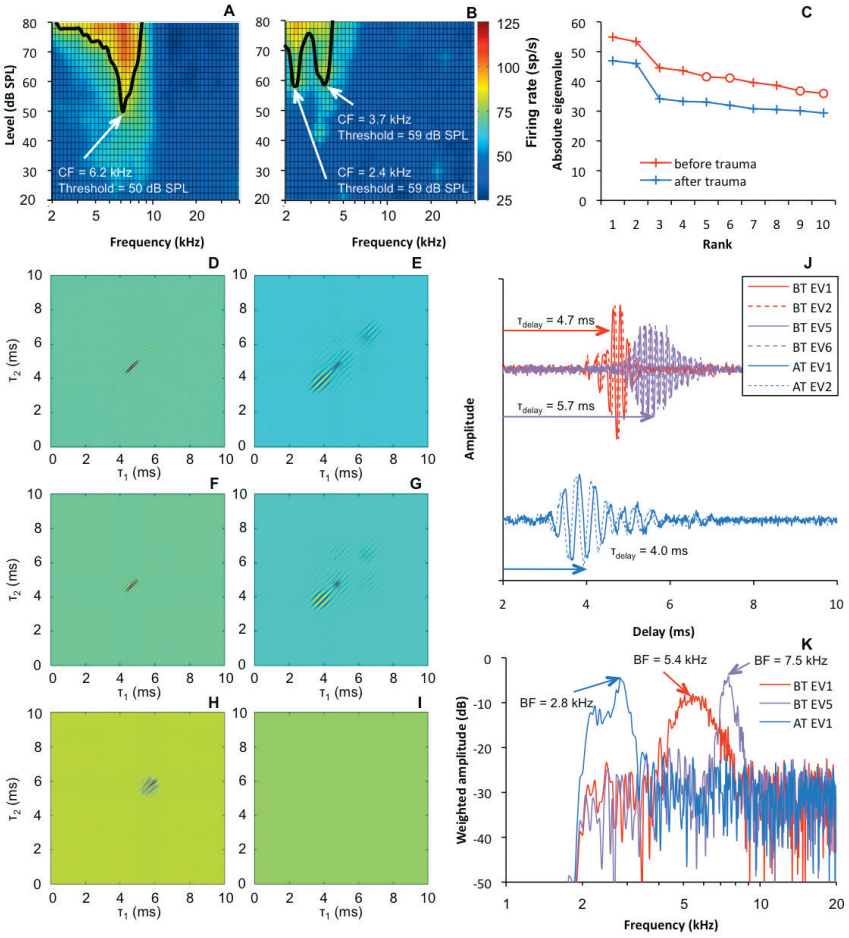

Figure 5.2 Representative example of a mid-CF multi unit. The excitatory receptive field is contoured by the excitatory tuning curve (black line) before **(A)** and after **(B)** acoustic trauma. **C)** The absolute eigenvalues of the ten highest-ranked subsystems before (red curve) and after (blue curve) acoustic trauma. Crosses depict subsystems with a positive eigenvalue, open circles depict subsystems with a negative eigenvalue. The second-order Wiener kernel before **(D)** and after **(E)** acoustic trauma. The original kernel of n = 2048 was zoomed in (0 – 10 ms); there were no stimulus-related oscillations outside this time window. The excitatory kernel, reconstructed from the subsystems with a positive eigenvalue, before **(F)** and after **(G)** acoustic trauma. The inhibitory kernel, reconstructed from the subsystems with a negative eigenvalue, before **(H)** and after **(I)** acoustic trauma. Since there were no inhibitory subsystems after trauma, the matrix consists of only zeros and has, therefore, only one color. **J)** Eigenvectors (EV) of the first- and third-ranked quadrature pairs, as derived from SVD analysis, depicted in the red and purple lines, respectively, before acoustic trauma (BT). The eigenvectors of the first quadrature pair after acoustic trauma (AT) are depicted in blue lines. The first quadrature pair (red and blue lines) consisted of two excitatory subsystems (with positive eigenvalues), the third quadrature pair (purple lines) consisted of two inhibitory subsystems (with negative eigenvalues). The highest-ranked and second highest-ranked eigenvector of the quadrature pair is depicted with a solid and a dashed line, respectively. **K)** The amplitude spectrum of the eigenvectors plotted in panel **J**, the same legend applies. Only the frequency response of the highest-ranked eigenvector (EV1 and EV5) of the quadrature pair is depicted here.

downward shift in frequency tuning could be observed, both in the responses to pure tones (CF) and in the stimulus-related oscillations of the second-order Wiener kernel (BF). In the high-CF multi unit, noise-evoked responses showed frequency selectivity (BF) after trauma, but tone-evoked responses did not (no CF). The BF that was apparent in the second-order kernel was shifted to a lower frequency as compared to before trauma.

3.4 Population characteristics

3.4.1 Spontaneous and noise-evoked activity

Figure 5.4 shows the effects of acoustic trauma on spontaneous and noise-evoked firing rates. For illustration, the low-CF units (CF < 3 kHz; blue triangles), mid-CF units (CF between 3 and 11 kHz; white squares), and high CF units (CF > 11 kHz; red circles) have been depicted with different markers. Spontaneous firing rates were significantly decreased immediately after acoustic trauma (Figure 5.4A; paired-sample T-test: $T(32) = 5.302$, $p < 0.001$). Noise-evoked firing rates were also significantly decreased by acoustic trauma (Figure 5.4B; paired-sample T-test: $T(32) = 3.031$, $p < 0.01$). The average reduction of the spontaneous firing rates (6.2 spikes/sec) alone could not account for the average reduction in the noise-evoked firing rates (29.0 spikes/sec).

3.4.2 Frequency selectivity and frequency tuning

Figure 5.5 compares the frequency tuning between before and after acoustic trauma, as determined with responses to pure tones (CF) and responses to the noise stimulus (BF). Low-CF multi units, depicted with blue triangles, retained frequency selectivity of the CF and the BF after acoustic trauma. Frequency selectivity of mid-CF multi units, depicted with white squares, was mildly affected by acoustic trauma. Excitatory receptive fields disappeared in two mid-CF multi units which had a CF > 8.4 kHz *before* trauma (Figure 5.5A), whereas all mid-CF multi units showed significant stimulus-related oscillations in the second-order kernels (BF) both before and after acoustic trauma (Figure 5.5B). The frequency selectivity of most high-CF multi units (red circles) was affected by acoustic trauma. A receptive field was apparent in one high-CF multi unit (Figure 5.5A) and a stimulus-related oscillation was apparent in the second-order kernel of three high-CF multi units (Figure 5.5B). The other units lacked frequency selectivity after acoustic trauma. Moreover, frequency tuning was also affected by acoustic trauma, when examining both the CF and the BF. In the multi units in which an excitatory CF could still be determined after acoustic trauma ($n = 21$), the CF was significantly reduced (Figure 5.5A; paired-sample T-test: $T(20) = 3.801$, $p < 0.005$). Similarly, in the multi units in which an excitatory BF could still be determined after acoustic trauma ($n = 26$), the frequency tuning of the BF was also significantly reduced (Figure 5.5B; paired-sample T-test: $T(25) = 2.836$, $p < 0.01$). In other words, neurons that were sensitive to high frequencies, had an altered sensitivity to lower frequencies after acoustic trauma, both

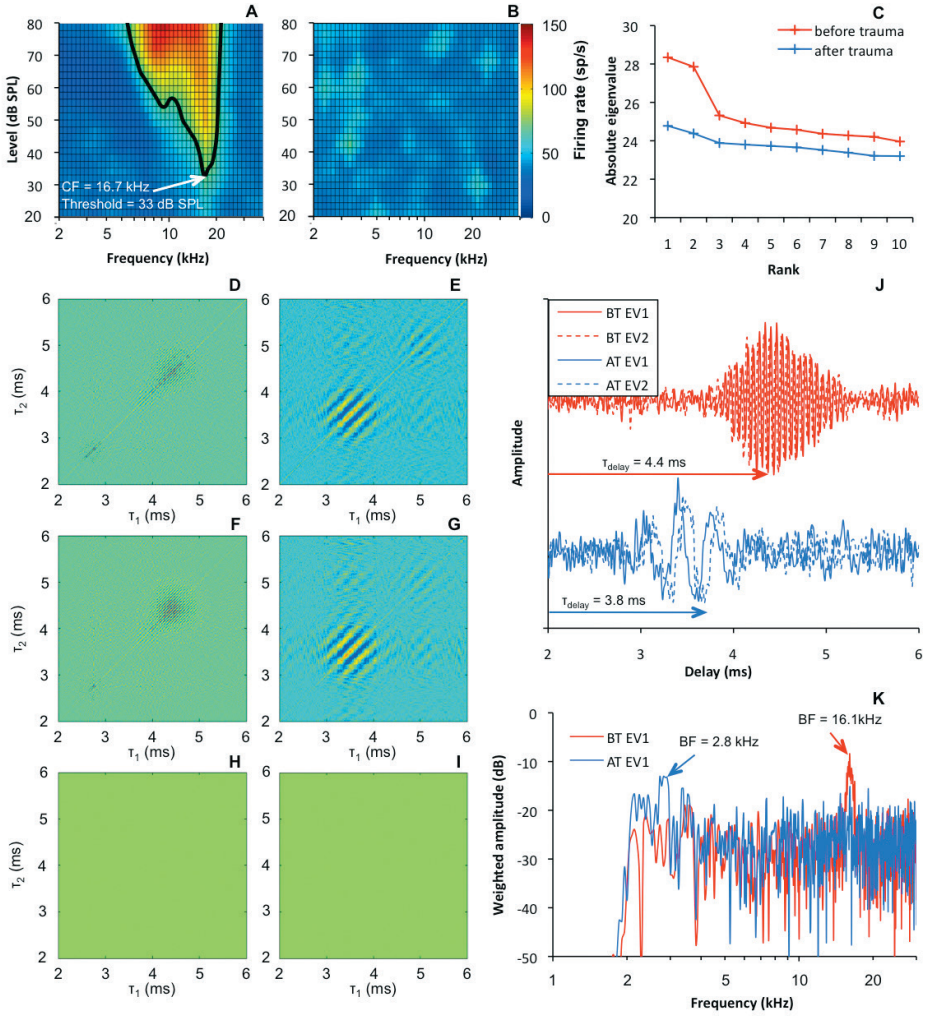

Figure 5.3 Representative example of a high-CF multi unit. Responses to pure tones before **(A)** and after **(B)** acoustic trauma. The excitatory receptive field is contoured by the excitatory tuning curve (black line). **C)** The absolute eigenvalues of the ten highest-ranked subsystems before (red curve) and after (blue curve) acoustic trauma. All subsystems had a positive eigenvalue. The second-order Wiener kernel before **(D)** and after **(E)** acoustic trauma. The original kernel of n = 2048 was zoomed in (2 – 6 ms); there were no stimulus-related oscillations outside this time window. The excitatory kernel, reconstructed from the subsystems with a positive eigenvalue, before **(F)** and after **(G)** acoustic trauma. The inhibitory kernel, reconstructed from the subsystems with a negative eigenvalue, before **(H)** and after **(I)** acoustic trauma (i.e. both are zero as there are no inhibitory subsystems, see panel **C**). **J)** Eigenvectors (EV) of the highest-ranked quadrature pair, as derived from SVD analysis, depicted in the red and blue lines for before (BT) and after (AT) acoustic trauma, respectively. The quadrature pairs consisted of excitatory subsystems (with positive eigenvalues). The highest-ranked and second highest-ranked eigenvector of the quadrature pair is depicted with a solid and a dashed line, respectively. **K)** The amplitude spectrum of the eigenvectors plotted in panel **J**, the same legend applies. Only the frequency response of the highest-ranked eigenvector (EV1) of the quadrature pair is depicted here.

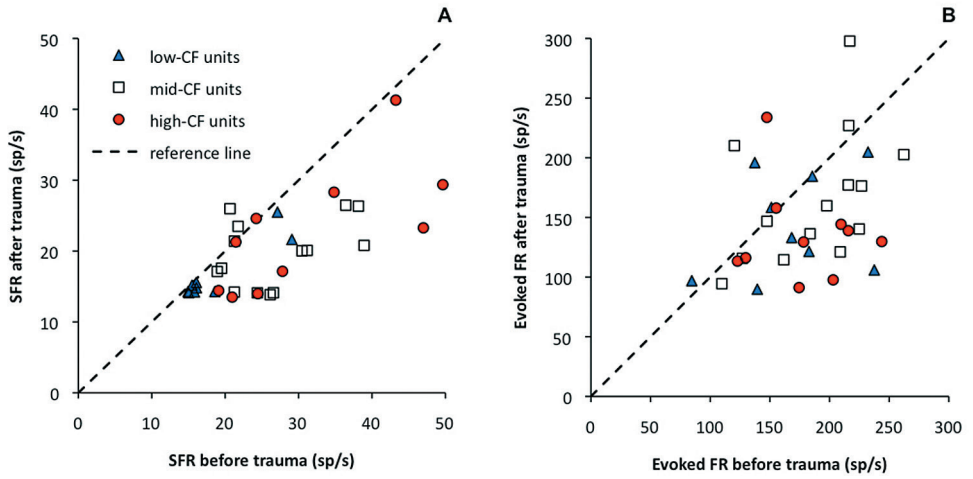

Figure 5.4 Spontaneous and noise-evoked firing rates. **A)** The spontaneous firing rate (SFR) in spikes/sec (sp/s) before acoustic trauma plotted against the SFR after acoustic trauma. A distinction has been made between low-CF units (CF < 3 kHz; depicted with blue triangles), mid-CF units (CF between 3 kHz and 11 kHz; depicted with white squares), and high-CF units (CF > 11 kHz; depicted with red circles). **B)** The noise-evoked firing rate (evoked FR) before acoustic trauma plotted against the evoked FR after acoustic trauma. The same legend as in panel **A** applies.

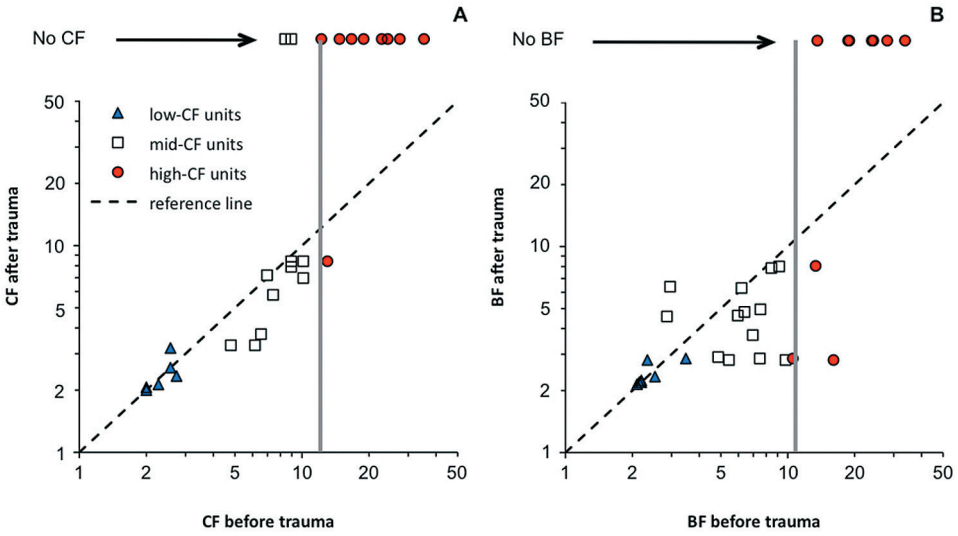

Figure 5.5 Frequency tuning before and after acoustic trauma. **A)** The excitatory CF before and after acoustic trauma. Multi units in which the excitatory receptive field disappeared after trauma are depicted at the top of the plot. The solid grey line indicates the trauma frequency (11 kHz). **B)** The excitatory BF of the highest-ranked eigenvector, derived from SVD of the second-order kernel, before and after acoustic trauma. Multi units in which no stimulus-related component in the second-order kernel could be observed after trauma are depicted at the top of the plot. The same legend as in panel **A** applies.

when observing the receptive fields (CF) and when observing the subsystems of the second-order kernels (BF).

Inhibitory responses to pure tones, and thus a corresponding inhibitory receptive field, were found in fifteen of the thirty-three multi units *before* acoustic trauma, all of which disappeared after acoustic trauma. Wiener-kernel analyses showed that inhibitory subsystems were also found in fifteen of the thirty-three multi units *before* acoustic trauma. However, after acoustic trauma, inhibitory subsystems, as revealed from responses to Gaussian noise, remained present in four multi units. In the other units (n = 11), inhibitory subsystems disappeared after acoustic trauma (see Figure 5.6, markers depicted at the top of the plot). The four multi units that retained inhibitory subsystems all were low-CF units and had a CF lower than or equal to 2.6 kHz (for an example, see Figure 5.1).

Inhibition-to-excitation ratios did not majorly change by acoustic trauma in these multi units (Figure 5.6, blue triangles). Furthermore, there was one low-CF multi unit (CF = 2 kHz) that did not have inhibitory subsystems before acoustic trauma, but had one significant inhibitory subsystem after trauma (see Figure 5.6, marker depicted at the far right of the plot). In all mid-CF and high-CF multi units, inhibitory subsystems disappeared as a result from acoustic trauma.

Together, these data show that excitation and inhibition as revealed from the Wiener kernels in low-CF multi units was not affected. Mid-CF multi units still had excitatory subsystems in response to noise, but did not have inhibitory subsystems anymore. In high-CF multi units, both excitation and inhibition was affected by acoustic trauma.

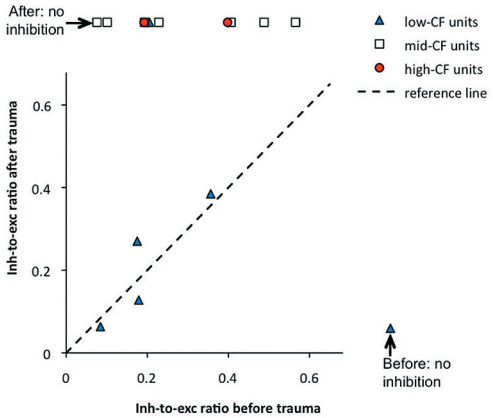

Figure 5.6 Inhibition before and after acoustic trauma. The inhibitory subsystems disappeared in all mid- and high-CF multi units that did have inhibitory subsystems before acoustic trauma (white squares and red circles at the top of the panel). In four low-CF multi units (blue triangles), inhibitory subsystems were preserved. The inhibition-to-excitation ratio, previously defined in Chapter 4, was not affected by acoustic trauma in these units.

3.4.3 Group delays

The group delay of the unit's highest-ranked eigenvector was not significantly changed by acoustic trauma (Figure 5.7; paired-sample T-test: $T(25) = 1.248$, $p = 0.223$). In the four multi units that had inhibitory subsystems before and after acoustic trauma (see Figure 5.6), the first inhibitory eigenvector had a longer group delay than the first excitatory eigenvector both before and after acoustic trauma.

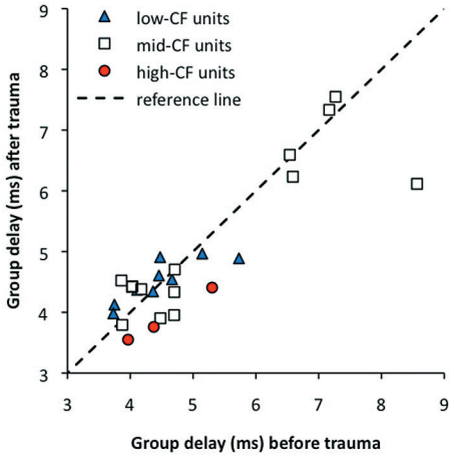

Figure 5.7 Group delays. The group delay of the highest-ranked eigenvector before acoustic trauma plotted against the group delay of the highest-ranked eigenvector after acoustic trauma.

4. Discussion

With this study, we showed that the effects of acoustic trauma can be identified with Wiener-kernel analysis. This analysis demonstrated that excitation and inhibition in low-CF multi units (CF < 3 kHz) was not affected, inhibition in mid-CF multi units (CF between 3 kHz and 11 kHz) disappeared whereas excitation remained, and excitation and inhibition in high-CF multi units (CF > 11 kHz) both disappeared as a result from acoustic trauma by an 11-kHz tone. This specific differentiation could not be identified with receptive-field analysis, which showed that inhibitory responses to the presented pure tones disappeared in all units. Furthermore, we showed that multi units were tuned to lower frequencies immediately after trauma as compared to before acoustic trauma. This could be observed in the receptive-field analysis (excitatory CF) as well as in the Wiener-kernel analysis (excitatory BF). And lastly, we showed that spontaneous and noise-evoked firing rates were significantly decreased immediately after acoustic trauma.

Inhibitory responses to pure tones, and thus also inhibitory receptive fields and tuning curves, disappeared in all units immediately after acoustic trauma. Furthermore, Wiener-kernel analyses showed that inhibitory subsystems disappeared in mid-CF and high-CF multi units, but not in low-CF multi units. The mid-CF multi units are of the most interest, since they retained their excitatory components but not their inhibitory components, and thus showed a clear disruption of the balance between excitation and inhibition.

The apparent discrepancy between Wiener-kernel analysis and tone-evoked receptive-field analysis can be understood by considering a basic difference between the analyses. A tone-evoked response is always the net result of excitation and inhibition. Presumably, the excitatory receptive field (areas within the black contour in panels A of Figures 5.1 – 5.3) is the result of excitatory and inhibitory input to the IC neuron being studied. Hence, the inhibitory strength in a unit's response can only be assessed from inhibitory receptive fields that are distinct from the excitatory receptive field. In contrast, the Wiener-kernel analysis is able to disentangle excitation and inhibition within the excitatory passband of the neuron (Yamada and Lewis, 1999; Chapter 4). In other words, it is possible to estimate the relative contribution of excitation and inhibition at stimulus frequencies that overall excite the neuron. Consequently, the tone-evoked receptive field and Wiener kernels reflect different measures of excitation and inhibition (see also Chapter 4).

Our results are consistent with molecular studies, that show a reduction in inhibitory neurotransmitters and their receptors in the IC following acoustic trauma (Szczepaniak and Møller, 1995; Milbrandt et al., 2000; Dong et al., 2010a). Furthermore, our results correspond to a disrupted balance of excitation and inhibition following acoustic trauma, and additionally showed that the disrupted balance resides specifically at multi units with a CF directly below the trauma frequency (Scholl and Wehr, 2008; Noreña, 2011; Llano et al., 2012; Chapter 2).

These results may be related to the neural mechanisms involved in hyperacusis. It has been suggested that hyperacusis is related to an upregulation of central gain in the brainstem (Gu et al, 2010; Knipper et al, 2013; Hickox and Liberman, 2014). Our results indicate that tone-induced acoustic trauma affects inhibition of mid-frequency neurons tuned to frequencies below the trauma frequency. The sensitivity of these neurons remained relatively unaffected. This provides a potential substrate for hyperactivity in response to auditory stimuli of moderate levels, which might be an equivalent of hyperacusis (Zeng, 2013).

The release of inhibition, as described above, could have also been involved in the changes we observed in the excitatory CF and excitatory BF, that shifted towards lower frequencies (Wang et al., 2002). Since these results were obtained immediately following acoustic trauma, it is not likely that the downward shift in frequency tuning resulted from the generation of new pathways towards the high-CF and mid-CF multi units. This indicates that rather a damage in inhibitory pathways unmasked sensitivity to the lower frequencies. Furthermore, a downward shift in frequency tuning of auditory neurons following an acoustic trauma-induced high-frequency hearing loss is consistent with previous findings in the

auditory cortex and the IC (Noreña and Eggermont, 2003, 2005; Yang et al., 2011; Niu et al., 2013).

A reduction in spontaneous firing rate of the IC immediately following acoustic trauma has previously been shown by Niu and colleagues (2013). However, other studies, including Chapter 2 of the current thesis, have reported no change in the spontaneous firing rate immediately after exposure (Noreña and Eggermont, 2003; Chapter 2). The within-unit design of the current study allowed us to directly compare firing rates of one multi unit before and after acoustic trauma, which provided additional sensitivity for this reduction as compared to the study in Chapter 2. Furthermore, noise-evoked firing rates were also significantly reduced immediately after acoustic trauma. Our results showed that the average reduction in spontaneous firing rate alone could not account for the reduction in noise-evoked firing rate. This indicated that an additional mechanism should have accounted for the reduced noise-evoked firing rates, such as a reduced sensory input due to acoustical damage at the periphery. Our findings are consistent with previous studies in the IC, that likewise showed unchanged or reduced firing rates evoked by a number of pure tones immediately after acoustic trauma (Sun et al., 2012; Chapter 2).

In summary, we showed that Wiener-kernel analysis confirmed and complemented current knowledge about the disrupted balance between excitation and inhibition following acoustic trauma in the IC. The use of Gaussian noise as a stimulus gave an advantage over pure tones, when studying excitation and inhibition. By using Wiener-kernel analysis and a decomposition of the second-order kernel with SVD, additional information about inhibitory responses that occur within the frequency band of excitation could be unraveled. This showed that the balance between excitation and inhibition in mid-CF units, that resided at the lower edge of the exposure frequency, was particularly vulnerable for acoustic trauma. These results are of potential interest as a central neural correlate of noise-induced hyperacusis.

Acknowledgements

The authors want to thank Annemieke Smit-van Oosten, Michel Weij, and Andre Zandvoort for technical support during the experiments and Russ Snyder for showing us the surgical procedures involved in the IC recordings.

This work was supported by the Heinsius Houbolt Foundation and the Stichting Gehoorgestoorde Kind. The study is part of the research program of our department: Healthy Aging and Communication.

Chapter 6

Spontaneous behavior in noise and silence: a possible new measure to assess tinnitus in guinea pigs

A.N. Heeringa, M.J.H. Agterberg, and P. van Dijk

Published in: Frontiers in Neurology (2014), 5: 207. doi: 10.3389/fneur.2014.00207.

Abstract

This study describes two experiments that were conducted in search for a behavioral paradigm to test for tinnitus in guinea pigs. Conditioning paradigms are available to determine the presence of tinnitus in animals and are based on the assumption that tinnitus impairs their ability to detect silent intervals in continuous noise. Guinea pigs have not been subjected to these paradigms yet, therefore we investigated whether guinea pigs could be conditioned in the two-way shuttle box paradigm to respond to silent intervals in noise. Even though guinea pigs could be trained relatively easy to respond to the presence of a noise interval, training guinea pigs to silent intervals in noise was unsuccessful. Instead, it appeared that they became immobile when the continuous stimulus was suddenly stopped. This was confirmed by the next experiment, in which we subjected guinea pigs to alternating intervals of noise and silence with a random duration between 30 – 120 s. Indeed, guinea pigs were significantly longer immobile during silence compared to during noise. By interpreting immobility as a signature of perceiving silence, we hypothesized that the presence of tinnitus would reduce immobility in silence. Therefore, we unilaterally exposed one group of guinea pigs to an 11-kHz tone of 124 dB SPL for 1 hour. A subset of the exposed animals was significantly more active in silence, but also more active in noise, as compared to the control group. The increased mobility during silent intervals might represent tinnitus. However, the increased mobility in noise of this group implies that the observed behavior could have derived from e.g. an overall increase in activity. Therefore, conducting validation experiments is very important before implementing this method as a new screening tool for tinnitus. Follow-up experiments are discussed to further elucidate the origin of the increased mobility in both silence and noise.

Keywords: guinea pigs; tinnitus; behavioral model; shuttle box; auditory; spontaneous behavior

Abbreviations: ABR, auditory brainstem response; CAR, conditioned avoidance response; CS, conditioned stimulus; RM-ANOVA, repeated-measures analysis of variance; UCS, unconditioned stimulus

1. Introduction

In the search for a treatment for tinnitus, animal models have proven to be useful to correlate tinnitus-inducing treatments, such as noise exposure, with neurophysiological changes in the central auditory system (Salvi et al., 1990; Noreña and Eggermont, 2003; Shore et al., 2008). However, the validity of these animal models critically depends on a behavioral paradigm to test whether an animal perceives tinnitus.

In the last few decades, several behavioral paradigms have been developed, which are all based on the assumption that perception of tinnitus impairs the ability to detect silence (Turner, 2007). Current models can be roughly divided between two categories: 1) conditioning paradigms, in which animals are trained to respond to silent intervals in background noise (Jastreboff et al., 1988a), and 2) startle reflex paradigms, in which the acoustic startle reflex is inhibited by a short silent gap in background noise preceding the startle stimulus (Turner et al., 2006). In both paradigms, it is determined whether animals are still able to detect a silent interval after a tinnitus-inducing treatment, such as noise exposure or salicylate.

Guinea pigs are frequently used to study neurophysiological changes after tinnitus-inducing treatments (e.g. Jastreboff and Sasaki, 1986; Takemura et al., 2004; Noreña et al., 2010; Mulders et al., 2011). Recent studies, that make use of the startle reflex paradigm, suggest that guinea pigs are indeed able to experience tinnitus (Dehmel et al., 2012; Robertson et al., 2013). However, the startle reflex paradigm needs to be adjusted for optimal assessment of tinnitus in guinea pigs (Berger et al., 2013). On the contrary, as to our knowledge, conditioning paradigms have not been used to assess tinnitus in guinea pigs yet.

One successful paradigm to condition guinea pigs to acoustic stimuli was presented by Philippens and colleagues (Philippens et al., 1992). This paradigm involved the use of a two-way shuttle box (Diamond and Neff, 1957). Within a few days of training, guinea pigs learn to shuttle from one compartment to the other upon presentation of a narrowband noise, i.e. the conditioned stimulus (CS). By their shuttle behavior, they avoid an unpleasant stream of air that serves as the unconditioned stimulus (UCS).

The initial aim of the current study was to develop a conditioning model to detect tinnitus in guinea pigs by using the shuttle-box paradigm. Experiment 1 examined the ability of guinea pigs to be trained in the shuttle box to a silent interval in continuous noise. Although training guinea pigs to shuttle at the presence of noise as CS was relatively easy, they could not be trained to shuttle in response to a silent interval in background noise. Instead, it appeared that the behavioral activity of the animals was inhibited during the silent interval. Therefore, we designed another experiment to investigate spontaneous behavior of guinea pigs during silence. In experiment 2 of the present study, guinea pigs were positioned in the shuttle box during alternating intervals of noise and silence. We evaluated the mobility of guinea pigs during silence and noise, respectively. This spontaneous behavior might explain the failure to train guinea pigs to silence (experiment 1). Furthermore, in experiment 2, a subgroup of animals was unilaterally exposed for one hour to an 11-kHz tone of 124 dB sound

pressure level (SPL), which has been previously proposed to induce tinnitus in guinea pigs (Robertson et al., 2013). We hypothesized that animals that hear tinnitus are no longer able to experience silence, and will show increased mobility during the silent intervals.

2. Methods

This study includes two experiments. The results of experiment 1 were used to design experiment 2. Both experiments were approved by the Animal Experiment Committee of the University of Groningen in compliance with Dutch law and regulations (DEC-RUG # 6068C and 6068E, respectively).

2.1 Experiment 1: Training to respond to noise and silent intervals

2.1.1 Animals

For experiment 1, ten male adult albino guinea pigs (Dunkin Hartley; Harlan Laboratories, Horst, the Netherlands), weighing between 300 and 360 grams at the start of the experiment, were divided over two experimental groups. Group 1 was first trained to noise and subsequently to silent intervals in continuous noise; group 2 was only trained to silent intervals in continuous noise. During the ten-day acclimatization period, the animals were socially housed in the Central Animal Facility of the University Medical Center Groningen on a 12-hour light:12-hour dark cycle, and were handled every other day. Food and water were provided ad libitum. In the housing room, temperature and humidity were kept constant, and background noise from a radio was present at 50 dB(A). One guinea pig was excluded based on a negative Preyer's reflex at the start of the training (Böhmer, 1988).

2.1.2 The shuttle box

The shuttle box, adapted from Agterberg et al. (2010), consisted of two compartments of equal size (23 x 23 x 23 cm), which were connected by a passage (Agterberg et al., 2010). Infrared beams placed on each side of the passage detected shuttling of the guinea pig between compartments. A forceful stream of air (maximum duration 20 s), that was directed downwards into the compartment where the guinea pig was at that moment, and that terminated upon shuttling, served as the UCS. Guinea pigs were trained to avoid the UCS by shuttling from one compartment to the other upon presentation of the CS. The CS was either a band-limited noise (2-19 kHz, 6 dB/octave slope, 78 dB SPL, 15 s) or a silent interval (15 s) in continuous noise (2-19 kHz, 6 dB/octave slope, 78 dB SPL). Note that in the last case the absence of sound, rather than the noise, served as CS. Acoustic stimuli were presented by two Piezo tweeters (PH8; Velleman) placed above each of the compartments of the shuttle box, respectively. The inter-trial interval had a random duration between 20 and 30 s during training to noise as CS (as described by Agterberg et al., 2010), and a random duration between 60 and 90 s during training to silent intervals as CS (as described by Sansone and

Bovet, 1970). This behavioral training paradigm has been described previously with respect to detection of acoustic stimuli with different sound levels (Agterberg et al., 2010) and with respect to detection of intracochlear electrical stimulation (Agterberg and Versnel, 2014). Custom-made LabView software (National Instruments corp.) generated acoustic stimuli, controlled UCS and CS presentation, and acquired shuttle responses. Background noise in the experimental room was on average 44 dB(A) and was attenuated by the use of a sound-attenuating box, which was placed over the shuttle box.

2.1.3 Behavioral training

In preparation for training, guinea pigs were allowed to habituate to the shuttle box for twenty minutes per day. Prior to training with noise as CS, guinea pigs were simply placed in the shuttle box and habituated in silence, and prior to training with silent intervals, the habituation occurred in the presence of a continuous noise of 78 dB SPL. A shuttle response during the CS was scored as a correct avoidance response (CAR). The first two training sessions consisted of ten trials. During the remaining sessions, the number of trials per session was increased to twenty. In order to prevent excessive exposure to the UCS, sessions were ended when animals failed to demonstrate a CAR for seven consecutive trials. Habituation and training always started on Wednesday and consisted of five and ten working days, respectively. There were no habituation and training sessions during the weekends.

2.1.4 Auditory brainstem response recordings

To verify that the guinea pigs were able to hear the acoustic stimuli, hearing thresholds were determined after the last training session by recording auditory brainstem responses (ABRs) to a broadband click of 0.1 ms. Guinea pigs were anesthetized with isoflurane (5% for initiating and 2% for maintenance of the anesthesia) in a mixture of medical air and oxygen. Body temperature was maintained at 38.5 °C by a heating pad, and heart rate and blood oxygen saturation were monitored using a pulsoximeter. Recording electrodes were placed subdermally at the vertex and behind each pinna. Signals were generated by a real-time processor (RP2.1, Tucker Davis Technologies Inc.), attenuated (PA5, TDT Inc.), and presented by an electrostatic speaker driver and speaker (ED1 and ES1, respectively; TDT Inc.). The free-field speaker (ES1) was positioned at approximately 2 cm in front of the nose of the animal. ABRs were amplified (EG&G Instruments, 5113 pre-amp), recorded by a second real-time processor, and saved on a PC using BioSigRP software (TDT Inc.). Stimulus presentation level started at 97 dB SPL and decreased with steps of 10 dB. ABRs were averaged over 1000 presentations. Thresholds were considered the lowest stimulus level to which distinct ABR waves were observed.

2.2 Experiment 2: Spontaneous behavior in noise and in silence

2.2.1 Animals

For experiment 2, fifteen guinea pigs, weighing between 376 and 488 grams at the start of the experiment, were used. The guinea pigs were divided over two groups: an experimental group (n = 10) that was exposed to a loud tone and a control group (n = 5) that was sham-exposed. The experimental group was larger because previous studies demonstrated that unilateral overexposure leads to tinnitus in only a subset of animals (Dehmet et al., 2012; Coomber et al., 2014). (Sham-) exposure was applied in the afternoon of day 1 and spontaneous behavior to noise and silence was assessed in the morning of the following day. ABRs were recorded immediately before and after (sham-) exposure, and after behavioral testing (Figure 6.2). Housing conditions were similar to conditions in experiment 1.

2.2.2 Auditory brainstem response

ABRs for experiment 2 were acquired with the same equipment as used in experiment 1 (section 2.1.4), but were measured for both ears separately. The free-field speaker was positioned against the pinna of the ipsilateral ear and the contralateral ear was plugged with wax (ohropax; OTC Medical BV). ABRs were recorded for responses to 0.1 ms clicks and to pure tones of 3 kHz, 6 kHz, 11 kHz, 15 kHz, and 22 kHz (3 ms duration, 0.2 ms $\cos^2$ ramps). Stimuli were calibrated using a measuring microphone (Bruël & Kjær; type 2670) and amplifier (B&K; type 2610). ABR thresholds were evaluated by an observer that was blind for stimuli and treatments.

2.2.3 Sound exposure

Anesthesia and monitoring of the animals during sound exposure were as described in section 2.1.4. The cone of a Piezo tweeter was removed and a custom-made funnel was attached to the speaker. The narrow end of the funnel was positioned inside the ipsilateral ear and the contralateral ear was plugged with wax to reduce air-conduction of the trauma stimulus. A continuous 11-kHz tone of 124 dB SPL was presented for 1 h to the anesthetized animal. The stimulus was designed in RPvdsEx (TDT, Inc.), generated by RP2.1 (TDT, Inc.) and amplified by a Philips amplifier (Philips PM 5170). The stimulus was calibrated at the narrow end of the funnel by a measuring microphone (B&K; type 2670) and amplifier (B&K; type 2610). The sham-exposed group was treated as the experimental group, without the stimulus being presented by the speaker.

2.2.4 Testing of behavioral activity in noise and silence

Spontaneous behavior of guinea pigs in noise and silence was studied in the shuttle box. The stimulus (designed by custom-made programs in MatLab [2010b, Mathworks]), consisted of alternating noise (band limited between 2-19 kHz, 88 dB SPL) and silence intervals. Noise

and silence intervals had durations equal to 30 s, 60 s, 90 s, and 120 s. The intervals were presented in a quasi-random order. However, each session started with a noise interval. Every noise and silence interval was presented twice, hence the total duration of behavioral testing was 20 minutes. For each animal, the order of durations of the intervals within the stimulus were individually randomized. Examples of the above-described stimulus can be found in Figure 6.4. The spontaneous behavior of the guinea pig and the acoustic stimulus were recorded with a smart phone (iPhone 4S, Apple Inc.), that was positioned approximately 1 m above the shuttle box.

Video recordings were muted and analyzed (VLC media player, version 1.1.5) at 0.33 times the rate, by an observer blind for the treatment of the animal. Spontaneous behavior was scored for every second, as either immobile, moving, walking, or shuttling. Moving refers to movements that did not involve a change of location, e.g. movements of the head. Walking refers to relocation of at least one of the paws. In shuttling, the animal moved from one compartment of the shuttle box to the other, i.e. a shuttle response. One shuttle response counted for one second. If an animal showed two types of behavior within one second, the most active type of behavior was scored for. Thus, immobility was only scored when the animal was sitting still for the entire second. In the analyses on group level, immobility (in percentage of time) was chosen as the main outcome measure.

2.3 Statistics

Statistical analyses were performed using repeated-measures analysis of variance (RM-ANOVA) and Student's T-test, as appropriate (IBM SPSS Statistics; Version 19). Significance was determined at $p < 0.05$. Data in figures display mean ± sem.

3. Results

3.1 Experiment 1: Training to respond to noise and silence intervals

ABRs to a free-field broadband click revealed that hearing thresholds ranged from 26 to 47 dB SPL across animals. This indicated that all animals could hear the noise of 78 dB SPL, which was either presented as a CS or as a continuous noise with a silent interval. Within ten training sessions to noise as CS (n1 – n10), guinea pigs of group 1 gradually increased their mean performance from < 10% CAR in session one (n1) to approximately 80% CAR in session ten (n10). This is indicative of a learning effect over time (Figure 6.1, red curve, sessions n1 – n10; RM-ANOVA: $F = 9.048$, $p < 0.001$).

Both experimental groups were tested for their ability to condition to a silent interval in continuous noise as CS. Animals in group 1, who were previously trained to noise, showed no scores above 10% CAR in any training session (Figure 6.1, red curve, sessions s1 – s10). Guinea pigs of group 2, that were naïve for training in the shuttle box, had no scores above 0% CAR in any of the ten training sessions (Figure 6.1, blue curve, session s1 – s10).

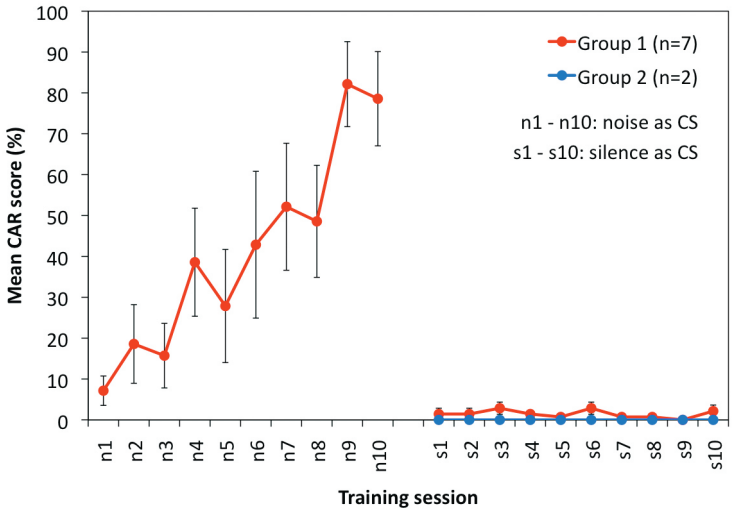

Figure 6.1 Results of experiment 1: training to respond to noise and silent intervals. Mean (± sem) CAR scores of guinea pigs of group 1 trained to noise (n=7, red circles, session n1 – n10) and subsequently trained to silence (session s1 – s10), and of guinea pigs of group 2 (n=2, blue circles) trained only to silence (session s1 – s10). RM-ANOVA revealed that performance of group 1 increased during session n1 – n10 ($F = 9.048$, $p < 0.001$). In contrast, the animals did not show any performance increase during training to silence (s1-s10 of group 1 and 2 combined, RM-ANOVA: $F = 0.696$, $p = 0.585$).

3.2 Experiment 2: Spontaneous behavior in noise and in silence

Auditory thresholds assessed before exposure (ABR 1 in Figure 6.2) were similar between the control and the experimental group, for all measured stimuli (Figure 6.3A, RM-ANOVA: n.s.). Immediately following exposure (ABR 2 in Figure 6.2), thresholds of the exposed ear of the experimental group were elevated for all stimuli, except 3 kHz (Figure 6.3B, orange circles; RM-ANOVA: $F(5,80) = 25.125$, $p < 0.001$, Bonferroni corrected paired T-tests, $p < 0.05$). One day after exposure (ABR 3 in Figure 6.2), thresholds partly recovered, but were still significantly elevated, except for 3 kHz and 6 kHz (Figure 6.3B, purple circles; RM-ANOVA: $F(5,85) = 18.426$, $p < 0.001$, Bonferroni corrected paired T-tests, $p < 0.05$).

Thresholds of the sham-exposed ears were not affected (Figure 6.3B, squares; RM-ANOVA: n.s.). In addition, unilateral (sham-)exposure did not affect the auditory thresholds of the unexposed ear (Figure 6.3C; RM-ANOVA: n.s.), indicating that the unilateral exposure only affected the ipsilateral ear. Accordingly, all animals were able to hear the stimulus with at least one ear at the day of behavioral testing. The (normal-hearing) control animals were predominantly immobile during silent intervals, as can be seen in the representative example of spontaneous behavior of a sham-exposed guinea pig (C3) during noise and silence intervals (Figure 6.4A; noise intervals are indicated with shaded columns, silence intervals with white columns). This animal was immobile during silence for 99.5% of the time (597 of 600 s).

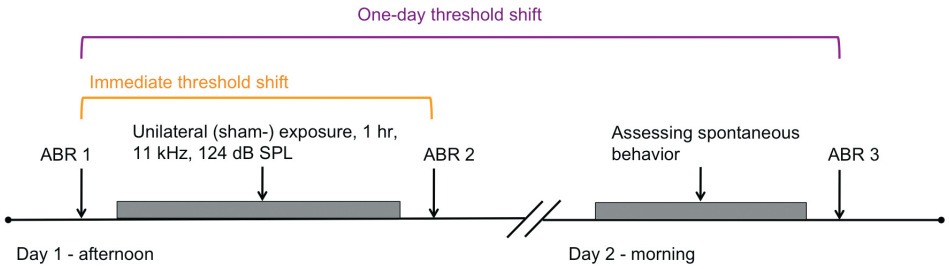

Figure 6.2 Timeline of experiment 2. In the afternoon of day 1, guinea pigs were either unilaterally exposed to an 11-kHz pure tone of 124 dB SPL, or sham-exposed for 1 hour. ABRs were measured immediately before and after the (sham-) exposure, indicated by ABR 1 and ABR 2, respectively. The difference between ABR 1 and ABR 2 was considered the immediate threshold shift (in orange). In the morning of the subsequent day, behavioral responses to noise and silence were assessed. ABRs were measured subsequently (ABR 3). The difference between ABR 1 and ABR 3 was considered the one-day threshold shift (purple).

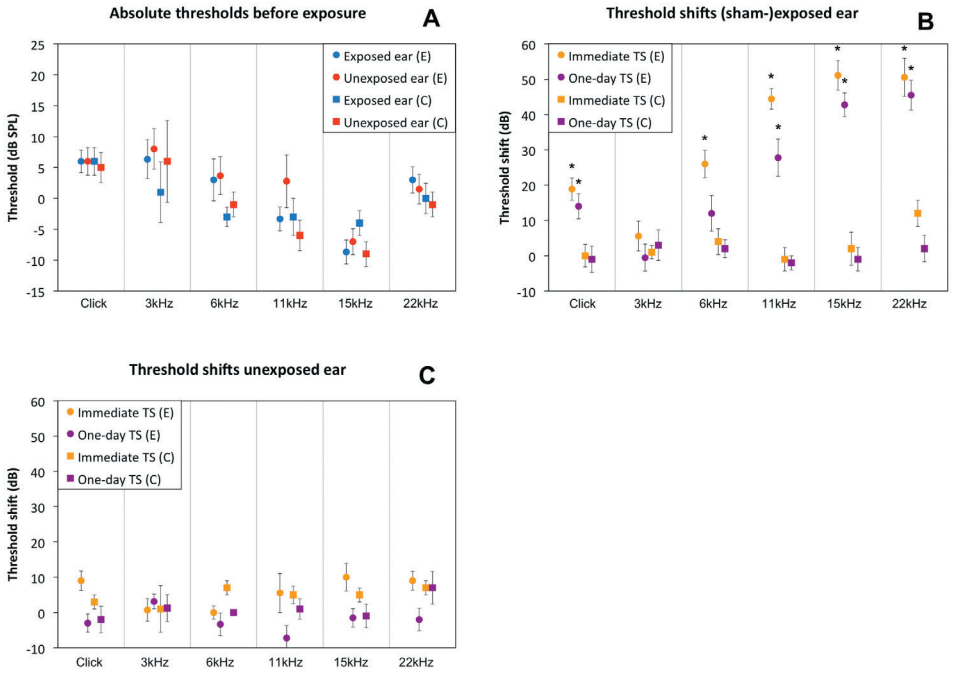

Figure 6.3 Auditory thresholds and sound-induced threshold shifts. Absolute hearing thresholds before exposure were similar between the control group (squared markers) and the experimental group (circled markers). Before exposure, there were no differences between the two ears in both groups (red vs. blue markers) **(A)**. Threshold shifts immediately (orange curves) and one day (purple curves) after overexposure in the exposed ear **(B)** and the unexposed ear **(C)** of the experimental group (circled markers) and the control group (squared markers). * indicates a significant threshold shift relative to ABRs before exposure (ABR 1; T-tests Bonferroni corrected, $p < 0.05$).

During noise intervals, guinea pig C3 was immobile for only 73% of the time (438 of 600 s) and engaged in the other scored behaviors for the remaining time, i.e. shuttle (1%), walking (8%), and moving (18%). Studying spontaneous behavior of the sound-exposed animals, however, revealed that immobility during silence varied more in the sound-exposed group compared to the sham-exposed group. Figure 6.4B displays a representative example of a guinea pig (E1) that showed spontaneous behavior that was similar to the control animals. This animal was immobile during silence for 97.2% of the time (583 of 600 s). In noise, guinea pig E1 was immobile for only 75.8% of the time (455 of 600 s) and was moving and walking for 20% and 4.2% of the time, respectively. Guinea pig E1 did not shuttle in any interval of the stimulus. On the contrary, guinea pig E8 became less immobile in the silent intervals after approximately ten minutes of behavioral testing. On average, this animal was immobile during silence for 84.2% of the time (505 of 600 s; Figure 6.4C). Additionally, guinea pig E8 shuttled six times during the recorded time, of which twice during a silent interval. Furthermore, guinea pig E2 was relatively active during most of the silent intervals and was immobile for 57.8% of the time in silence (347 of 600 s). This animal shuttled 22 times in total, of which 8 times in the silent intervals.

Exposed guinea pigs were divided between an 'affected' and an 'unaffected' group based on their immobility in silence. The mean immobility in silence (98.4%) minus three times the standard deviation of the control group (3 x 0.98%) was the criterion above which an animal of the exposed group was classified as 'unaffected'. When the immobility in silence of an exposed animal was lower than the criterion, it was classified as an 'affected' animal. Six of the ten exposed guinea pigs (E1, E3, E4, E5, E7, and E10) showed similar behavior during silence as the control animals (>95.5% immobility in silence) and were classified as 'unaffected'. The remaining four exposed guinea pigs (E2, E6, E8, and E9) had a immobility in silence lower than the 95.5%, and were classified as 'affected' (Figure 6.5A).

Sham-exposed animals were significantly longer immobile during silence than during noise (Figure 6.5B, blue bars; paired-sample T-test: $T(4) = 7.240$, $p < 0.005$). Furthermore, sham-exposed animals shuttled on average 8 times during noise intervals (range 5-11), yet, they never shuttled in the silent intervals. The percentage immobility of the 'affected' group was significantly different from both the control group and the 'unaffected' group, both in silence and in noise (Figure 6.5B; RM-ANOVA: $F(2,12) = 20.06$, $p < 0.001$, Bonferroni corrected pair-wise comparisons). The effect of acoustic condition on immobility was significant (RM-ANOVA: $F(1,12) = 164.7$, $p < 0.001$) and there was no interaction between acoustic condition and the groups (RM-ANOVA: $p > 0.68$).

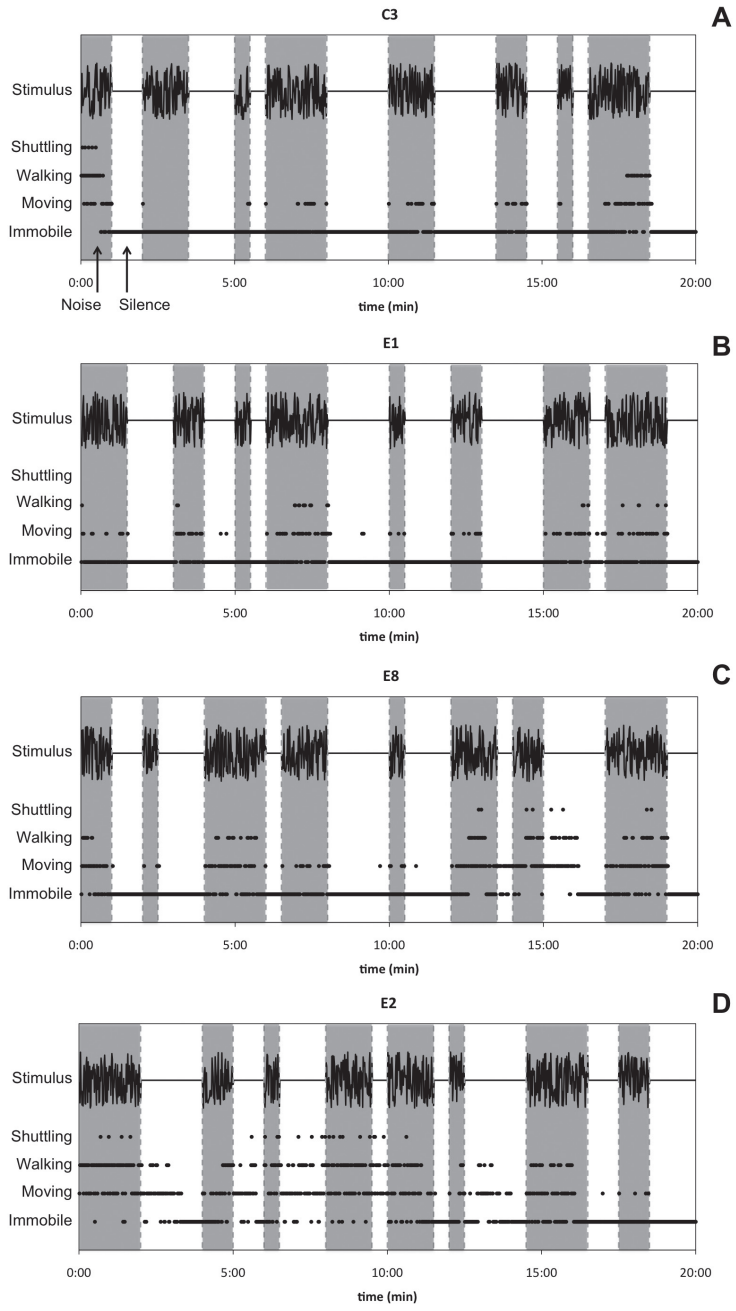

Figure 6.4 Raw data of spontaneous behavior in noise and silence. Examples of behavior during noise (shaded timeframes) and silence (unshaded timeframes) of a control animal **(A)**, an exposed animal classified as 'unaffected' **(B)**, and two exposed animals classified as 'affected' (**C** and **D**, respectively). Every dot represents one second, every second was classified for either immobile, moving, walking, or shuttling (see Material and Methods, section 2.3.3). As can be seen, the two animals classified as 'affected' **(C, D)** were more active during silent intervals compared to the control **(A)** and the 'unaffected' animal **(B)**.

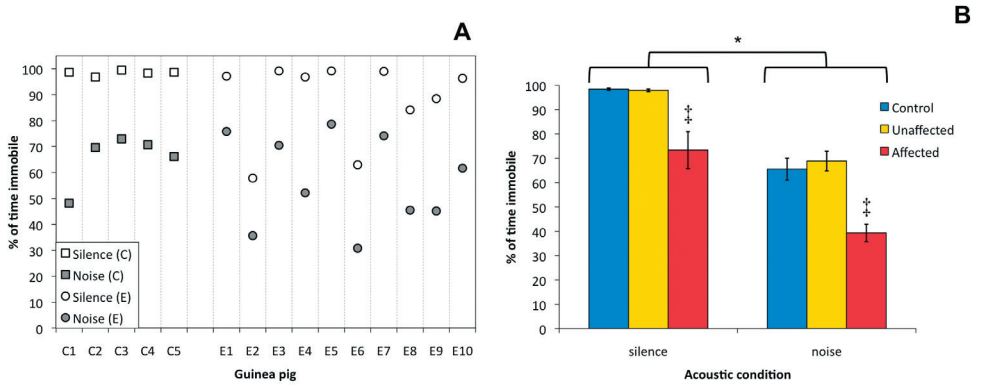

Figure 6.5 Immobility in noise and silence. **A)** Individual immobility (% of time) in silence (white markers) and in noise (gray markers) for the control group (C1 – C5; squares) and the exposed group (E1 – E10; circles). **B)** Mean immobility (% of time) ± sem during noise and during silence for the control group (blue), the 'unaffected' group (yellow), and the 'affected' group (red). There was a significant difference between immobility in noise and in silence (*, RM-ANOVA: $F(1,12) = 164.7$, $p < 0.001$). Furthermore, the 'affected' group was significantly less immobile than the control group and the 'unaffected' group, both in silence and in noise (‡, RM-ANOVA: $F(2,12) = 20.06$, $p < 0.001$, Bonferroni corrected pair-wise comparisons).

4. Discussion

The present data demonstrate that guinea pigs can be trained relatively easy to shuttle in response to an acoustic CS. However, training to shuttle in response to silent intervals in noise was unsuccessful (experiment 1). We showed in experiment 2 that normal-hearing guinea pigs hardly moved during silence, while they frequently moved during presentation of noise. This natural tendency for immobility during silence may explain the failure to train guinea pigs to silence in experiment 1. Furthermore, unilateral exposure to a loud sound led to a decrease in immobility during silence in a subset of the exposed animals. This might suggest that these exposed animals (labeled as ´affected´) no longer experienced silence: they may have perceived tinnitus. However, these animals were also more active in noise compared to the control animals. Therefore, it is not clear whether the 'affected' animals were under stimulus control, i.e. the increased activity in both silence and noise could have been the result from additional factors other then the presented acoustic stimuli. These additional factors might include tinnitus, but can also involve, for example, an overall increase in general activity or anxiety. Accordingly, conducting several validation experiments is crucial before this method can be reliably used as a screening tool for tinnitus in guinea pigs. These necessary validation experiments are extensively discussed below and should further elucidate the origin of the abnormal behavior of these animals.

By showing that guinea pigs can be trained within ten days to respond with a shuttle response to a noise interval, we confirmed earlier studies with the shuttle box (Philippens

et al., 1992; Agterberg et al., 2010; Agterberg and Versnel, 2014). It has been shown that guinea pigs can generalize this response to other sound levels and to intracochlear electrical stimulation (Agterberg et al., 2010; Agterberg and Versnel, 2014). Guinea pigs can also be trained to respond to pure tones, although in different training paradigms (Crifò, 1973; Prosen et al., 1978; Bakin et al., 1996; Galván and Weinberger, 2002; Hu et al., 2009). In spite of these positive findings, training guinea pigs to respond to silent intervals (CS) in noise was unsuccessful, both in naïve and previously trained animals. Instead, during experiment 1, guinea pigs seemed to become immobile at the onset of silence. This might explain why a successful conditioning model to test for tinnitus in guinea pigs has not been reported in literature yet.

Experiment 2 confirmed that, indeed, normal-hearing guinea pigs demonstrated significantly more immobility in silence than in noise. Moreover, normal-hearing guinea pigs did not demonstrate a single spontaneous shuttle response during a silent interval, while during noise, they demonstrated on average 8 spontaneous shuttle responses in 10 minutes. The mobility during a noise interval might have been crucial for successful training in the shuttle box in experiment 1, and explains why training to silent intervals was unsuccessful.

Furthermore, in experiment 2, the guinea pigs in the experimental group were unilaterally exposed for one hour to an 11-kHz tone of 124 dB SPL. This type of acoustic trauma has previously been proposed to induce tinnitus in guinea pigs (Robertson et al., 2013). Our results showed that a subset of the exposed animals, classified as 'affected', were more active both in noise and in silence (see Figure 6.5B). This finding can be due to several factors, which are described in the following paragraphs.

For example, natural variation in general activity might be an explanation for this behavior. A natural variation in anxiety and exploratory behavior is apparent in mice and rats (Kazlauckas et al., 2005; Herrero et al., 2006). Therefore, it is conceivable that the guinea pigs in the 'affected' group were more active by nature, resulting in less immobility in both silence and noise. However, the finding that normal-hearing animals hardly moved in silence was a robust result, as reflected by the failed training in experiment 1, the control group of experiment 2, several pilot experiments with normal-hearing guinea pigs in our lab (data not shown), and by the literature (Agterberg and Versnel, 2014). Specifically, in the control group of experiment 2 the mean immobility rate was 98.4% with a standard deviation of 0.98%. The immobility of the four animals classified as 'affected' was between 10 and 42 standard deviations from the mean of the control group. Therefore, it is unlikely that the increased mobility of the affected guinea pigs is caused by natural variation across all animals.

Another factor, that could be involved in the observed increase in behavioral activity in noise and silence, is the hearing loss induced by the sound exposure. Previous research has shown that hearing loss affects the startle response (Lobarinas et al., 2013). However, the startle response is a reflex. In contrast, the behavior of the current study is likely to be not a reflex, since it is expressed as long as at least 120 s. Moreover, note that both the 'affected' and the 'unaffected' animals in the exposed group had a unilateral hearing loss. Thus, the

presence of unilateral hearing loss can probably not explain the abnormal behavior in the 'affected' group.

One could argue that the observed behavior in the 'affected' group might have been a result of stress and anxiety, since numerous interactions between the auditory and limbic system have been demonstrated (Kraus and Canlon, 2012). In the current study, all animals were under anesthesia during the (sham) exposure. Thus the stress induced by the procedure is being controlled for, and the actual traumatizing noise is most likely not experienced by the exposed animals. Any stress that the exposed animals might have, could have derived from damage due to the noise exposure. For example, noise trauma, applied under anesthesia, can affect brain structures, such as the neurogenesis in the hippocampus (Kraus et al., 2010), which would presumably affect behavior. Indeed, Zheng and colleagues found that tinnitus-inducing noise exposure impairs several instinctive behaviors, such as impulsive control and social interaction, but not anxiety (Zheng et al., 2011a, 2011b). Moreover, if the 'affected' animals were more anxious, they would presumably show a decrease, rather than an increase, in activity due to freezing behavior, which is a well-established measure for anxiety (Crawford and Masterson, 1982; Rodgers, 1997; Hagenaars et al., 2014). Thus stress and anxiety can probably not account for the increased mobility of the animals in the 'affected' group.

Another explanation for the abnormal behavior in the 'affected' animals is that they perceived tinnitus. Namely, by interpreting immobility as a signature of perceiving silence, the presence of tinnitus would decrease the amount of immobility in silence, because the animals might not detect complete silence anymore. As such, tinnitus would function as a masker of the silence. Therefore, one possible explanation for the increased activity in silence is that these animals perceived tinnitus that masked the silent intervals. Similar to earlier studies demonstrating that unilateral trauma leads to tinnitus in only a subset of guinea pigs (Dehmel et al., 2012; Coomber et al., 2014), not all exposed animals demonstrated this increased activity during silence. This finding is also consistent with the observation that acoustic trauma in humans does not lead to tinnitus in all human subjects (Kitcher et al., 2012; Degeest et al., 2014). Previous psychophysical studies in humans suggest that tinnitus does not mask the offset of sound; listeners with tinnitus can still detect silent gaps in noise (Campolo et al., 2013; Fournier and Hébert, 2013). Thus, the increased activity in silence of the exposed 'affected' animals is rather related to the inability to detect complete silence, than to an inability to detect the offset of the noise. There were different degrees of increased activity in silence within animals labeled as ´affected´. This could reflect that this test is more sensitive for one animal with tinnitus than for the other. However, it could also reflect different characteristics or intensities of tinnitus. The latter is reasonable, because there are considerable inter-individual differences in the characteristics of tinnitus induced by noise exposure, both in humans and in laboratory animals (Coomber et al., 2014; Degeest et al., 2014). The increased mobility in noise could be explained by the presence of hyperacusis, i.e. an oversensitivity to sound, which is reported to be often comorbid with tinnitus (Schecklmann et al., 2014). This could have resulted in a more intense perception of the

already quite loud noise stimulus of 88 dB SPL. Thus the range of behaviors observed in the 'affected' animals could reflect the range of tinnitus characteristics.

However, validation experiments are crucial before the abnormal behavior can be attributed to tinnitus. The fact that the control and the 'unaffected' animals show a different behavior in noise and silence, respectively, shows that they are most likely under control of the acoustic stimulus (Sidman, 2008). However, the 'affected' animals are (at least) partly not under stimulus control, since they are mobile in silence but also show increased activity in noise. Above, we hypothesized that the perception of tinnitus can explain the increased activity in silence. However, numerous confounding effects of noise exposure could have also controlled their behavior, such as unilateral hearing loss, hyperacusis, motoric changes, generalized hyperactivity, stress, and anxiety. The following validation experiments are proposed to confirm or deny our hypothesis that the abnormal behavior of the affected group is due to tinnitus (Heffner and Harrington, 2002; Heffner and Heffner, 2012; von der Behrens, 2014):

1. Measuring corticosterone levels before behavioral testing can determine whether there is a correlation between stress and spontaneous behavior in noise and silence.
2. Inducing stress in normal-hearing animals before behavioral testing may show the effects of stress and anxiety on the behavior of guinea pigs in noise and silence.
3. An ear-plugging experiment, which is also used to validate other tinnitus behavioral models (Bauer and Brozoski, 2001; Heffner and Koay, 2005; Lobarinas et al., 2013), can reveal whether unilateral conductive hearing loss affects immobility in silence. However, one should interpret the outcomes with caution, since conductive hearing loss may also induce tinnitus (Mills and Cherry, 1984).
4. If the increased activity in both noise and silence of the 'affected' animals is due to a generalized increase in activity, it should be independent of the acoustic characteristics of the noise. The increased activity should be observed for both weak and strong noise stimuli. Instead, if the increased activity during noise is caused by hyperacusis, it would disappear when softer stimuli are used. Thus, repeating these experiments with weaker stimuli, might test whether the abnormal behavior is due to an generalized increase in activity or due to hyperacusis (and tinnitus during the silent intervals).
5. In a within-subject design, spontaneous behavior could be assessed before and after sound exposure. This could test for a contribution of a natural variation in general activity as an explanation for the differences between the 'affected' and 'unaffected' animals.
6. To determine whether the behavior of the 'affected' animals could be due to the perception of a sound (i.e. tinnitus), a tinnitus-like sound can be presented to a normal-hearing guinea pig during the entire testing period of the current paradigm (Jastreboff et al., 1988b). Behavior in silence and noise that is similar to that of the 'affected' animals, supports the hypothesis that this behavior is due to the perception of a sound, which would be tinnitus in the 'affected' animals.

7. Testing other tinnitus-inducing agents, such as salicylate, for their effect on the behavior of guinea pigs in noise and silence can also reveal whether the observed behavior in the 'affected' group could be a result of tinnitus (Guitton et al., 2003). In this experiment, one should keep in mind that certain drugs might also have their own effect directly on behavior, independently from their effect on the auditory system.
8. Cross-validation against other behavioral models to test for tinnitus, for example the startle reflex paradigm, may provide further validation (Berger et al., 2013).
9. It would further validate our measure when neurophysiological changes that are often attributed to tinnitus are found in the 'affected' but not in the 'unaffected' animals (Jastreboff and Sasaki, 1986; Takemura et al., 2004; Noreña et al., 2010; Mulders et al., 2011).

As discussed previously, current behavioral animal models for tinnitus can be divided in two categories: 1) conditioning paradigms (Jastreboff et al., 1988a), and 2) startle reflex paradigms (Turner et al., 2006). If the above-described phenomenon does indeed represent tinnitus in guinea pigs, it would be adding a new category to the existing behavioral tinnitus models. An advantage of the current model is that no training is required, which allows efficient assessment in large groups of animals. Furthermore, if the observed behavior is indeed instinctive, as expected, aging and other factors that influence learning and memory are not likely to affect outcomes.

In conclusion, guinea pigs could be trained relatively easy to detect noise in an active avoidance task, but did not show this trained response to silent intervals in continuous noise (experiment 1). Apparent immobility during silent intervals explains this finding (experiment 2). Further, we showed that a subset of noise-exposed animals was less immobile during silence and noise. We suggested that this abnormal behavior may be due to tinnitus and hyperacusis, respectively. However, conducting several validation experiments is very important before implementing this method as a new measure to detect tinnitus. Therefore, a number of experiments have been proposed that may further elucidate the origin of the abnormal behavior.

Acknowledgements

We want to thank Hans Segenhout for his help with setting up the equipment, Nima Ilbegi for his help with conducting experiment 1, and Minne Bonnema for technical support. We also want to thank Huib Versnel from the Department of Otorhinolaryngology and Head and Neck Surgery of the University Medical Center Utrecht, for providing us with the shuttle box and its corresponding software.

This study was supported by the Heinsius Houbolt Foundation, the Stichting Gehoorgestoorde Kind, and the NWO (grant number 114024021). The study is part of the research program of our department in Groningen: Healthy Aging and Communication.

Chapter 7

Discussion and Conclusion

A.N. Heeringa

Preface

The overarching aim of the current dissertation was to study the underlying pathophysiological mechanism(s) of noise-induced tinnitus and hyperacusis. Specifically, I studied the immediate and long-term effects of acoustic trauma on (1) wave amplitudes of the auditory brainstem response (ABR), (2) evoked and spontaneous activity in the inferior colliculus (IC), and (3) spontaneous behavior in noise and silence. I found that the amplitude of ABR wave I is reduced up to four weeks after bilateral acoustic trauma, whereas the amplitude of ABR wave IV is already normal one week after trauma, suggesting an increased central gain between the auditory nerve and the auditory midbrain (Chapter 2). Furthermore, inhibition in the IC is reduced by acoustic trauma, both in response to pure tones and in response to a noise stimulus, likewise implying an increase in central gain in the auditory midbrain (Chapter 2, Chapter 5). Moreover, my results showed that spontaneous activity in the IC is not majorly affected by acoustic trauma (Chapter 2). If any, it is slightly reduced shortly after trauma (Chapter 5). Envelope coding in the IC is enhanced immediately after trauma, suggesting that processing of complex sound features is also altered by acoustic trauma (Chapter 3). Moreover, my experiments showed that the Wiener-kernel analysis technique is applicable to spike trains of the IC (Chapter 4) and can be used as a tool to study the effects of acoustic trauma on response characteristics of the IC (Chapter 5). Last, the behavioral experiments showed that normal-hearing guinea pigs are active in noise, but immobile in silence. Unilateral acoustic trauma results in an altered pattern of this spontaneous behavioral activity in a subgroup of guinea pigs, which includes an increased mobility in silence and in noise (Chapter 6). This suggests that spontaneous behavior in noise and silence might potentially serve as a new measure to detect tinnitus in guinea pigs.

These individual experiments each provide answers to single, specific research questions. However, ideally, these experiments together should be combined in one comprehensive experiment. In one animal, neurophysiological measures, i.e. ABR wave amplitudes, spontaneous activity, evoked activity, and Wiener kernels, and behavioral activity could be assessed. If the behavioral paradigm can be further validated, this might provide insight into whether the animal perceives tinnitus and/or suffers from hyperacusis. Then, the neurophysiological fingerprints of acoustic trauma could be correlated to tinnitus and/or hyperacusis. Such a complete animal model would allow us to thoroughly and reliably study the effectiveness and mode of action of specific drug treatments. This is an important next step in the line of research described in this dissertation.

In the following sections, I will discuss the contributions of the neurophysiological and behavioral findings to the current literature. Subsequently, I will discuss the limitations and provide suggestions for future directions to establish a reliable animal model for tinnitus and hyperacusis. This chapter finishes with a concluding section describing the scientific and clinical implications that can be drawn from the results of this dissertation.

Neurophysiology

Increased central gain

One of the main theories regarding pathological mechanisms behind tinnitus and hyperacusis is called the increased central-gain theory (Noreña, 2011; Knipper et al., 2013; Zeng, 2013; Auerbach et al., 2014). This theory implies that a sensory system responds to a deprived external input with an abnormal homeostatic response in order to maintain a balanced state. This abnormal homeostatic response can involve an increased sensitivity to incoming signals as well as an amplification of the spontaneous activity. It has been hypothesized that the first explains the presence of hyperacusis, whereas the latter corresponds to tinnitus (e.g. Zeng, 2013). Increased hearing thresholds clearly imply a deprived sensory input to the central auditory system. However, recent studies have shown that noise-induced temporary threshold shifts can also result in a permanent deprivation of sensory input by means of the degeneration of the cochlear nerve (Kujawa and Liberman, 2009; Lin et al., 2011). This phenomenon has been termed "hidden hearing loss". The results of the current dissertation are discussed with respect to the increased central-gain theory, both as a result of elevated hearing thresholds and as a result of "hidden hearing loss".

In Chapter 2, I found that a sound-induced temporary threshold shift is associated with a reduction in the ABR wave I amplitude up to four weeks after acoustic trauma. This implies that the integrity of the auditory nerve is compromised by the acoustic trauma, even though the auditory thresholds fully recovered (Lin et al., 2011). Moreover, the amplitude of ABR wave IV recovered as soon as the thresholds recovered (after one week). Together, this suggests a mechanism that amplifies the reduced sensory input between the auditory nerve and the auditory midbrain. These findings are consistent with studies on ABR waves of tinnitus patients with normal audiograms that likewise demonstrate reduced wave I amplitudes but normal amplitudes of wave V (Kehrle et al., 2008; Schaette and McAlpine, 2011; Gu et al., 2012). Wave I amplitudes are also reduced in normal-hearing people with self-reported exposure to loud sounds (Stamper and Johnson, 2014). Even though the initial findings of a reduced wave I amplitude were found in tinnitus patients, it is not clear whether it is a neural marker of tinnitus and/or hyperacusis. In laboratory animals, "hidden hearing loss", as reflected by a decreased wave I amplitude and a reduced ribbon count, is thought to correspond with the generation of hyperacusis (Hickox and Liberman, 2014). Furthermore, when equally exposed animals are classified as either "tinnitus" or "no-tinnitus", it appears that all exposed animals, regardless of the classification, have a reduced wave I amplitude, whereas in the "tinnitus" animals, a *reduced* wave IV amplitude is found (Rüttiger et al., 2013). Since behavioral experiments were not conducted with the animals of Chapter 2, the observed ABR wave amplitude changes cannot be directly assigned to tinnitus, hyperacusis, or both. However, the altered ABR wave amplitudes are consistent with the presence of "hidden hearing loss" and with an increased central gain along the auditory pathway.

The increased central-gain theory is also related to the balance between inhibition and excitation in the central auditory system (Noreña, 2011; Zeng, 2013). Healthy homeostatic neural activity is regulated by excitatory and inhibitory interactions, among others (Turrigiano and Nelson, 2004). Therefore, a disrupted balance between excitation and inhibition in the direction of an increased excitation or a decreased inhibition could cause increased central gain. Inhibition and excitation can be studied by using molecular techniques, e.g. by investigating inhibitory and excitatory neurotransmitters and their receptors, and by using neurophysiological techniques, as performed in the current dissertation. Chapter 2 of this dissertation shows that the amount of inhibitory responses to pure tones is significantly reduced up to two weeks after acoustic trauma associated with a temporary threshold shift. On the contrary, the amount of excitatory responses is not decreased, but rather increased in response to low-frequency pure tones. Furthermore, Chapter 5 shows that inhibitory receptive fields disappear in all IC multi units immediately after acoustic trauma, whereas excitatory receptive fields remain present in the multi units with a characteristic frequency lower than the trauma frequency of 11 kHz. Inhibitory subsystems, as revealed from singular-value decomposition of the second-order Wiener kernel, are only present in multi units with a low characteristic frequency < 3 kHz. In contrast, excitatory subsystems were present in multi units with a characteristic frequency (*before* trauma) of up to 16 kHz. This indicates that in the IC, inhibition in particular is vulnerable for acoustic trauma, as revealed with receptive-field analysis and with Wiener-kernel analysis. My results indicate that acoustic trauma results in a decrease of inhibitory components in the IC, which is consistent with the increased central-gain theory (Noreña, 2011). Furthermore, my results are consistent with molecular studies, which show that acoustic trauma results in a down-regulation of inhibitory neurotransmitters and their corresponding receptors (Szczepaniak and Møller, 1995; Dong et al., 2010a, 2010b), and with neurophysiological studies, which show that noise-induced hearing loss amplifies excitatory responses in the IC (Willott and Lu, 1982; Salvi et al., 1990; Niu et al., 2013). A reduction of inhibition in the central auditory system has been suggested to be correlated to tinnitus and to hyperacusis (Knipper et al., 2010; Wang et al., 2011; Sun et al., 2014). Since the guinea pigs of Chapter 2 and Chapter 5 were not subjected to behavioral paradigms, it is not certain whether the acoustic-trauma induced neurophysiological changes presented in this dissertation reflect tinnitus, hyperacusis, or both. However, it can be speculated that they are an underlying mechanism of hyperacusis, as altered stimulus-driven activity in the IC has previously been linked to hyperacusis (Gu et al., 2010; Eggermont, 2013; Zeng, 2013).

As mentioned above, an increased central gain can also induce alterations in spontaneous spiking activity of the central auditory system. Naturally, the characteristics of spontaneous activity are specifically relevant in the absence of acoustic stimulation, making it an attractive neural correlate for the central pathophysiology of tinnitus (Kaltenbach, 2011; Noreña, 2011; Zeng, 2013; Eggermont and Roberts, 2014). Indeed, previous studies have shown that spontaneous firing rates in the IC are increased following a tinnitus-inducing noise exposure (Mulders and Robertson, 2009; Manzoor et al., 2013). However, the results of

the current dissertation show that spontaneous firing rates measured immediately, one week, two weeks, and four weeks after acoustic trauma do not significantly increase (or decrease) as compared to the control group (Chapter 2). If any, when comparing spontaneous activity in the same unit before and immediately after acoustic trauma, there is a small but significant decrease (Chapter 5). Therefore, considering the lack of hyperactivity in the inferior colliculus multi-unit recordings, it was concluded that the bilaterally exposed animals were not experiencing tinnitus, but rather hyperacusis.

In summary, my results support the theory that acoustic trauma induces an increased gain in the central auditory system. The results derived from analyses of ABR wave amplitudes, excitatory and inhibitory processes, and spontaneous activity all suggest the presence of hyperacusis, rather than tinnitus.

Enhanced envelope coding

Acoustic trauma can also alter the coding of more complex features of an acoustic stimulus, such as the envelope. Coding envelope cues properly are important when processing complex, meaningful sounds, such as speech (Shannon et al., 1995). My results showed that the neural response, phase-locked to the envelope of the acoustic stimulus, is altered immediately after acoustic trauma (Chapter 3). Modulation gain, i.e. the strength of the neural phase-locked response relative to the modulation depth of the acoustic stimulus, is increased after acoustic trauma in IC neurons. Specifically, multi units with characteristic frequencies below the trauma frequency (< 11 kHz) show enhanced envelope coding in response to modulation frequencies below 256 Hz. This finding is consistent with responses in the auditory nerve and in auditory-evoked potentials after noise-induced hearing loss (Kale and Heinz, 2010; Zhong et al., 2014), but have not been shown before in the IC.

The observed change in envelope coding at the level of the IC might be an underlying neural mechanism for the problems that hearing-impaired people encounter when listening in noisy environments (Bayat et al., 2013). Envelope information that derives from fluctuating background noises, such as competing speakers, might act as a distraction when pathologically amplified in the central auditory system. Previous studies showed that patients with sensorineural hearing loss also have normal to better-than-normal envelope detection thresholds (Moore and Glasberg, 2001; Füllgrabe et al., 2003). In addition, the increased modulation gain in phase-locked responses of the IC after acoustic trauma might be corresponding to the acoustic trauma-induced increased central gain, as discussed above.

Wiener kernels

By recording a system's response to a broadband Gaussian white noise, a set of Wiener kernels can be computed. These kernels provide a description of the nonlinear system that is being studied (Eggermont, 1993). Wiener kernels have been extensively described for noise-evoked spike trains of the auditory nerve of a variety of species (van Dijk et al., 1994, 1997; Yamada and Lewis, 1999; Lewis et al., 2002a, 2002b; Recio-Spinoso et al., 2005; Temchin et al., 2005;

Sneary and Lewis, 2007). Furthermore, there are also two studies describing Wiener kernels of noise-evoked spike trains recorded at the ventral cochlear nucleus (Wickesberg et al., 1984; Recio-Spinoso and van Dijk, 2006), only one of which reports successful recordings of the second-order kernels (Recio-Spinoso and van Dijk, 2006). In order to get an interpretation for the functional properties of the second-order kernels, they can be decomposed with singular-value decomposition into a series of subsystems, consisting of a filter function (eigenvector) and a gain value (eigenvalue; Yamada and Lewis, 1999). The eigenvectors allow us to obtain frequency responses and group delays and the eigenvalues provide a relative weight factor to the eigenvector. Furthermore, the sign of the eigenvalue indicates whether the subsystem contributes positively or negatively to the neural response, corresponding to excitation or inhibition, respectively. Singular-value decomposition has successfully been applied to recordings of the auditory nerve and the cochlear nucleus (Yamada and Lewis, 1999; Lewis et al., 2002a, 2002b; Temchin et al., 2005; Recio-Spinoso and van Dijk, 2006; Sneary and Lewis, 2007).

Since Wiener kernels, complemented with singular-value decomposition, reveal many response characteristics, including excitatory and inhibitory components, we hypothesized that it might be beneficial for studies that aim to understand the neurophysiological consequences of acoustic trauma. However, Wiener-kernel analyses had not been previously applied for noise-evoked spike trains of the IC. Therefore, the applicability of the Wiener-kernel analysis technique for noise-evoked spike trains of the IC was studied in the experiments described in Chapter 4 of the current dissertation. This chapter shows that significant first- and second-order kernels can be identified for spike trains of the IC.

In Chapter 5, the changes induced by acoustic trauma were studied using Wiener-kernel analysis. As discussed above, these changes can include altered excitation, altered inhibition, or both. Application of Wiener-kernel analysis on noise-evoked spike trains has a particular advantage over studying tone-evoked neural activity. The response to a tone is the summed result of excitation and inhibition. Hence, it is difficult to attribute any changes due to acoustic trauma to either excitation, inhibition, or both. In contrast, singular-value decomposition of Wiener kernels computed from noise-evoked spike trains allows for the explicit separation of excitation and inhibition in the neural response. In other words, a change due to acoustic trauma can be specifically linked to a change due to either excitation or inhibition. Using this analysis technique, the effects of acoustic trauma on the excitatory and inhibitory components of the IC were studied (Chapter 5). The results of this study have been discussed previously in the context of the increased central-gain theory (see section 'increased central gain'): acoustic trauma essentially cancels inhibition, but not excitation, in neurons that are tuned to frequencies below the edge of the trauma frequency.

Spontaneous behavior

Progress in research on the pathophysiological mechanisms of tinnitus and hyperacusis critically depends on a reliable behavioral animal model that determines whether the

animal being studied has tinnitus and/or hyperacusis. Furthermore, a behavioral model will be essential when testing promising treatments for tinnitus and hyperacusis. A number of different paradigms were available when I started this project in 2010 (Turner, 2007). However, none had been tested on guinea pigs. Today, there are two studies showing that the startle reflex paradigm can be applied to determine tinnitus in guinea pigs (Dehmel et al., 2012; Berger et al., 2013). I started by developing a conditioning paradigm to determine tinnitus in guinea pigs (Jastreboff and Sasaki, 1994).

Previous studies showed that guinea pigs could be trained in a shuttle box to shuttle to the other compartment in the presence of a 15-s noise burst (Philippens et al., 1992; Agterberg et al., 2010). Therefore, we aimed at training guinea pigs in the shuttle box to respond to a silent interval in continuous noise. However, it seemed that the guinea pigs inhibited their activity during the silent intervals, demonstrating that such a conditioning paradigm with silent intervals was not readily applicable as a measure for tinnitus in guinea pigs. In our subsequent experiments, the spontaneous behavior in silence was further studied as a possible measure to detect tinnitus in guinea pigs (Chapter 6). The idea behind this measure is that normal-hearing guinea pigs show a clear distinction in spontaneous behavior during silence as compared to during noise, i.e. they are mobile during noise, whereas they do not move during silence. We hypothesized that guinea pigs with tinnitus do not perceive complete silence and, therefore, do not show this typical behavior during silence. My results showed that some guinea pigs with unilateral sound-induced hearing loss have an increased mobility during silence as well as during noise (Chapter 6). Validation experiments, as those extensively described in the discussion of Chapter 6, are essential before attributing these observations to tinnitus, hyperacusis, or both. However, the observed behavior during the silent intervals of the experiment strongly suggests that a subgroup of the traumatized animals indeed perceived tinnitus.

Limitations

Below, three methodological aspects are discussed that impacted the application or interpretation of the results reported in the current dissertation.

Anesthesia

The use of anesthetics during the neurophysiological recordings and during the exposure of the animals to acoustic trauma was, due to important ethical reasons, unavoidable. Isoflurane was used as an anesthetic during acoustic trauma for the animals that were allowed to recover from the acoustic trauma (Chapter 2, Chapter 6). During the neurophysiological procedures, a mixture of ketamine and xylazine was used to anesthetize the animals. Thus the effects of immediate acoustic trauma in Chapter 2, Chapter 3, and Chapter 5 resulted from exposure applied under ketamine/xylazine anesthesia. It has been shown that isoflurane has a protective effect on noise-induced hearing loss and noise-induced tinnitus (Kim et al., 2005; Norman et al., 2012). Furthermore, ketamine is known to be an antagonist of the *N*-methyl-

D-aspartate (NMDA) receptor, which binds glutamate, and inner ear damage from acoustic overexposure is thought be facilitated by glutamate excitotoxicity (Puel, 1995). This suggests that, without the anesthetics, the damage could have been even more severe. Thus the noise damage as described in this dissertation may be underestimated as compared to that in real-life (unanaesthetized) situations.

Unilateral vs. bilateral acoustic trauma

In the neurophysiological experiments of the current dissertation, the animals were exposed to a free field bilateral acoustic-trauma stimulus (Chapter 2, Chapter 3, Chapter 5), as this is similar to most conditions where humans may acquire acoustic trauma. However, in the behavioral experiment of the current dissertation, a unilateral acoustic-trauma stimulus was used (Chapter 6). The reason for applying unilateral trauma was that by traumatizing only one ear, there is a smaller chance that the behavioral outcomes are confounded by hearing loss, since the unexposed ear retains normal auditory thresholds.

Even though the trauma stimulus was the same in all experiments (1-h exposure of an 11-kHz pure tone of 124 dB SPL), the mode of exposure could have induced a separate set of behavioral and neurophysiological changes. For example, spontaneous firing rates in the IC show separate characteristics in animals with bilateral acoustic trauma compared to animals with unilateral acoustic trauma (Ma et al., 2006). Furthermore, the olivocochlear system, which is activated by bilaterally presented sounds, protects the ear from damage by acoustic trauma (Liberman, 1988; Maison and Liberman, 2000). Hence, unilateral acoustic trauma likely results in more severe damage than bilateral trauma, due to the lack of protective mechanisms mediated by the efferent system. This should be considered when directly comparing the neurophysiological results with the behavioral results of the current dissertation, as well as when comparing the current results with the literature.

Contemplations about behavioral paradigms to test for tinnitus and hyperacusis

Ever since the first behavioral paradigm for tinnitus was published in the '80s (Jastreboff et al., 1988a), there has been no agreement in the current literature on the best measure to determine tinnitus in laboratory animals (Hayes et al., 2014). Both the conditioning paradigms and the startle reflex paradigms have advantages and disadvantages (Heffner and Heffner, 2012). An important concern regarding all behavioral models for tinnitus in laboratory animals is whether the behavior actually reflects tinnitus, and not something else. First of all, the assumption must be made that the animal being studied is in fact capable of experiencing a conscious percept, such as tinnitus. The next difficulty is that animals in behavioral paradigms for tinnitus can never be under stimulus control, as the stimulus that we would want them to act upon is a percept that is in their head, and thus beyond the 'control' of the scientist (Sidman, 2008). These questions, although very interesting, lie beyond the scope of this dissertation. The assumption that laboratory animals are capable of experiencing tinnitus is made in all studies on behavioral models as well as in Chapter 6 of this dissertation.

Looking forward

The next step along this line of research is to combine the electrophysiological recordings with the behavioral measure that has been suggested for tinnitus. As such, an animal model can be developed in which promising treatments that are applied at the round window of the cochlea can be tested (Muehlmeier et al., 2011). Accordingly, the effectiveness of the treatments can be evaluated by the behavioral paradigm, whereas the mode of action can be studied by the range of neurophysiological changes induced by acoustic trauma, as those described in this dissertation. The following notions are personal suggestions about the direction in which I think this research should further go.

First of all, I believe that the variability in the exposed animals is of great interest. Future studies could focus on the neurophysiological differences between the animals with normal and with abnormal behavior in noise and silence. Next, I consider reaching a consensus about the most reliable behavioral measure to determine tinnitus and/or hyperacusis in animal as an important aim for the future, if we want to directly compare results from different laboratories around the world. Furthermore, performing neuroimaging studies in laboratory animals with tinnitus would allow for a better translation between the animal studies and the human studies. Also, I believe that scientists working with animal models can move further in the direction that is taken by neuroimaging studies, namely looking at the brain as a whole instead of single locations. For example, an experiment in which *in vivo* electrophysiological recordings are made simultaneously at several locations in the auditory central system would be very interesting. Moreover, I think it is important to realize that the pathophysiological mechanism(s) of tinnitus and hyperacusis are not likely to be static, but rather dynamic in time, especially within the first hours, days, and weeks after the acoustic trauma, as is also illustrated by Chapter 2. Investigating a mechanism at only one time point is as brief as a photo, whereas we would want to know the whole movie. Therefore, in order to better understand a mechanism, one should always take multiple time points into account. And last, to understand a pathophysiological mechanism thoroughly, I think that combining neurophysiology with molecular techniques is of great importance. Molecular findings can also provide useful targets for future treatments.

The ideal experiment would combine all these aspects and different approaches, i.e. behavioral, neurophysiological, and molecular, into one animal experiment. I believe that the methodological issues that are raised by combining these approaches into one experiment are some of the most urgent issues to solve in the near future.

Conclusion

The overarching aim of the current dissertation was to study the underlying pathophysiological mechanism(s) of noise-induced tinnitus and hyperacusis. The experiments that were conducted for the current dissertation have filled some small gaps in the current literature. Together with other important scientific work, these findings might eventually help to find

the pathophysiological mechanism(s) of noise-induced tinnitus and hyperacusis. Specifically, this dissertation shows that neurophysiological correlates of acoustic trauma in the inferior colliculus include a decrease in inhibition, an increase in excitation, and enhanced envelope coding. Furthermore, this dissertation shows that Wiener kernels are applicable to study spike trains of the inferior colliculus and are an appropriate technique to further study the pathophysiological consequences of acoustic trauma. Last, a possible new measure to determine tinnitus in guinea pigs is reported.

By studying the consequences of acoustic trauma, the results of this dissertation can make a contribution to the current knowledge about underlying mechanisms of noise-induced tinnitus and hyperacusis. Therefore, these findings are of interest to auditory neurophysiologists that work on the pathophysiological mechanisms of tinnitus and hyperacusis. Showing that Wiener kernels can be measured in the inferior colliculus might provide a new tool to study these pathological mechanisms, as these analyses provide information on the balance between excitation and inhibition in a relatively straightforward way. Furthermore, my work has contributed to the literature on behavioral models for tinnitus by describing a possible new measure to assess tinnitus in guinea pigs.

The society of today expects its participants to stay active for a longer time. This underlines the importance of people not having to be hindered by hearing loss, tinnitus, or hyperacusis. Knowledge about the consequences of acoustic trauma raises more awareness in society about the traumatizing effects of overexposure. Above all, advances in research on neurophysiological correlates of acoustic trauma, tinnitus, and hyperacusis might provide new avenues to discover treatments that alleviate the burden for patients suffering from these debilitating conditions. Contributing to that goal was my motivation in conducting this research.

References

Agterberg MJH, van den Broek M, Philippens IHCHM (2010) A less stressful animal model: a conditioned avoidance behaviour task for guineapigs. Lab Anim 44:206-10. doi: 10.1258/la.2009.009096.

Agterberg MJ, Versnel H (2014) Behavioral responses of deafened guinea pigs to intracochlear electrical stimulation: a new rapid psychophysical procedure. Hear Res 313:67-74. doi: 10.1016/j.heares.2014.04.011.

Auerbach BD, Rodrigues PV, Salvi RJ (2014) Central gain control in tinnitus and hyperacusis. Front Neurol 5:206. doi:10.3389/fneur.2014.00206.

Bakin JS, South DA, Weinberger NM (1996) Induction of receptive field plasticity in the auditory cortex of the guinea pig during instrumental avoidance conditioning. Behav Neurosci 110(5):905-13.

Bauer CA, Brozoski TJ, Rojas R, Boley J, Wyder M (1999) Behavioral model of chronic tinnitus in rats. Otolaryngol Head Neck Surg 121(4):457-462.

Bauer CA, Brozoski TJ (2001) Assessing tinnitus and prospective tinnitus therapeutics using a psychophysical animal model. J Assoc Res Otolaryngol 2(1):54-64.

Bayat A, Farhadi M, Pourbakht A, Sadjedi H, Emamdjomeh H, Kamali M, Mirmomeni G (2013) A comparison of auditory perception in hearing-impaired and normal-hearing listeners: an auditory scene analysis study. Iran Red Crescent Med J 15(11):e9477. doi:10.5812/ircmj.9477.

Berger JI, Coomber B, Shackleton TM, Palmer AR, Wallace MN (2013) A novel behavioural approach to detecting tinnitus in the guinea pig. J Neurosci Methods 213(2):188-195. doi:10.1016/j.jneumeth.2012.12.023.

Böhmer A (1988) The Preyer reflex - an easy estimate of hearing function in guinea pigs. Acta Otolaryngol 106:368-72.

Bronkhorst AW, Plomp R (1992) Effect of multiple speechlike maskers on binaural speech recognition in normal and impaired hearing. J Acoust Soc Am 92(6):3132-3139.

Buño W Jr (1978) Auditory nerve fiber activity influenced by contralateral ear sound stimulation. Exp Neurol 59(1):62-74.

Campolo J, Lobarinas E, Salvi R (2013) Does tinnitus "fill in" the silent gaps? Noise Health 15(67):398-405. doi: 10.4103/1463-1741.121232.

Carney LH, Yin TCT (1989) Responses of low-frequency cells in the inferior colliculus to interaural time differences of clicks: excitatory and inhibitory components. J Neurophysiol 62(1):144-161.

Clopton BM, Winfield JA (1973) Tonotopic organization in the inferior colliculus of the rat. Brain Res 56:355-8.

Coomber B, Berger JI, Kowalkowski VL, Shackleton TM, Palmer AR, Wallace MN (2014) Neural changes accompanying tinnitus following unilateral acoustic trauma in the guinea pig. Eur J Neurosci 40(2):2427-41. doi: 10.1111/ejn.12580.

Crawford M, Masterson FA (1982) Species-specific defense reactions and avoidance learning. Pav J Biol Sci 17(4):204-14.

Crifò S (1973) Shiver-audiometry in the conditioned guinea-pig (simplified Anderson-Wedenberg test). Acta Otolaryngol 75:38-44.

Dauman R, Bouscau-Faure F (2005) Assessment and amelioration of hyperacusis in tinnitus patients. Acta Otolaryngol 125(5):503-509.

de Boer E, de Jongh HR (1978) On cochlear encoding: potentialities and limitations of the reverse-correlation technique. J Acoust Soc Am 63(1):115-135.

Degeest S, Corthals P, Vinck B, Keppler H (2014) Prevalence and characteristics of tinnitus after leisure noise exposure in young adults. Noise Health 16(68):26-33. doi: 10.4103/1463-1741.127850.

Dehmel S, Eisinger D, Shore SE (2012) Gap prepulse inhibition and auditory brainstem-evoked potentials as objective measures for tinnitus in guinea pigs. Front Syst Neurosci 6:42. doi:10.3389/fnsys.2012.00042.

Diamond IT, Neff WD (1957) Ablation of temporal cortex and discrimination of auditory patterns. J Neurophysiol 20(3):300-15.

Dong S, Rodger J, Mulders WHAM, Robertson D (2010a) Tonotopic changes in GABA receptor expression in guinea pig inferior colliculus after partial unilateral hearing loss. Brain Res 1342:24-32. doi:10.1016/j.brainres.2010.04.067.

Dong S, Mulders WHAM, Rodger J, Woo S, Robertson D (2010b) Acoustic trauma evokes hyperactivity and changes in gene expression in guinea-pig auditory brainstem. Eur J Neurosci 31(9):1616-1628. doi:10.1111/j.1460-9568.2010.07183.x.

Duan M, Agerman K, Ernfors P, Canlon B (2000) Complementary roles of neurotrophin 3 and a N-methyl-D-aspartate antagonist in the protection of noise and aminoglycoside-induced ototoxicity. PNAS 97(13):7597-7602.

Dunnebier EA, Segenhout JM, Wit HP, Albers FWJ (1997) Two-phase endolymphatic hydrops: a new dynamic guinea pig model. Acta Otolaryngol 117:13-19.

Duque D, Pérez-González D, Ayala YA, Palmer AR, Malmierca MS (2012) Topographic distribution, frequency, and intensity dependence of stimulus-specific adaptation in the inferior colliculus of the rat. J Neurosci 32(49):17762-17774. doi:10.1523/JNEUROSCI.3190-12.2012.

Eggermont JJ, Johannesma PIM, Aertsen AMH (1983) Reverse-correlation methods in auditory research. Q Rev Biophys 16(3):341-414.

Eggermont JJ (1993) Wiener and Volterra analyses applied to the auditory system. Hear Res 66:177-201.

Eggermont JJ, Roberts LE (2004) The neuroscience of tinnitus. Trends Neurosci 27(11):676-682.

Eggermont JJ (2013) Hearing loss, hyperacusis, or tinnitus: what is modeled in animal research? Hear Res 295:140-149. doi:10.1016/j.heares.2012.01.005.

Eggermont JJ, Roberts LE (2014) Tinnitus: animal models and findings in humans. Cell Tissue Res (Epub ahead of print) doi:10.1007/s00441-014-1992-8.

Ehret G, Romand R (Eds.) (1997) The Central Auditory System. New York, NY: Oxford University Press.

Ehret G (1997) The auditory midbrain, a "shunting yard" of acoustical information processing. In: Ehret G, Romand R (eds) The Central Auditory System. Oxford University Press, New York, pp 259-316.

Fournier P, Hébert S (2013) Gap detection deficits in humans with tinnitus as assessed with the acoustic startle paradigm: does tinnitus fill in the gap? Hear Res 295:16-23. doi: 10.1016/j.heares.2012.05.011.

Füllgrabe C, Meyer B, Lorenzi C (2003) Effect of cochlear damage on the detection of complex temporal envelopes. Hear Res 178:35-43.

Furman AC, Kujawa SG, Liberman MC (2013) Noise-induced cochlear neuropathy is selective for fibers with low spontaneous rates. J Neurophysiol 110(3):577-586. doi:10.1152/jn.00164.2013.

Galván VV, Weinberger NM (2002) Long-term consolidation and retention of learning-induced tuning plasticity in the auditory cortex of the guinea pig. Neurobiol Learn Mem 77:78-108. doi:10.1006/nlme.2001.4044.

Gilles A, de Ridder D, van Hal G, Wouters K, Kleine Punte A, van de Heyning P (2012) Prevalence of leisure noise-induced tinnitus and the attitude toward noise in university students. Otol Neurotol 33(6):899-906. doi:10.1097/MAO.0b013e31825d640a.

Grimault N, Bacon SP, Micheyl C (2002) Auditory stream segregation on the basis of amplitude-modulation rate. J Acoust Soc Am 111(3):1340-1348.

Gu JW, Halpin CF, Nam EC, Levine RA, Melcher JR (2010) Tinnitus, diminished sound-level tolerance, and elevated auditory activity in humans with clinically normal hearing sensitivity. J Neurophysiol 104:3361-3370. doi:10.1152/jn.00226.2010.

Gu JW, Herrmann BS, Levine RA, Melcher JR (2012) Brainstem auditory evoked potentials suggest a role for the ventral cochlear nucleus in tinnitus. J Assoc Res Otolaryngol 13(6):819-833. doi:10.1007/s10162-012-0344-1.

Guitton MJ, Caston J, Ruel J, Johnson RM, Pujol R, Puel J-L (2003) Salicylate induces tinnitus through activation of cochlear NMDA receptors. J Neurosci 23(9):3944-52.

Hagenaars MA, Oitzl M, Roelofs K (2014) Updating freeze: aligning animal and human research. Neurosci Biobehav Rev 47C:165-76. doi: 10.1016/j.neubiorev.2014.07.021.

Hayes SH, Radziwon KE, Stolzberg DJ, Salvi RJ (2014) Behavioral models of tinnitus and hyperacusis in animals. Front Neurol 5:179. doi:10.3389/fneur.2014.00179.

Heeringa AN, van Dijk P (2014) The dissimilar time course of temporary threshold shifts and reduction of inhibition in the inferior colliculus following intense sound exposure. Hear Res 312:38-47. doi:10.1016/j.heares.2014.03.004.

Heffner HE, Harrington IA (2002) Tinnitus in hamsters following exposure to intense sound. Hear Res 170:83-95.

Heffner HE, Koay G (2005) Tinnitus and hearing loss in hamsters (Mesocricetis auratus) exposed to loud sound. Behav Neurosci 119(3):734-42.

Heffner HE, Heffner RS (2012) Behavioral tests for tinnitus in animals. In: Tinnitus. Eggermont JJ et al., (Eds.) New York: Springer Science+Business Media. p21-58.

Henry KS, Heinz MG (2013) Effects of sensorineural hearing loss on temporal coding of narrowband and broadband signals in the auditory periphery. Hear Res 303:39-47.

Hermes DJ, Aertsen AMHJ, Johannesma PIM, Eggermont JJ (1981) Spectro-temporal characteristics of single units in the auditory midbrain of the lightly anesthetised grass frog (*Rana temporaria L.*) investigated with noise stimuli. Hear Res 5:147-178.

Herrero AI, Sandi C, Venero C (2006) Individual differences in anxiety trait are related to spatial learning abilities and hippocampal expression of mineralocorticoid receptors. Neurobiol Learn Mem 86(2):150-9.

Hickox AE, Liberman MC (2014) Is noise-induced cochlear neuropathy key to the generation of hyperacusis or tinnitus? J Neurophysiol 111:552-564. doi:10.1152/jn.00184.2013.

Hu B, Lin X, Huang L-S, Yang L, Feng H, Sui J-F (2009) Involvement of the ipsilateral and contralateral cerebellum in the acquisition of unilateral classical eyeblink conditioning in guinea pigs. Acta Pharmacol Sin 30(2):141-52. doi: 10.1038/aps.2008.18.

Jastreboff PJ, Sasaki CT (1986) Salicylate-induced changes in spontaneous activity of single units in the inferior colliculus of the guinea pig. J Acoust Soc Am 80(5):1384-91.

Jastreboff PJ, Brennan JF, Sasaki CT (1988a) An animal model for tinnitus. Laryngoscope 98(3):280-286.

Jastreboff PJ, Brennan JF, Coleman JK, Sasaki CT (1988b) Phantom auditory sensation in rats: an animal model for tinnitus. Behav Neurosci 102(6):811-822.

Jastreboff PJ, Sasaki CT (1994) An animal model of tinnitus: a decade of development. Am J Otol 15(1):19-27.

Joris PX, Verschooten E (2013) On the limit of neural phase locking to fine structure in humans. Adv Exp Med Biol 787:101-108. doi:10.1007/978-1-4614-1590-9_12.

Kale S, Heinz MG (2010) Envelope coding in auditory nerve fibers following noise-induced hearing loss. J Assoc Res Otolaryngol 11(4):657-673. doi:10.1007/s10162-010-0223-6.

Kaltenbach JA (2011) Tinnitus: models and mechanisms. Hear Res 276:52-60. doi:10.1016/j.heares.2010.12.003.

Kazlauckas V, Schuh J, Dall'Igna OP, Pereira GS, Bonan CD, Lara DR (2005) Behavioral and cognitive profile of mice with high and low exploratory phenotypes. Behav Brain Res 162(2):272-8.

Kehrle HM, Granjeiro RC, Sampaio ALL, Bezerra R, Almeida VF, Oliveira CA (2008) Comparison of auditory brainstem response results in normal-hearing patients with and without tinnitus. Arch Otolaryngol Head Neck Surg 134(6):647-651. doi:10.1001/archotol.134.6.647.

Kim JU, Lee HJ, Kang HH, Shin JW, Ku SW, Ahn JH, … Chung JW (2005) Protective effect of isoflurane anesthesia on noise-induced hearing loss in mice. Laryngoscope 115(11):1996-1999.

Kitcher ED, Ocansey G, Tumpi DA (2012) Early occupational hearing loss of workers in a stone crushing industry: our experience in a developing country. Noise Health 14(57):68-71. doi: 10.4103/1463-1741.95134.

Knipper M, Zimmermann U, Müller M (2010) Molecular aspects of tinnitus. Hear Res 266:60-69. doi:10.1016/j.heares.2009.07.013.

Knipper M, van Dijk P, Nunes I, Rüttiger L, Zimmermann U (2013) Advances in the neurobiology of hearing disorders: recent developments regarding the basis of tinnitus and hyperacusis. Prog Neurobiol 111:17-33. doi:10.1016/j.pneurobio.2013.08.002.

Korenberg MJ, Hunter IW (1990) The identification of nonlinear biological systems: Wiener kernel approaches. Ann Biomed Eng 18:629-654.

Kraus KS, Mitra S, Jimenez Z, Hinduja S, Ding D, Jiang H, … Salvi RJ (2010) Noise trauma impairs neurogenesis in the rat hippocampus. Neurosci 167(4):1216-26. doi: 10.1016/j.neuroscience.2010.02.071.

Kraus KS, Canlon B (2012) Neuronal connectivity and interactions between the auditory and limbic systems. Effects of noise and tinnitus. Hear Res 288:34-46. doi: 10.1016/j.heares.2012.02.009.

Kujawa SG, Liberman MC (2009) Adding insult to injury: cochlear nerve degeneration after "temporary" noise-induced hearing loss. J Neurosci 29(45):14077-14085. doi:10.1523/JNEUROSCI.2845-09.2009.

Langers DRM, de Kleine E, van Dijk P (2012) Tinnitus does not require macroscopic tonotopic map reorganization. Front Syst Neurosci 6:2. doi:10.3389/fnsys.2012.00002.

Lanting CP, de Kleine E, van Dijk P (2009) Neural activity underlying tinnitus generation: results from PET and fMRI. Hear Res 255:1-13. doi:10.1016/j.heares.2009.06.009.

Lewis ER, Henry KR, Yamada WM (2002a) Tuning and timing of excitation and inhibition in primary auditory nerve fibers. Hear Res 171:13-31.

Lewis ER, Henry KR, Yamada WM (2002b) Tuning and timing in the gerbil ear: Wiener-kernel analysis. Hear Res 174:206-221.

Liberman MC (1988) Response properties of cochlear efferent neurons: monaural vs. binaural stimulation and the effects of noise. J Neurophysiol 60(5):1779-1798.

Liberman MC (1989) Rapid assessment of sound-evoked olivocochlear feedback: Suppression of compound action potentials by contralateral sound. Hear Res 38:47-56.

Lin HW, Furman AC, Kujawa SG, Liberman MC (2011) Primary neural degeneration in the guinea pig cochlea after reversible noise-induced threshold shift. J Assoc Res Otolaryngol 12(5):605-616. doi:10.1007/s10162-011-0277-0.

Llano DA, Turner J, Caspary DM (2012) Diminished cortical inhibition in an aging mouse model of chronic tinnitus. J Neurosci 32(46):16141-16148. doi:10.1523/JNEUROSCI.2499-12.2012.

Lobarinas E, Hayes SH, Allman BL (2013) The gap-startle paradigm for tinnitus screening in animal models: limitations and optimization. Hear Res 295:150-60. doi: 10.1016/j.heares.2012.06.001.

Ma WLD, Hidaka H, May BJ (2006) Spontaneous activity in the inferior colliculus of CBA/J mice after manipulations that induce tinnitus. Hear Res 212:9-21.

Maison SF, Liberman MC (2000) Predicting vulnerability to acoustic injury with a noninvasive assay of olivocochlear reflex strength. J Neurosci 20(12):4701-4707.

Manzoor NF, Gao Y, Licari F, Kaltenbach JA (2013) Comparison and contrast of noise-induced hyperactivity in the dorsal cochlear nucleus and inferior colliculus. Hear Res 295:114-123. doi:10.1016/j.heares.2012.04.003.

Milbrandt JC, Holder TM, Wilson MC, Salvi RJ, Caspary DM (2000) GAD levels and muscimol binding in rat inferior colliculus following acoustic trauma. Hear Res 147:251-260.

Mills RP, Cherry JR (1984) Subjective tinnitus in children with otological disorders. Int J Pediatr Otorhinolaryngol 7(1):21-7.

Moore BCJ, Glasberg BR (2001) Temporal modulation transfer functions obtained using sinusoidal carriers with normally hearing and hearing-impaired listeners. J Acoust Soc Am 110(2):1067-1073.

Muehlmeier G, Biesinger E, Maier H (2011) Safety of intratympanic injection of AM-101 in patients with acute inner ear tinnitus. Audiol Neurootol 16(6):388-397. doi:10.1159/000322641.

Mulders WH, Robertson D (2009) Hyperactivity in the auditory midbrain after acoustic trauma: dependence on cochlear activity. Neuroscience 164(2):733-746. doi:10.1016/j.neuroscience.2009.08.036.

Mulders WHAM, Robertson D (2011) Progressive centralization of midbrain hyperactivity after acoustic trauma. Neuroscience 192:753-760. doi:10.1016/j.neuroscience.2011.06.046.

Mulders WHAM, Ding D, Salvi R, Robertson D (2011) Relationship between auditory thresholds, central spontaneous activity, and hair cell loss after acoustic trauma. J Comp Neurol 519:2637-47. doi: 10.1002/cne.22644.

Niu Y, Kumaraguru A, Wang R, Sun W (2013) Hyperexcitability of inferior colliculus neurons caused by acute noise exposure. J Neurosci Res 91(2):292-299. doi:10.1002/jnr.23152.

Noreña AJ, Eggermont JJ (2003) Changes in spontaneous neural activity immediately after an acoustic trauma: implications for neural correlates of tinnitus. Hear Res 183:137-153.

Noreña AJ, Eggermont JJ (2005) Enriched acoustic environment after noise trauma reduces hearing loss and prevents cortical map reorganization. J Neurosci 25(3):699-705.

Noreña AJ, Moffat G, Blanc JL, Pezard L, Cazals Y (2010) Neural changes in the auditory cortex of awake guinea pigs after two tinnitus inducers: salicylate and acoustic trauma. Neuroscience 166:1194-209. doi: 10.1016/j.neuroscience.2009.12.063.

Noreña AJ (2011) An integrative model of tinnitus based on a central gain controlling neural sensitivity. Neurosci Biobehav Rev 35(5):1089-1109. doi:10.1016/j.neubiorev.2010.11.003.

Norman M, Tomscha K, Wehr M (2012) Isoflurane blocks temporary tinnitus. Hear Res 290:64-71. doi:10.1016/j.heares.2012.03.015.

Philippens IHCHM, Melchers BPC, Wolthuis OL (1992) Active avoidance behavior in guinea pigs: effects of physostigmine and scopolamine. Pharmacol Biochem Beh 42:285-9.

Pollak GD, Xie R, Gittelman JX, Andoni S, Li N (2011) The dominance of inhibition in the inferior colliculus. Hear Res 274(1-2):27-39. doi:10.1016/j.heares.2010.05.010.

Prosen CA, Petersen MR, Moody DB, Stebbins WC (1978) Auditory thresholds and kanamycin-induced hearing loss in the guinea pig assessed by a positive reinforcement procedure. J Acoust Soc Am 63(2):559-66.

Puel JL (1995) Chemical synaptic transmission in the cochlea. Prog Neurobiol 47(6):449-476.

Recio-Spinoso A, Temchin AN, van Dijk P, Fan Y-H, Ruggero MA (2005) Wiener-kernel analysis of responses to noise of chinchilla auditory-nerve fibers. J Neurophysiol 93:3615-3634. doi:10.1152/jn.00882.2004.

Recio-Spinoso A, van Dijk P (2006) Analysis of responses to noise in the ventral cochlear nucleus using Wiener kernels. Hear Res 216-217:7-18.

Rees A, Palmer AR (1989) Neuronal responses to amplitude-modulated and pure-tone stimuli in the guinea pig inferior colliculus, and their modification by broadband noise. J Acoust Soc Am 85(5):1978-1994.

Rieke F, Warland D, de Ruyter van Steveninck R, Bialek W (1999) Spikes, exploring the neural code. MIT press, London.

Robertson D, Bester C, Vogler D, Mulders WHAM (2013) Spontaneous hyperactivity in the auditory midbrain: relationship to afferent input. Hear Res 295:124-9. doi: 10.1016/j.heares.2012.02.002

Rodgers RJ (1997) Animal models of 'anxiety': where next? Behav Pharmacol 8(6-7):477-96.

Rüttiger L, Ciuffani J, Zenner HP, Knipper M (2003) A behavioral paradigm to judge acute sodium salicylate-induced sound experience in rats: a new approach for an animal model on tinnitus. Hear Res 180:39-50.

Rüttiger L, Singer W, Panford-Walsh R, Matsumoto M, Lee SC, Zucotti A, … Knipper M (2013) The reduced cochlear output and the failure to adapt the central auditory response causes tinnitus in noise exposed rats. PLoS One 8(3):e57247. doi:10.1371/journal.pone.0057247.

Salvi RJ, Hamernik RP, Henderson D (1978) Discharge patterns in the cochlear nucleus of the chinchilla following noise induced asymptotic threshold shift. Exp Brain Res 32(3):301-320.

Salvi RJ, Saunders SS, Gratton MA, Arehole S, Powers N (1990) Enhanced evoked response amplitudes in the inferior colliculus of the chinchilla following acoustic trauma. Hear Res 50:245-258.

Salvi RJ, Wang J, Ding D (2000) Auditory plasticity and hyperactivity following cochlear damage. Hear Res 147:261-274.

Sansone M, Bovet D (1970) Avoidance learning by Guinea pigs. Q J Exp Psychol 22(3):458-61.

Schaette R, McAlpine D (2011) Tinnitus with a normal audiogram: physiological evidence for hidden hearing loss and computational model. J Neurosci 31(38):13452-13457. doi:10.1523/JNEUROSCI.2156-11.2011.

Schecklmann M, Landgrebe M, Langguth B, TRI Database Study Group (2014) Phenotypic characteristics of hyperacusis in tinnitus. PLoS One 9(1):e86944. doi:10.1371/journal.pone.0086944.

Scholl B, Wehr M (2008) Disruption of balanced cortical excitation and inhibition by acoustic trauma. J Neurophysiol 100:646-656. doi:10.1152/jn.90406.2008.

Shannon RV, Zeng FG, Kamath V, Wygonski J, Ekelid M (1995) Speech recognition with primarily temporal cues. Science 270(5234):303-304.

Shore SE (2005) Multisensory integration in the dorsal cochlear nucleus: unit responses to acoustic and trigeminal ganglion stimulation. Eur J Neurosci 21(12):3334-3348.

Shore SE, Koehler S, Oldakowski M, Hughes LF, Syed S (2008) Dorsal cochlear nucleus responses to somatosensory stimulation are enhanced after noise-induced hearing loss. Eur J Neurosci 27:155-68. doi: 10.1111/j.1460-9568.2007.05983.x

Sidman M (2008) Reflections on stimulus control. Behav Analyst 31(2):127-35.

Sneary MG, Lewis ER (2007) Tuning properties of turtle auditory nerve fibers: evidence for suppression and adaptation. Hear Res 228:22-30.

Stamper GC, Johnson TA (2014) Auditory function in normal-hearing, noise-exposed human ears. Ear Hear (Epub ahead of print).

Stolzberg D, Hayes SH, Kashanian N, Radziwon K, Salvi RJ, Allman BL (2013) A novel behavioral assay for the assessment of acute tinnitus in rats optimized for simultaneous recording of oscillatory neural activity. J Neurosci Methods 219(2):224-232. doi:10.1016/j.jneumeth.2013.07.021.

Sun W, Deng A, Jayaram A, Gibson B (2012) Noise exposure enhances auditory cortex responses related to hyperacusis behavior. Brain Res 1485:108-116. doi:10.1016/j.brainres.2012.02.008.

Sun W, Fu Q, Zhang C, Manohar S, Kumaraguru A, Li J (2014) Loudness perception affected by early age hearing loss. Hear Res 313:18-25. doi:10.1016/j.heares.2014.04.002.

Szczepaniak WS, Møller AR (1995) Evidence of decreased GABAergic influence on temporal integration in the inferior colliculus following acute noise exposure: a study of evoked potentials in the rat. Neurosci Lett 196:77-80.

Takemura K, Komeda M, Yagi M, Himeno C, Izumikawa M, Doi T, … Yamashita T (2004) Direct inner ear infusion of dexamethasone attenuates noise-induced trauma in guinea pig. Hear Res 196:58-68.

Temchin AN, Recio-Spinoso A, van Dijk P, Ruggero MA (2005) Wiener kernels of chinchilla auditory-nerve fibers: verification using responses to tones, clicks, and noise and comparison with basilar-membrane vibrations. J Neurophysiol 93:3635-3648. doi:10.1152/jn.00885.2004.

Turner JG, Brozoski TJ, Bauer CA, Parrish JL, Myers K, Hughes LF, Caspary DM (2006) Gap detection deficits in rats with tinnitus: a potential novel screening tool. Behav Neurosci 120(1):188-195.

Turner JG (2007) Behavioral measures of tinnitus in laboratory animals. Prog Brain Res 166:147-156.

Turrigiano GG, Nelson SB (2004) Homeostatic plasticity in the developing nervous system. Nat Rev Neurosci 5(2):97-107.

van der Heijden M, Joris PX (2003) Cochlear phase and amplitude retrieved from the auditory nerve at arbitrary frequencies. J Neurosci 23(27):9194-9198.

van Dijk P, Wit HP, Segenhout JM, Tubis A (1994) Wiener kernel analysis of inner ear function in the American bullfrog. J Acoust Soc Am 95(2):904-919.

van Dijk P, Wit HP, Segenhout JM (1997) Dissecting the frog inner ear with Gaussian noise. I. Application of high-order Wiener-kernel analysis. Hear Res 114:229-242.

von der Behrens W (2014) Animal models of subjective tinnitus. Neural Plast 2014:741452. doi:10.1155/2014/741452.

Wada SI, Starr A (1983a) Generation of auditory brain stem responses (ABRs). II. Effects of surgical section of the trapezoid body on the ABR in guinea pigs and cat. Electroencephalogr Clin Neurophysiol 56(4):340-351.

Wada SI, Starr A (1983b) Generation of auditory brain stem responses (ABRs). III. Effects of lesions of the superior olive, lateral lemniscus and inferior colliculus on the ABR of the guinea pig. Electroencephalogr Clin Neurophysiol 56(4):352-366.

Walton JP, Frisina RD, O'Neill WE (1998) Age-related alteration in processing of temporal sound features in the auditory midbrain of the CBA mouse. J Neurosci 18(7):2764-2776.

Wang J, Salvi RJ, Powers N (1996) Plasticity of response properties of inferior colliculus neurons following acute cochlear damage. J Neurophysiol 75(1):171-183.

Wang J, Ding D, Salvi RJ (2002) Functional reorganization in chinchilla inferior colliculus associated with chronic and acute cochlear damage. Hear Res 168:238-249.

Wang H, Brozoski TJ, Caspary DM (2011) Inhibitory neurotransmission in animal models of tinnitus: maladaptive plasticity. Hear Res 279:111-117. doi:10.1016/j.heares.2011.04.004.

Wickesberg RE, Dickson JW, Gibson MM, Geisler CD (1984) Wiener kernel analysis of responses from anteroventral cochlear nucleus neurons. Hear Res 14:155-174.

Willott JF, Lu SM (1982) Noise-induced hearing loss can alter neural coding and increase excitability in the central nervous system. Science 216(4552):1331-1334.

Yamada WM, Lewis ER (1999) Predicting the temporal responses of non-phase-locking bullfrog auditory units to complex acoustic waveforms. Hear Res 130:155-170.

Yang S, Weiner BD, Zhang LS, Cho SJ, Bao S (2011) Homeostatic plasticity drives tinnitus perception in an animal model. Proc Natl Acad Sci USA 108(36):14974-14979. doi:10.1073/pnas.1107998108.

Yin TCT, Kuwada S (1983) Binaural interaction in low-frequency neurons in inferior colliculus of the cat. II. Effects of changing rate and direction of interaural phase. J Neurophysiol 50(4):1000-1019.

Zeng FG (2013) An active loudness model suggesting tinnitus as increased central noise and hyperacusis as increased nonlinear gain. Hear Res 295:172-179. doi:10.1016/j.heares.2012.05.009.

Zheng XY, Henderson D, Hu BH, Ding DL, McFadden SL (1997) The influence of the cochlear efferent system on chronic acoustic trauma. Hear Res 107:147-159.

Zheng Y, Hamilton E, Stiles L, McNamara E, de Waele C, Smith PF, Darlington CL (2011a) Acoustic trauma that can cause tinnitus impairs impulsive control but not performance accuracy in the 5-choice serial reaction time task in rats. Neurosci 180:75-84. doi: 10.1016/j.neuroscience.2011.02.040.

Zheng Y, Hamilton E, McNamara E, Smith PF, Darlington CL (2011b) The effects of chronic tinnitus caused by acoustic trauma on social behaviour and anxiety in rats. Neurosci 193:143-53. doi: 10.1016/j.neuroscience.2011.07.026.

Zhong Z, Henry KS, Heinz MG (2014) Sensorineural hearing loss amplifies neural coding of envelope information in the central auditory system of chinchillas. Hear Res 309:55-62. doi:10.1016/j.heares.2013.11.006.

Zuccotti A, Kuhn S, Johnson SL, Franz C, Singer W, Hecker D, … Knipper M (2012) Lack of brain-derived neurotrophic factor hampers inner hair cell synapse physiology, but protects against noise-induced hearing loss. J Neurosci 32(25):8545-8553. doi:10.1523/JNEUROSCI.1247-12.2012.

Summary

Acoustic Trauma

Damage caused by prolonged exposure to loud noise is called acoustic trauma. The most well-known consequence of acoustic trauma is an increase in hearing thresholds, i.e. hearing impairment. However, acoustic trauma can also cause ringing in the ears, which is called tinnitus in medical terms. Tinnitus is a common phenomenon: nearly 90% of adolescents report having had a tinnitus at least once. However, there are also people who constantly have tinnitus. This can be very disabling. Additional symptoms that are common with tinnitus are difficulties with concentrating, insomnia, and stress, which can sometimes turn into depression and even attempted suicides. Furthermore, acoustic trauma can also cause hyperacusis, a condition in which the patient is hypersensitive to sounds of normal volume. Unfortunately, at present there are no treatments available that are able to consistently cure tinnitus and hyperacusis.

One reason for the lack of a treatment is the fact that we do not completely understand the underlying mechanisms of tinnitus and hyperacusis. It is known that, in addition to damage in the ear, the brain also plays an important role in the development of tinnitus and hyperacusis. Therefore most of the research described in this dissertation is focused on the brain. More specifically, I studied the consequences of acoustic trauma on the function of the brain: in other words, the neurophysiological consequences of acoustic trauma. Because neurophysiology in humans can only be studied indirectly, the current studies were conducted in laboratory animals. The last chapter is devoted to the question of how we can determine if animals have tinnitus or hyperacusis. The overarching purpose of this dissertation is to contribute to the development of an animal model to test treatments for tinnitus and hyperacusis.

Recording brain activity in a laboratory animal

The central auditory system is defined as the brain areas that are processing acoustic information (see the figure on the front page of this dissertation). The brain cells (neurons) in these regions communicate with each other by means of electrical signals, or action potentials. By analyzing the patterns of these action potentials, the processing of sound can be studied. Action potentials of neurons can be recorded by implanting an electrode in the brain of the experimental animal. The rate at which a neuron fires action potentials is also called the neural activity. By presenting specific sounds, different auditory neurons increase or decrease their spontaneous neural activity, which is referred to as excitation and inhibition, respectively. **Chapter 2** shows that acoustic trauma results in a disturbed balance

between excitation and inhibition. In particular, the number of neurons showing inhibition is decreased after acoustic trauma.

This result was subsequently confirmed and further investigated by analyzing neural activity using the Wiener kernel technique. Wiener kernels are determined by cross-correlating the presented sound with the evoked action potentials. The sound frequencies to which the neuron responds can be extracted from these kernels. It can also be determined whether this response is excitatory or inhibitory. In **Chapter 4**, the application of the Wiener kernel technique is described for neural activity of the inferior colliculus. Next, in **Chapter 5**, Wiener kernels are applied on neural activity measured before and immediately after acoustic trauma. By calculating the Wiener kernels we have gained more insight into the balance between excitation and inhibition in neurons of normal-hearing animals and how this balance is disturbed due to acoustic trauma. It turns out that mainly in mid-frequency neurons, which respond to frequencies just below the trauma frequency, no inhibition and only excitation is present after acoustic trauma.

Decreased inhibition in auditory neurons will generally lead to higher firing rates in response to sound. It can be assumed that this will cause sounds to be perceived louder than normal. Thus, reduced inhibition might lead to hyperacusis. This is part of the reason why this dissertation asserts that an acoustic trauma-induced disturbed balance between excitation and inhibition could be an underlying mechanism of hyperacusis.

Neurons of the auditory system also code for the slower fluctuations of the amplitude of a sound (the amplitude modulations). These are encoded for by timing the action potentials at a specific phase of the amplitude modulation, also called phase locking. **Chapter 3** describes the effects of acoustic trauma on the degree of phase locking in the inferior colliculus. It appears that neurons respond more strongly to amplitude modulations after acoustic trauma. This may underlie the problems that people with hearing loss encounter with understand speech in fluctuating (amplitude modulated) background noise.

How can we ask a guinea pig if he has tinnitus or hyperacusis?

In order to determine whether acoustic trauma-induced abnormalities in neural activity correlate with tinnitus or hyperacusis, behavioral models have been developed. A behavioral model is defined as a method which can determine from the behavior of the animal whether it has tinnitus or hyperacusis. Models that determine tinnitus are based on the assumption that the animal with tinnitus does not perceive silence. This dissertation describes a potential new method to determine tinnitus (and perhaps hyperacusis) in a laboratory animal, in this case, the guinea pig. This method is based on the finding that guinea pigs show different natural behavior during noise and in silence. In silence, they sit still and in noise, guinea pigs will move and walk around. **Chapter 6** shows that guinea pigs that have been exposed to acoustic trauma are also active during the silent intervals. This suggests that they may not have perceived silence and have tinnitus. When it has been determined whether the degree

of activity during sound correlates with sound intensity, this method could possibly also be used to determine hyperacusis in laboratory animals.

Conclusions

In summary, this dissertation shows that acoustic trauma is not limited to hearing loss in the ear, but also has several consequences for the processing of sound in the central auditory system. Acoustic trauma disturbs the balance between excitation and inhibition in the mid-frequency neurons and enhances the response to amplitude modulations in the inferior colliculus. These findings, in combination with the proposed new behavior model, will potentially contribute to the development of an animal model in which a direct relationship can be established between the neurophysiological effects of acoustic trauma and the presence of tinnitus or hyperacusis. Such an animal model opens new pathways for further investigation of the mechanisms of tinnitus and hyperacusis, and for the development of treatments.

Samenvatting

Geluidstrauma

De schade die je op kan lopen door langdurige blootstelling aan hard geluid wordt geluidstrauma genoemd. Het meest bekende gevolg van geluidstrauma is een verhoging van de gehoordrempels, oftewel slechthorendheid. Echter, geluidstrauma kan ook leiden tot oorsuizen, ook wel tinnitus genoemd in medische termen. Tinnitus komt veel voor; bijna 90% van de adolescenten zegt wel eens tinnitus te hebben gehad. Echter, er is ook een groep mensen die constant een tinnitus heeft. Hier kan men veel last van krijgen. Bijkomende klachten die vaak voorkomen met langdurige tinnitus zijn concentratieproblemen, slapeloosheid en stress, welke soms over kunnen gaan in depressie en zelfs zelfmoordneiging. Verder kan geluidstrauma ook leiden tot hyperacusis, een conditie waarin de patiënt overgevoelig is voor geluiden met normale geluidssterkte. Helaas zijn er tot op heden geen behandelingen beschikbaar die tinnitus en hyperacusis kunnen doen verdwijnen.

Een van de redenen voor het ontbreken van een behandeling is het feit dat we de onderliggende mechanismes van tinnitus en hyperacusis nog niet precies begrijpen. Wel is bekend dat, naast gehoorschade in het oor, de hersenen ook een belangrijke rol spelen bij het ontstaan van tinnitus en hyperacusis. Het grootste deel van het onderzoek dat is beschreven in dit proefschrift is daarom gericht op de hersenen. In deze studies worden de consequenties van geluidstrauma op de functie van de hersenen, oftewel de neurofysiologische consequenties van geluidstrauma, bestudeerd. Omdat neurofysiologie in de mens alleen indirect bestudeerd kan worden is het huidige onderzoek uitgevoerd in proefdieren. Het laatste hoofdstuk is gewijd aan de vraag of we kunnen vaststellen of het proefdier tinnitus of hyperacusis heeft. Het doel van dit proefschrift is om bij te dragen aan de ontwikkeling van een proefdiermodel voor het testen van behandelingen voor tinnitus en hyperacusis.

Meten van hersenactiviteit in een proefdier

Een deel van de hersenen is voornamelijk gericht op het verwerken van geluid. Deze gebieden worden samen ook wel het centraal auditief systeem genoemd (zie de figuur op de voorpagina van dit proefschrift). De hersencellen (neuronen) in deze gebieden communiceren met elkaar door middel van elektrische signalen, de actiepotentialen. Door de patronen van deze actiepotentialen te analyseren kan de verwerking van geluid bestudeerd worden. Actiepotentialen van neuronen kunnen gemeten worden door een elektrode te implanteren in de hersenen van het proefdier. De vuurfrequentie waarmee een neuron actiepotentialen afgeeft wordt ook wel de neurale activiteit genoemd. Door het aanbieden van specifieke geluiden wordt de spontane neurale activiteit van verschillende neuronen dan wel verhoogd (excitatie) of verlaagd (inhibitie). **Hoofdstuk 2** laat zien dat geluidstrauma resulteert in een

verstoorde balans tussen excitatie en inhibitie. Met name het aantal neuronen dat inhibeert is verminderd na geluidstrauma.

Dit resultaat is vervolgens bevestigd en verder onderzocht door de neurale activiteit te analyseren met de Wiener kernel techniek. Wiener kernels worden uitgerekend door het gepresenteerde geluid te correleren met de actiepotentialen. De geluidsfrequenties waarop het neuron reageert kunnen vervolgens afgeleidt worden uit de kernels. Ook kan bepaald worden of deze reactie exciterend of inhiberend is. In **hoofdstuk 4** wordt de toepassing van de Wiener kernel techniek op neurale activiteit van de inferior colliculus beschreven. Vervolgens worden in **hoofdstuk 5** Wiener kernels toegepast op neurale activiteit gemeten voor geluidstrauma en direct na geluidstrauma. Door het uitrekenen van de Wiener kernels hebben we meer inzicht gekregen in hoe de balans tussen excitatie en inhibitie is opgebouwd in neuronen van normaalhorende proefdieren en hoe deze balans is verstoord als gevolg van geluidstrauma. Het blijkt dat er voornamelijk in de mid-frequente neuronen, welke reageren op frequenties net onder de trauma frequentie, wel excitatie maar geen inhibitie meer aanwezig is na geluidstrauma.

De verminderde inhibitie zal in het algemeen leiden tot een hogere vuurfrequentie van auditieve neuronen in response op geluid. We nemen aan dat dit er toe zal leiden dat geluiden over het algemeen als luider worden waargenomen. De verminderde inhibitie zou daarmee kunnen leiden tot hyperacusis. Mede daardoor wordt er in dit proefschrift gesteld dat de verstoorde balans van excitatie en inhibitie als gevolg van geluidstrauma een onderliggende pathologie is van hyperacusis.

Neuronen in het auditief systeem coderen ook voor de langzamere veranderingen van de sterkte van het geluid (de amplitude modulaties). Neuronen coderen hiervoor door hun actiepotentialen precies te timen met een bepaalde fase van de amplitude modulatie, ook wel phase locking genoemd. **Hoofdstuk 3** beschrijft de consequenties van geluidstrauma op de mate van phase locking in de inferior colliculus. Het blijkt dat neuronen sterker reageren op de amplitude modulaties na geluidstrauma. Dit kan ten grondslag liggen aan de problemen die mensen met gehoorverlies ervaren met het verstaan van spraak in fluctuerende (amplitude gemoduleerde) achtergrond geluiden.

Hoe kunnen we aan een cavia vragen of hij tinnitus of hyperacusis heeft

Om te bepalen of de afwijkingen in hersenactiviteit correleren met tinnitus of hyperacusis, zijn er gedragsmodellen ontwikkeld. Onder een gedragsmodel wordt een methode verstaan waarbij uit het gedrag van een proefdier kan wordt opgemaakt of hij tinnitus of hyperacusis heeft. De methodes voor het bepalen van tinnitus zijn gebaseerd op de aanname dat een proefdier geen stilte kan ervaren wanneer hij tinnitus heeft. Dit proefschrift beschrijft een mogelijk nieuwe methode om tinnitus (en wellicht hyperacusis) te bepalen in een proefdier, in dit geval de cavia. Deze methode is gebaseerd op de bevinding dat cavia's verschillend

natuurlijk gedrag laten zien in ruis en in stilte. In stilte zitten cavia's stil en in ruis zullen ze bewegen en rondlopen. **Hoofdstuk 6** laat zien dat cavia's die zijn blootgesteld aan geluidstrauma ook actief worden tijdens de stilte intervallen. Dit suggereert dat ze de stilte niet ervaren en mogelijk tinnitus hebben. Wanneer er is vastgesteld of de mate van activiteit tijdens geluid correleert met de luidheid van de ruis zou dit wellicht gebruikt kunnen worden voor het vaststellen van hyperacusis in het proefdier.

Conclusies

Samenvattend toont dit proefschrift dat geluidstrauma niet beperkt blijft tot gehoorschade in het oor, maar ook diverse consequenties heeft voor de verwerking van geluid in het centraal auditief systeem. Geluidstrauma verstoord de balans tussen excitatie en inhibitie in midfrequente neuronen en versterkt de reactie op amplitude modulaties in de inferior colliculus. Deze bevindingen, in combinatie met het voorgestelde nieuwe gedragsmodel, zullen mogelijk bijdragen aan de ontwikkeling van een proefdiermodel waarin een directe relatie gelegd kan worden tussen de neurofysiologische consequenties van geluidstrauma en de aanwezigheid van tinnitus of hyperacusis. Een dergelijk proefdiermodel opent nieuwe paden voor het verder onderzoeken van de mechanismes van tinnitus en hyperacusis en voor het ontwikkelen van behandelingen.

Acknowledgements

Pim, bedankt dat je altijd het vertrouwen in mij had om mij dit onderzoek te laten uitvoeren. Ik heb enorm veel van je geleerd en je enthousiasme voor het auditieve onderzoek is erg aanstekelijk geweest.

Hans, je bent van onschatbare waarde geweest in het tot stand brengen van mijn experimenten. Ik ben je erg dankbaar voor alle kennis en expertise die je met me gedeeld hebt en voor de fijne samenwerking.

Martijn, niet alleen heb ik met plezier met je samengewerkt en veel van je geleerd over gedragsexperimenten met cavia's, ook ben ik je erg dankbaar voor je steun en wijze woorden over het leven als PhD student.

Acquiring my surgical skills to approach the inferior colliculus are all thanks to **Russ Snyder**. Thank you for showing me how to record neural activity from the inferior colliculus, a skill that was indispensable to complete this dissertation.

Verder wil ik de medewerkers van het CDP bedanken voor hun hulp tijdens mijn experimenten. Met name **Annemieke Smit-van Oosten, Michel Weij, André Zandvoort, Bianca Meijeringh** en **Ar Jansen**.

Ik bedank **Nima Ilbegi** en **Fedde Tigchelaar** voor hun bijdrage aan het uitvoeren en analyseren van de gedrags- en Wiener kernel experimenten, respectievelijk.

I want to thank the reading committee, **Gerard Borst, Natasha Maurits,** and **Richard Salvi**, for their time to evaluate this dissertation and for their insightful comments.

I want to thank **Terrin** and **Enja** for their valuable comments on earlier versions of the introduction and discussion, and the summary, respectively.

To all my colleagues at the ENT department, thank you for creating a great environment all those years, research-wise and 'gezellig'-wise!

Many thanks also to the **BCN** graduate school and in particular to everyone of the **PhD Council**.

To my friends: **Carina, Marnix, Inge**, **Jennifer**, **Melanie**, **Sygrid**, **Martijn**, **Marjolein**, **Rolinka**, **Paul**, **Emi**, **Jonathan**, **Stefan**, **Jessica**, **Tessa**, **Bonne**, and **the people of the Friday Afternoon Drinks Group**. Thank you for the vivid discussions and all the good times!

Lieve **Maaike** en **Astrid**, jullie zijn mijn steun en toeverlaat en de liefste vriendinnen die ik me kan wensen! Het is voor mij heel speciaal dat jullie mijn paranimfen zijn. Ik had het niet zonder jullie gekund.

In plak om by te kommen, om mysels te wêzen en om dochs nog ien kear út te lizzen wat ik ek alwer presys ûndersykje. Leave **Heit, Mem, Jorrit en Anita, Frida** en **Doutsen,** bedankt dat jim der altiid binne, foar jim lústerjend ear en foar jim wize wurden. Ek foar myn skoan famylje: **Laas, Jikkie, Martine en Klaes, Abe, Elles, Pieter Jissel en Thea, Elskemare** en **Liseanna**.

Leave **Minne**, do wiest der altiid foar my, yn alles wat dit ûndersyk op myn en ús paad hat brocht. Bedankt foar al dyn nuchtere en relativerende wurden at ik it even net mear wist, foar dyn sterke skouder en foar dyn steun yn alles wat ik doch.

Curriculum Vitae

Amarins N. Heeringa was born in 1986 in Deinum, the Netherlands. From 1998 until 2004, she went to the Atheneum at OSG Piter Jelles Âldlân. She started with Life Science & Technology at the University of Groningen in 2004, where she specialized in Molecular Physiology and Pharmacology.

After receiving her Bachelor's degree, she travelled for a year in South-East Asia and the United States, after which she started in 2008 with the Research Master Behavioural and Cognitive Neurosciences (BCN) at the University of Groningen. Within this master, she specialized in Molecular and Clinical Neuroscience and she performed two research projects. Her minor thesis was supervised by Dr. P. Meerlo at the University of Groningen and was titled: 'Does sleep deprivation affect hippocampal functioning?'. For her major thesis, she studied the role of the immune system in bone cancer-derived pain at the Université de Bordeaux 2, which was supervised by Dr. J.P. Konsman.

After graduating cum laude in 2010, she started working on a PhD project at the ENT department of the University Medical Center Groningen, which resulted in the current dissertation. Her project was supervised by Dr. P. van Dijk and was connected to the graduate school of Behavioural and Cognitive Neurosciences (BCN).

After finishing her PhD project, she moved to the US to do a postdoc at the Kresge Hearing Research Institute at the University of Michigan in the lab of Dr. S. Shore, studying non-auditory connections to the ventral cochlear nucleus.